Flexible Riser Fatigue Analysis

Studying Conservatism in Flexible Riser Fatigue Analysis and Development of an Engineering Model to Study Influencing Parameters of Local Wire Stress

Frederike Nugteren

Master of Science Thesis

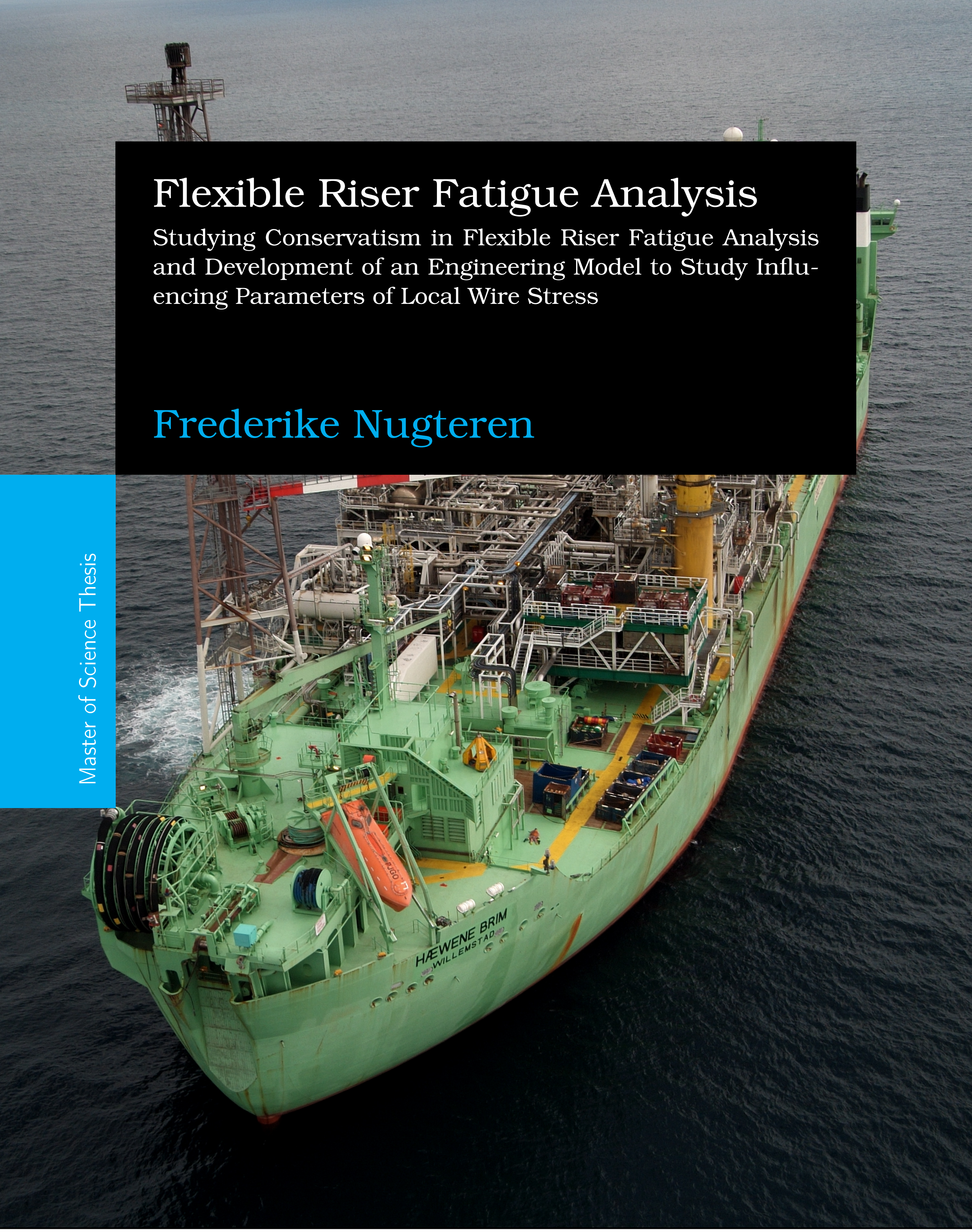

Delft University of Technology

Flexible Riser Fatigue Analysis

Studying Conservatism in Flexible Riser Fatigue Analysis and Development of an Engineering Model to Study Influencing Parameters of Local Wire Stress

Master of Science Thesis

For the degree of Master of Science in Offshore Engineering at Delft University of Technology

Frederike Nugteren

May 11, 2015

Faculty of Mechanical, Maritime and Materials Engineering (3mE) · Delft University of Technology

The work in this thesis was supported by Shell Projects & Technology. Their cooperation is hereby gratefully acknowledged.

Summary

Introduction

Purpose

Shell utilizes flexible risers in the North-Sea to connect Floating Production Storage and Offloading units to the sub-sea infrastructure. The floating facility, shallow water and harsh environmental conditions have been reasons to decide on flexibles. Unfortunately, flexible risers have a proven sensibility to numerous failure mechanisms and in too many cases the predicted service-life is not met.

In general, failure of the flexible riser is either caused by extreme conditions–the giant once in a 100yr wave–or by repetitive movements within (seemingly) safe margins; i.e fatigue. The latter is a big point of discussion in the context of service-life prediction as most in-field conditions deviate from design conditions. Main causes for deviation are outer sheath damage, the diffusion of gasses from the inner bore and divergent environmental conditions. Also the accuracy of fatigue assessment methodology needs improvement. To this date, behavioural software models cannot fully predict the motions and stresses as a response to the loads imposed on the flexible riser system.

Shell was involved in numerous Joint Industry Projects to contribute to and benefit from industry consensus on fatigue analysis methodologies. Full-scale experiments, knowledge and software development were a major focus of Shell engineers from the first utilization of flexibles up to the late nineties. Hereafter, focus shifted from research and development to outsourcing elaborate calculations to riser manufacturers and specialist engineering consultants. Hence adequate judgement of fatigue analysis reports remained as the in-house responsibility.

The incentive to refocus on flexible riser fatigue analysis and to develop knowledge and tools was a recent premature flexible riser replacement in the North-Sea. The situation was triggered by changed in-field conditions leading to insufficient fatigue life. However, dissection of the strength governing tensile armour layer and subsequent small-scale testing did not confirm this analysis result. Hence it was expected that costly consequences of over-conservative fatigue analyses —early replacement as well as over-dimensioning new designs— can and should be avoided in the future by restoring in-house expertise.

To establish this, Shell requested for a knowledge boost, an in-house software model and a renewed approach to address specialist consultants. Firstly to improve safety judgements after sudden in-field condition changes. Secondly to accommodate flexible riser fatigue analyses for future projects.

A knowledge boost, an in-house software model and a renewed approach to address specialist consultants combined with the criteria for a successful research project resulted in the following research objective:

Studying Conservatism in Flexible Riser Fatigue Analysis and Development of an Engineering Model to Study Influencing Parameters of Local Wire Stress

Project Scope & Methods

The Offshore Structures department is responsible for managing structural design and integrity analyses for offshore field developments scattered around the globe. Hence the operational safety throughout the service life of a particular structure or structural element. Flexible risers operated in the North-Sea have a fatigue-critical design due to their slenderness combined with harsh operational conditions. Consequently, integrity management of flexible risers is governed by failure prevention through metal fatigue of the tensile armour wires.

In present work, integrity management is defined as: identifying changed in-field conditions and deciding on a safe but cost-effective approach to match the flexible riser service life to the desired field life. The riser design, fatigue analysis and monitoring & inspection strategies can all three contribute to finding the best possible strategy. Not all aspects are fully investigated; new designs are not within the scope of present work. However, knowledge inquiries and model development raises the potential of future in-house fatigue analyses for field development concepts considering flexible risers.

First, the focus of a literature review was on industry visions and fatigue life assessments. Hence fatigue analysis methodology —with a special focus on local modelling— was thoroughly investigated because this is the Shell and industry accepted method to define and assess fatigue life.

Secondly, a new strategy was developed to stretch the fatigue life after identifying a significant in-field changed condition. This guideline incorporates in-house analysis activities to enhance the collaboration with specialist consultants.

Changed environmental and operational conditions should be incorporated in the fatigue analysis within the limits of fixed geometry parameters. A local model captivates the direct influence on stress levels in the fatigue-critical tensile armour wires as a result of these new conditions. For the purpose of doing a pre-analysis independently, a new in-house analytical model was developed: ABC Fatigue.

Finally, a benchmark case-study illustrates the purpose, methodology and conclusions of such pre-analysis by analysing a typical flexible riser designed for North-Sea environmental conditions.

Literature Review

Integrity Management

Corrosion of armour wires has been thoroughly studied for the last 10-15 years. Currently the assumed dry-annulus conditions are usually not present during the service-life of the riser. A couple of serious failures of flexible risers were caused by corrosion of armour wires. The most important observation has been that all failed risers suffered from damaged outer sheaths hence the best way to avoid corrosion fatigue is to prevent breaches.

Manufactures of flexible risers highly recommend monitoring techniques able to deliver in-field data. Strain monitoring, by embedding strain sensing optical fibers, continuously measures strain rates in multiple wires around the circumference. The remaining fatigue life capacity is subsequently obtained from rainflow-counting the number of load cycles and strain amplitudes. At the end of a design life it is easy to evaluate life time extension options. Also this information can act as a solid basis to when unexpected conditions are encountered such as other bore conditions but also loads on the tensile armour wires.

Design specifications should be very specific and continuously evolve to account for unexpected mechanisms where application are used under new conditions. Verification of the riser system design assumptions is expected to evolve into monitoring the following:

- Metocean conditons (design input parameter)
- Vessel motions, especially heave and translational movement at tie-in location (design input parameter)
- Bend stiffener deflection for high risk applications (response parameter).
- Integrity of the annulus (design versus actual condition).

Fatigue Analysis Methodology & Conservatism

Fatigue analysis is defined as research that encompasses global dynamic motions and local stress in the tensile armour wires. Existing methodologies lack the consistency and level of transparency that is required to independently demonstrate the level of safety and conservatism in new flexible riser designs. The Fatigue Analysis Methodology Guidelines were a major step into reaching industry accepted methodology. This document is the main deliverable from the Real Life Joint Industry Project, managed by MCS. Their approach generally starts with simpler conservative calculations that can be safely applied to a riser designed far below the fatigue critical limit. For fatigue critical designs, more accurate and comprehensive methods are advised. Paragraph 2-2-1 and 2-2-2 cite the most important steps and assumptions associated to global and local analyses (Smith and Grealish).

This industry accepted design verification philosophy was not enough to completely resolve the technology protection issue. Propriety of knowledge and models still characterizes the industry. Universally recognized API Spec 17J and API Spec 17B are continuously updated to commingle consensus on minimum requirements between operators, suppliers and regulators. Technology evolves; new materials and new design design scenarios (deep water) introduce new failure mechanisms (Loback et al., 2010).

To ensure a fatigue life larger than the desired service life, the industry accepted fatigue analysis methodology is used. This is a three-step procedure:

1. Dynamic analysis to couple metocean conditions and riser motions. The fatigue critical zone/cross-section is detected for further analysis in the second step.
2. Quasi-static analysis to couple motions and stresses.
3. Fatigue life calculation transforms stresses to fatigue damage and includes additional safety.

The accuracy of calculation methodology is a topic of discussion; this calculation is over-conservative. Checking the actual presence of cracks and other indicators of failure is challenging in operational conditions. New initiatives such as embedding strain sensing optical fibers or frequent wire inspection to identify wire break are promising developments in order to match calculations with the actual damage accumulating in the material throughout its service life.

Local Modelling

The local fatigue analysis converts the global loading at selected hotspots to stress in the armour wires. The analysis requires a numerical model of the flexible pipe cross-section and an interface that is compatible with the global to local transposition procedures.

The general requirements for LA models are outlined as follows:

1. Verified against full-scale measurements.
2. Capable of modelling tension and curvature ranges.
3. Preferably account for hysteresis effects, if not already addressed in the global or intermediate analysis.
4. Take into account the effects of external pressure.
5. Stresses to be calculated at the four corners of the rectangular shaped wires normally used for tensile armour.
6. Preferably output stresses at eight points around the circumference, so that directionality effects can be considered.

Conservatism Indicators & Engineering Guideline

After identification of a changed condition a quick decision on a safe but cost-effective approach is required. The fatigue analysis methodology steps are analysed to identify assumptions which alter the level of conservatism. Furthermore, two hazardous scenario's and their impact on fatigue life are illustrated. A new approach is advised to support in-field flexible risers currently operated in the North-Sea region.

Fatigue Assessment Analysis: Conservatism Indicators

An overview of 31 conservatism indicators used in the three-step fatigue analysis is presented. To define these critical elements, literature on current methodology and local analysis techniques was studied in a literature review. The local analysis has been deeply investigated hence analysis elements are more detailed.

Advice: Engineering Guideline

Currently, Shell's actions after detection of a sudden hazard heavily rely on the advice given by specialist consultants. Their advice and expertise are essential however the following initial actions are advised to change the collaboration environment.

1. Collate and neatly store design conditions - i.e. all input values and model assumptions which were used for the initial fatigue analysis prior to riser installation.
2. Rate all conservatism indicators with "simple" or "elaborate" (table 3-2)to determine the extensiveness of the initial fatigue analysis.
3. Determine the current and desirable quality of load data obtained from monitoring and inspection activities. Collate and have them readily available in case a re-assessment is triggered.

4. Pro-actively analyse high-risk riser systems and strive for optimal input through monitoring, inspections and data management.

In case of a sudden hazard, fatigue life can be enhanced by implementing actual conditions instead of initial predictions (loads) and by elaborating the model (formats and responses) where possible. Pre-analyses and model runs can be done in-house, a verified model combined with recent operational data can quantify the impact of changed input data. Subsequent collaboration with specialist consultant is advised. ABC Fatigue's suitability for in-house pre-analyses is analysed trough model cross-validation and verification.

ABC Fatigue: From fundamental Theory to Algorithm

A new analytical software model was developed to study the major sources of conservatism in local fatigue analysis: ABC Fatigue. In general, two aspects can compromise the accuracy of a local fatigue analysis:

1. Input parameters are not correct: design conditions deviate from actual in-field measurements.
2. The methodology and/or algorithm is not correct.

ABC Fatigue should be capable to run a reasonably accurate local fatigue analysis with a main purpose to study parameter impact on wire-stress for pre-analysis and feed studies. Modelling the influence of hysteresis and irregular waves is desired. Furthermore, ABC Fatigue is based on analytical formulae, a preferred feature to search for linkages between load and response parameters for different riser cross-sections and load-cases.

Model A and B assess multiple wire-locations around the circumference and along the helix wire assuming constant loading characteristics, i.e. constant axisymmetric loading and constant curvature.

Hysteresis is incorporated in Model C; extending the algorithm of Model B by including periodic curvature to simulate regular and irregular wave patterns. This study is signified by diligent tracking of wire positions and superposing the responses from curvature cycles.

Model A

The imposed loads in this analysis are internal pressure p_{in}, external pressure p_{out} and external tension T_{ex}. The expected physical behaviour of the flexible riser in this axisymmetric analysis is signified by:

1. Stress in the metallic armour wires σ_i for N helical layers i.
2. Contact pressures $p_{C,i}$ and $p_{C,i+1}$ pressing inside and outside of layers i.
3. Symmetric deformation of the riser cross section: elongation ΔL, expansion Δa and torsion $\Delta\theta$.

The load is shared among the N metallic layers according to wire laying angle and helix radius. A process of load transmission, based on the stress-strain constitutive relation for linear materials, introduces contact pressure transmission trough the armour layers. The model response is based on finding the radial, circumferential and longitudinal equilibrium and to define the load distribution among each metallic layer. The correct calculation of stress in the wires in this axisymmetric analysis is mainly challenged by the helical shape of the armour layers and the composite character of the flexible riser.

The approach by Feret and Bournazel (1987) still holds as the basis for most contemporary axisymmetric analyses. Parameters, relations and assumptions proposed in this theory are also the fundamental basis of Part A. The influence of torsion $\Delta\theta$ is assumed to be negligible and is not taken into account.

The algorithm of Model A can be summarized as follows:

1. An initial expansion Δa_0 and elongation ΔL_0 are assumed to simulate a constitutive response.
2. The wire-stress in each layer i as a response to the imposed deformation is calculated and the approximate values for wall tension $\sum F_{ap,i}$ and total pressure differential $\sum p_{ap,i}$ are derived from wire-stresses.
3. The total wall tension F_t and total pressure differential p_t are calculated from the initial load conditions.
4. Through an iterative approach the correct deformation, hence equilibrium, is determined by checking $F_t = F_{ap}$ and $p_t = p_{ap}$ after each iteration cycle.
5. The final wire stresses are subsequently used to calculate the pressure differential p_i through each layer from the inner bore to the outer layer. Finally, the layer pressure differentials are subtracted from the inner-bore pressure p_{in} to calculate the net contact pressures $p_{C,i}$ between each concentric layer.

Model B

For axisymmetric loads, analytical stress calculations are highly accurate. For a-symmetric deformation, or bending, a tenuous and non-linear stiffness characteristic compromises the stress-response calculation. Hence, bending analysis did not converge to a general analytical model as presented for axisymmetric analysis by Feret and Bournazel.

However, an acceptable approach has been developed. This method is based on the friction induced axial shear stress and local bending of the individual wire induced by riser curvature. To evaluate both responses, the riser section is viewed from the global (cross-section) perspective and the local wire perspective.

The physical behaviour as a response to a curvature Ω_2, or curvature radius R_2 is signified by:

1. Friction stress σ_f; an axial shear stress emerging during the wire stick-condition, reaching a constant maximum value after reaching the full slip-condition.
2. Local bending stress σ_b in two orthogonal directions H_2 and H_3, dependent global curvature.
3. Total alternating stress σ_a resulting from the superposition of friction and local bending stress.

Compressive and tensile forces emerge from bending the riser cross-section. A thin-walled steel cylinder would show linear shortening of the compressive side and similarly elongation on the tensile side as a response to curvature Ω.

However, the layered and helical character of the flexible riser introduces non-linear strain behaviour for each concentric layer i when following helix wire wrapped around the layer circumference. Friction stress σ_f and bending stress σ_b are superposed with the static stress σ_s calculated by Model A to find the total wire stress σ_t. The global axis-system is labelled $X_{1,2,3}$ and the local (helix-wire) axis-system as $H_{1,2,3}$.

The algorithm of Model B can be summarized as follows:

1. Define additional geometry and curvature loading b, t and Ω_{max}.
2. Define friction coefficient and calculate critical curvature and
3. Calculate friction stresses by extending the domain of a quarter pitch to all 360 circumferential locations.
4. Calculate lateral and transverse bending and superpose to find total bending stress for all circumferential positions ψ.
5. Superposition of friction and bending stress to find total stress σ_a for all circumferential positions ψ.

Model C

In Model C cyclic curvature is introduced. Extreme response values are measured at cycle top and crest to define the maximum stress range experienced in the numerous wires around the circumference. A crucial uncertainty regards the direction and magnitude of wire slip and the relation with curvature. Wire slip results in a major change of riser stiffness and non-linear stress accumulation in the wires around the circumference.

The bending theory as used in Model B is continuously repeated for each curvature level $\Omega(t)$ at $t_{i+1} = t_i + \Delta t$ for $i = 0 - 2\pi$.

The assumed conditions used in this generic theory are as follows

1. A cyclic curvature $\Omega(t)$ is applied to a local section with length L; the riser is repetitively bent into a torus with up and downward orientation.
2. Quasi-static frequency domain: no dynamic acceleration and incorporation of mass.
3. Wire-slip only in longitudinal direction H_1: no change of wire laying angle in the bent state according to loxodromic assumption.

Full-slip conditions:

1. Modelling one curvature load-cycle with constant curvature amplitude in the quasi-static frequency domain.
2. Linear relationship between curvature increment $d\Omega$ and slip distance ΔH.
3. Wires are immediately in full-slip condition in the first time-step after curvature sign change thus $d\Omega = 0$.

Stick-slip conditions:

1. Stick-condition pertains until axial shear force is higher than available friction force. At initiation of first curvature increment and at maxima and minima of curvature reversals, wire slip is zero.

2. The stick region is delineated by the critical curvature; stick condition emerges as $d\Omega < \Omega_{cr}$ and pertains after sign change of $d\Omega$ until the sum of curvature increments is larger than the critical curvature.
3. Ten cycles c_c are modelled;
    - Constant or Irregular Ω_a.
    - Instead of 2 reversals for a full cycle, reversals range between 1.75-2.25.
4. First cycle is identical to tenth cycle regarding amplitude and reversals.

ABC Fatigue: Model Validation & Verification

A clear distinction exists between the "Physical response" and the "Model response". The former being the real response seen under operational conditions and/or experiments, the latter obtained from mathematical relations. Minimal differences are desired as model predictions hence fatigue life estimates are consequently reliable and operational safety judgements —based on a fatigue life re-assessment including updated conditions— can be made without hesitation.

Response parameters of Model A were cross-validated with Flexpipe, an industry accepted model used and owned by Technip (Technip). Model B was cross-validated with Helica, a newly developed (Skeie et al., 2012) and also industry accepted model by DNV.

The verification criterion is used to determine the suitability of ABC for pre-analysis; incorporating in-field environmental and operational conditions to study their impact on stress range hence their potential to raise the fatigue life of the flexible riser.

Model A: contact pressure and wire stress

The following validation statements can be made with regard to axisymmetric analysis:

- The model can accurately calculate the axial wire stresses from constant pressure and tension existing in the first three metallic layers, i.e. for both pressure and tensile oriented armour, within relevant operational domains.
- The response of the outer tensile armour is not validated. Load sharing relations defined for the two tensile armours are tenuous, also in literature.
- Contact pressure between the first and second pressure armour is aligned with the design calculations.
- Contact pressures between second pressure armour, inner tensile armour and outer tensile are over-conservative. However the slope of the curves are aligned, indicating a correct method. High values calculated by ABC Fatigue are presumably related to the the omission of plastic layers.

Model B: stress range

In general, the sign of friction stress is correct for all circumferential locations and both inner and outer tensile armour. However, assumptions were made to match the riser geometry and case-study data was presented in graphical forms. Hence, data-quality of the case-study compromise the reliability of both validations. Based on data quality, the validation cycle of Model B-Helica is more trustworthy than the second scheme used for Model B-Life6. Consequently, the latter does not influence model validation statements.

The following statements can be made

- Response data presented by (Skeie et al., 2012) studied the inner tensile armour thus no possible comparison for outer tensile armour.
- The values of friction stress and total stress are within a 1-4% deviation range.

Verification

ABC Fatigue —a superposition of Model A and Model B— is currently not suitable for elaborate in-house local analysis. Three out of six criteria are not satisfied. In theory, follow-up on the third action presented in table 5-10 is sufficient to finalize a local model which is ready for data comparison, e.g. with specialist consultants and riser manufacturers. This relatively simple enhancement would enable in-house pre-analyses within the limit of the inner tensile armour. In addition, information exchange is advised to design the post-processing application.

Benchmark Case-Study

A model experiment was carried out to signify the impact of changing design loads. This is evident as in-field measurements —i.e. monitoring of operational and metocean conditions and inspections of sudden and accumulated riser damage— prove deviations from initial predicted values used for flexible riser design and corresponding fatigue life calculation.

Present work advises imitation of this experiment (or then called pre-analysis) by Shell engineers to study the fatigue life margins of their flexible riser portfolio and to determine positive and negative fatigue life contributions from various input parameters. Also the relative impact of each input parameter is important to determine highly influential parameters which can potentially alter the fatigue life. Elaborate analysis by specialist consultants should subsequently investigate these predictions by generating accurate values —i.e. within the limits of current state-of-art model technology— resulting in a strategy to alter the fatigue life in case of critical fatigue life.

The influence of environmental loads is studied by deviation of the curvature and tension ranges. Operational load is signified by the inner-bore pressure. Parameter domains are derived from a 6 inch production riser operated by Shell in the North-Sea. Wire-stress accumulation, or stress-range, is relevant as this parameter is proportional to fatigue life.

Research Questions and Methodology

Research Objective: Signify the impact of changing design loads.

Four research questions were formulated to study the influence of environmental and operational conditions:

Question 1: What is the relative influence of pressure, tension and wire dimension the critical curvature; i.e. magnitude of friction stress?

Question 2: What is the influence of the bi-linear response behaviour, i.e. wire-slip?

Question 3: Which circumferential location governs the stress calculation?

Question 4: Is the maximum stress range always acting at the same circumferential location?

Six experiments were carried out:

1. Pressure range - Stress range
2. Tension range - Stress range
3. Wire width range - Stress range
4. Curvature range - Stress range (Benchmark pressure/tension)
5. Curvature range - Stress range (High pressure)
6. Curvature range - Stress range (High tension)

Influence of changing input parameters

Firstly, increasing pressure, tension and wire width all result in larger stress alternations for equal curvature levels. Pressure has the largest influence followed by wire width and tension.

Secondly, curvature-wire stress relations are linear and positive for all wire locations and three load conditions (Benchmark, high pressure, high tension) ψ, the slope of this relation increases for circumferential positions ψ towards the neutral axis at $\psi = 270$ as expected according to initial friction stress dominance and accumulating bending stresses for increasing curvature levels.

Thirdly, for this riser a pressure variation has a large impact on the curvature response compared to tension. The low pressure curvature - high pressure curvature multiplication factor is $c = 0.88$ and the low tension curvature - high tension curvature multiplication factor is $c = 0.53$.

Governance of friction stress

Increasing pressure, tension and wire width all result in a higher critical curvature value; i.e. wire slip is delayed. Pressure is clearly dominating this mechanism. However, tension also contributes and for other tension domains (deep water) this influence could become governing.

Circumferential maximum stress position

For a curvature value of Ω=0.01 1/m (benchmark), the maximum stress is always located at the outer fiber of the riser cross-section. The threshold value Ω_b indicating local bending dominance is not reached.

The threshold curvature is $\Omega_b = 0.027$ 1/m for the benchmark conditon. High pressurizing delays wire slip and maintains the highest stress range in the wire located at the outer fiber. High tension brings the threshold value Ω_b to 0.031 1/m.

Circumferential max moves to $\psi_{max} = 220°$ and the stress level is 10% higher than in the outer fiber at $\psi = 180°$. This is only 5% for the high-tension load-case. In high pressurized condition there is no difference.

This mechanism raises the question: What wires eventually govern fatigue life?

Irregular waves

Model C is not properly cross-validated. However, the impact of hysteresis was modelled indicatively; a precedence of load-cycles definitely influences the relationship between curvature magnitude and wire stress-range as expected.

Impact of changing design conditions

Each pre-analysis should incorporate an investigation of the load parameters pressure and tension cross-evaluated with an array of significant curvature domains. The study of this riser showed a predominant influence from pressure. Diligent study of pressure logs and the reformulation of one or multiple pressure load-cases can result in longer fatigue life.

Similarly the influence of friction coefficient is advised. The determination of this parameter is often tenuous but the impact can be large (proportional to the critical curvature hence initial friction stress).

Also a pre-analysis for the given curvature ranges can point out the location of maximum wire-stresses and the position of this maximum. If wire-slip and hysteresis are properly introduced by validating Model C, this mechanism probably redistributes the maximum stress among the circumferential wires hence lowering the stress ranges.

Conclusions

State-of-Art knowledge

Current knowledge development in the context of fatigue analysis of flexible risers is focused on monitoring of operational data and incorporation of corrosion fatigue. The former can potentially reduce conservatisms from the global and local analysis steps. The latter mechanism inevitably diminishes the fatigue life however incorrect annulus environment predictions induce over-conservatisms.

A big step towards industry consensus and transparency of Fatigue Analysis Methodology was established in the Real Life JIP (2006). However, propriety of software models is still the main compromiser of model development and methodology consensus .

In the context of local modelling, three model theories can be used to simulate axisymmetric load-response behaviour. Pioneering work published in 1987 still hols as the state-of-art analytical method. Theory to simulate the rigourous bending behaviour is not converged and clearly published. Various analytical models are used by manufacturers, research institutes and regulators for design and research purposes. Their publications commonly refer to similar basic formulations with minor enhancements. Most studies conclude with a satisfactory model-validation through full-scale experiments and/or reference models. However fundamental differences regarding slip direction, stick-slip mechanism and cycle repetition are blurring true model fundaments, capabilities and limits.

To conclude, industry investigations are focused on stimulating data monitoring and management, small-scale testing and stimulating tranparency of hysteresis formulations applied in the bending model.

Flexible Riser Integrity Guideline

Currently, Shell's actions after detection of a sudden hazard heavily rely on the advice given by specialist consultants. Four actions are advised to change the collaboration environment. These actions are based on implementing actual conditions instead of initial predictions (loads) and elaborations of the local and global analysis models (formats and responses) where possible by determining the extensiveness of fatigue analyses through a rating system based on 31 conservatism indicators.

Pre-analyses and model runs can be done in-house, a verified model combined with recent operational data can quantify the impact of changed input data. Subsequent collaboration with specialist consultant is advised.

ABC Fatigue: in-house local model

ABC Fatigue —a superposition of Model A and Model B— is currently not suitable for elaborate in-house local analysis. Three out of six criteria are not satisfied. In theory, a tension domain enhancement is sufficient to finalize a local model ready for data comparison, e.g. with specialist consultants and riser manufacturers. This relatively simple enhancement would enable in-house pre-analyses within the limit of the inner tensile armour.

Model C incorporates wire-slip and the stick-slip behaviour. However, this application is not validated hence the study of irregular waves and hysteresis was not possible in present work.

Case-study

The study of a 6 inch case-study riser showed a predominant influence from pressure. Diligent study of pressure logs and the reformulation of one or multiple pressure load-cases can result in longer fatigue life.

Recommendations

Restore balance

Currently, Shell's actions after detection of a sudden hazard heavily rely on the advice given by specialist consultants. Their advice and expertise are essential however a new action plan is advised to change the collaboration environment.

In addition, Shell can boost industry knowledge development by good data management, currently a company focus point. Documenting all operational load, response and condition parameters stimulates in-house model development and also enables a mutually beneficial collaboration with specialist consultants. This simultaneously restores the balance of knowledge reliability on external expertise. The specialist consultant averages the total stress around the circumference. Find out what averaging assumption are being used.

Pre-analyses

Imitation of the case-study experiment is advised to study the fatigue life margins of Shell's flexible riser portfolio and to determine positive and negative fatigue life contributions from various input parameters. Each pre-analysis should incorporate an investigation of the load parameters pressure and tension cross-evaluated with an array of significant curvature domains. In addition, information exchange is advised to design the post-processing application.

Similarly, the study of friction coefficient impact is advised. The determination of this parameter is often tenuous but the impact can be large (proportional to the critical curvature hence initial friction stress).

Also a pre-analysis for the given curvature ranges can point out the location of maximum wire-stresses and the position of this maximum. If wire-slip and hysteresis are properly introduced by verifying Model C, this mechanism can be studied. Ideally, this would redistribute the maximum stress among the circumferential wires hence lowers stress ranges and fatigue life.

Model development

Model C extension is recommended to fully benefit from ABC fatigue when dealing with sudden hazardous operational conditions. A full time-trace of tension and curvature and subsequent rainflow-counting generates more realistic stress-ranges by including wire position changes and corresponding friction and bending stresses. Full-scale measurements of curvature loads versus wire-slip responses of the (inner) tensile armour required.

Although the inner tensile armour is assumed to be fatigue critical, it is strongly recommended to introduce a new relation for the axisymmetric response of the outer tensile armour. Cross-model validation would be sufficient however full-scale validation experiments are advised.

Full-scale validation

A full-scale validation strives for alignment between experiment and model load-response variables. Present work clearly presents an overview of all model variables hence relatively little effort is required to design an experiment and to validate ABC Fatigue accordingly.

Furthermore, experimental data is required to validate ABC Fatigue up to industry standards. Currently, all three manufacturers of flexible pipe own a private test rig hence data is potentially generated and exchanged. However there should be a clear incentive, such as JIP involvement, to retrieve test data. Manufacturers are hesitant to disclose data other than presented in the JIP wrap-up report and have full rights over all data even when tests are managed by independent test facilities such as Marintek in Norway.

Table of Contents

List of Figures

List of Tables

Chapter 1

Introduction

This chapter will touch upon all main elements of the work carried out throughout this Master Thesis. First section 1-1 elaborates on the study goals in terms of project criteria, the research proposal by Shell and the resulting research objective.

Section 1-2 introduces flexible risers and their special characteristics compared to (normal) steel risers. Also the three main research elements of present work are introduced: Integrity Management, Fatigue Analysis Methodologies & Conservatism and Local Modelling.

Finally, section 1-3 summarizes the work that has been carried out in forms of the research methods and report structure.

1-1 Purpose

The main study-goal was finalizing the Offshore Engineering master program and writing a Master Thesis on an industry based research proposal. This was done in collaboration with TU Delft and Shell Projects and Technology, Rijswijk. Their proposed study of fatigue analysis of flexible risers raised the potential of a fundamental and challenging research thesis in the context of structural mechanics.

1-1-1 Project Criteria: TU Delft

The following elements guided towards the delivery of a satisfactory research study to graduate as a Master of Science in Offshore Engineering. The criteria for a successful 9-month research project were defined as follows:

1. Finding and understanding relevant theory of structure mechanics.
2. Scrutinize the development of major themes and research area's linked to this structure by conducting a literature study.
3. Select the state-of-art knowledge basis for a mechanical model and include new theoretical approaches.
4. Validate the model by using experimental data or cross-validation.

5. Find behavioural linkages by generating and studying model-data.
6. Conclude the study by presenting research methodology, results and recommendations.

This was achieved by modelling the mechanical behaviour of a flexible riser. Skills in preparing and executing fundamental research, effective project management and designing for practical engineering solutions were growing simultaneously.

1-1-2 Research Proposal: Conservatism in Fatigue Analysis of Flexible Risers

Shell utilizes flexible risers in the North-Sea to connect Floating Production Storage and Offloading units to the sub-sea infrastructure. The floating facility, shallow water and harsh environmental conditions have been reasons to decide on flexibles. Unfortunately, flexible risers have a proven sensibility to numerous failure mechanisms and in too many cases the predicted service-life is not met.

In general, failure of the flexible riser is either caused by extreme conditions–the giant once in a 100yr wave–or by repetitive movements within (seemingly) safe margins; i.e fatigue. The latter is a big point of discussion in the context of service-life prediction as most in-field conditions deviate from design conditions. Main causes for deviation are outer sheath damage, the diffusion of gasses from the inner bore and divergent environmental conditions. Also the accuracy of fatigue assessment methodology needs improvement. To this date, behavioural software models cannot fully predict the motions and stresses as a response to the loads imposed on the flexible riser system.

Shell was involved in numerous Joint Industry Projects to contribute to and benefit from industry consensus on fatigue analysis methodologies. Full-scale experiments, knowledge and software development were a major focus of Shell engineers from the first utilization of flexibles up to the late nineties. Hereafter, focus shifted from research and development to outsourcing elaborate calculations to riser manufacturers and specialist engineering consultants. Hence adequate judgement of fatigue analysis reports remained as the in-house responsibility.

The incentive to refocus on flexible riser fatigue analysis and to develop knowledge and tools was a recent premature flexible riser replacement in the North-Sea. The situation was triggered by changed in-field conditions leading to insufficient fatigue life. However, dissection of the strength governing tensile armour layer and subsequent small-scale testing did not confirm this analysis result. Hence it was expected that costly consequences of over-conservative fatigue analyses —early replacement as well as over-dimensioning new designs— can and should be avoided in the future by restoring in-house expertise.

To establish this, Shell requested for a knowledge boost, an in-house software model and a renewed approach to address specialist consultants. Firstly to improve safety judgements after sudden in-field condition changes. Secondly to accommodate flexible riser fatigue analyses for future projects.

1-1-3 Research Objective

A knowledge boost, an in-house software model and a renewed approach to address specialist consultants combined with the criteria for a successful research project as stated in section 1-1-1 resulted in the following research objective:

Studying Conservatism in Flexible Riser Fatigue Analysis and Development of an Engineering Model to Study Influencing Parameters of Local Wire Stress

1-2 Project Scope

Engineering responsibility incorporates ensuring the integrity of all analysed structural components. The life-cycle of a flexible riser is initiated with a robust riser design and a fatigue life always larger than the service life (multiplied by a factor). A selection of operational and environmental conditions is monitored continuously and the integrity is regularly checked through inspection. Both measures are used to identify changed conditions and this might induce a re-assessment of fatigue life, the necessity of this action is based on the judgement of Shell engineers. Figure 1-1 shows the sequence either resulting in continued service or riser replacement as a result of changed in-field conditions.

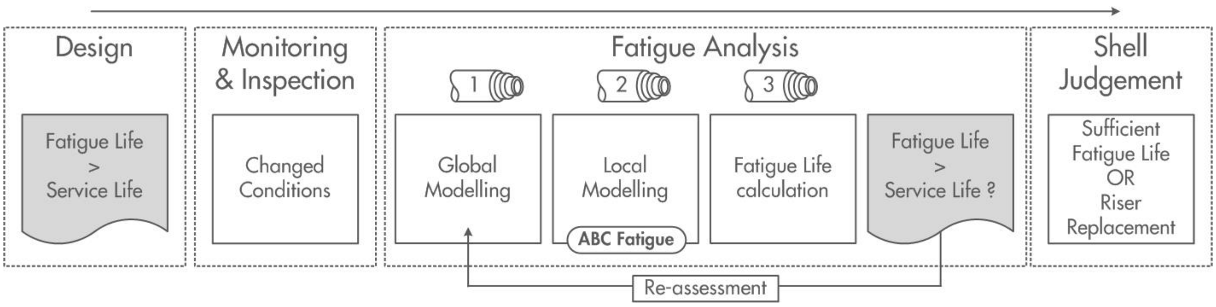

Figure 1-1: Action sequence induced by changed in-field conditions; resulting in continued operation or riser replacement.

In present work, integrity management is defined as: the identification of a changed condition and deciding on a safe but cost-effective approach. Integrity management organizes and steers the engineering work and can be considered of great importance. The riser design, fatigue analysis and monitoring & inspection strategies can all three contribute to a more reliable judgement. However, not all aspects are fully investigated in present work. Figure 1-2 indicates all focus points of this research, the three main elements in yellow.

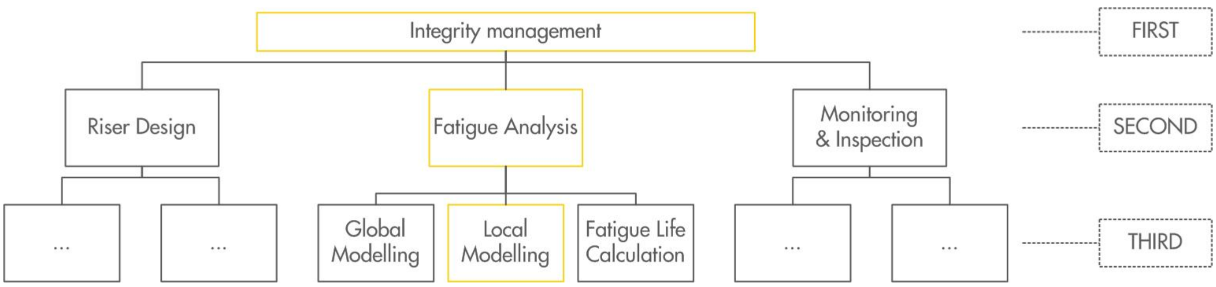

Figure 1-2: Scope of present work

First, this thesis touches upon integrity management. A new approach is developed to stretch the fatigue life after identifying a significant in-field change. Secondly, fatigue analysis is studied because this is the Shell and industry accepted method define and assess fatigue life. Thirdly local modelling has a major focus. This second step of the fatigue analysis procedure allows for studying changed environmental and operational conditions and its direct influence on stress levels in the fatigue-critical tensile armour wires. For this purpose, a new analytical model was developed: ABC Fatigue.

Consequently, new designs are not within the scope of present work. However, knowledge inquiries and model development raises the potential of future in-house fatigue analyses for development concepts considering flexible risers.

1-2-1 General: Flexible Risers

A flexible riser is a multilayer pipe with layers of different materials. The pipe connects a subsea production unit to the processing facility on the sea-surface. Often this is a floating facility such as a Floating Production Storage and Offloading unit, exerting horizontal and vertical motions on the riser.

Other than a rigid steel riser a flexible riser can perform under high-dynamic conditions — i.e. it is able to withstand large and cyclic bending moments without failure. In addition, the riser is capable of resisting tension arising from static and dynamic axial loads equivalent to steel risers.

Desired mechanical properties are highly influenced by the composite structure of the riser cross-section; all layers respond to loads from self-weight, internal and external pressure, floater-movements, waves and current in a synergistic way. Layers are either metallic (M) or plastic (P); principal functions are described in table 1-1 and depend on layer-material and layer-configuration. A typical riser cross-section is depicted in Figure 1-3a.

Table 1-1: From the riser bore to the outer sheath: layer properties

Name	Material	Configuration	Function
Carcass	M	Profiled steel strips	*Resistance to collapse*
Inner Liner	P	Continuous	*Confining product*
Pressure Armour	M	Z-shaped wires, short pitch	*Resistance to pressure(s)*
Tensile Armour	M	Rectangular wires, long pitch	*Mainly axial resistance*
Outer Sheath	P	Continuous	*Protection*
Anti-wear Sheath	P	Continuous	*Prevention of metallic-wear*

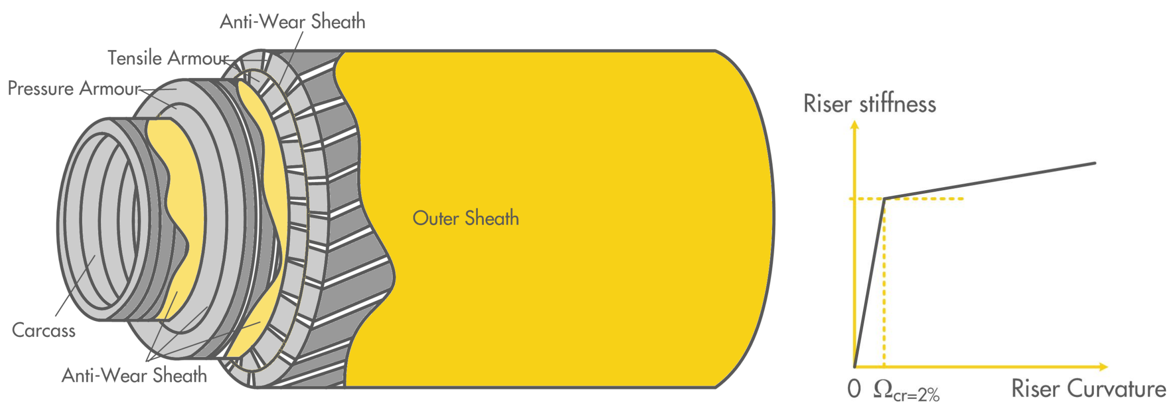

(a) Concentric layer composition (b) Bi-linear bending stiffness

Figure 1-3: Flexible Riser characteristics

As shown in figure 1-3a, steel layers are also present in the flexible riser. However, the steel layers are helically shaped and separated with plastic layers to confine fluids and gasses from the inner-bore and to prevent corrosive sea-water ingress. Load-sharing and slip between plastic and metallic layers introduce a bi-linear bending stiffness, see figure 1-3b. The initial riser stiffness can be compared to a rigid steel pipe and stress-strain response follows linear Euler Beam Theory.

The tensioned side of the riser is connected with the compressed side through the helix wire and wire-slip is induced after passing a critical curvature value Ω_{cr} as the material is pulled towards the outrados. Now the stiffness of the metal helix is no longer contributing to the global stiffness of the riser section and the flexible riser can be subjected to large curvature radii without yielding the metal wires. This characteristic is the reason that for North-Sea shallow water and harsh environmental conditions, flexible risers are essential to establish a safe connection between the subsea infrastructure and production facility.

1-2-2 Integrity Management

Integrity management is necessary to prevent riser failure caused by metal fatigue of tensile armour wires.

The initial riser design ensures a fatigue life larger than the planned service life of the flexible riser for the predicted environmental and operational conditions. Scheduled and continuous checks of relevant parameters will detect changes. A strategy is needed to first make a reliable judgement about the impact of these conditions on the fatigue life and secondly to take proper measures to guarantee a fatigue life larger than service life for the new situation.

Currently, the following steps usually characterize such situation:

1. Condition change is detected and first judgement is made about impact on fatigue life.
2. Specialist is involved. If advised, re-assessment of fatigue life is initiated.
3. Initial design conditions are used and new conditions are incorporated, usually with a negative impact on the fatigue life. Continued service or riser replacement is advised.
4. Specialist advice governs the final decision by Shell engineers.

Hesitance while judging the impact of changed conditions on the fatigue life is not desirable. Industry and especially operator's visions on integrity management activities are studied in chapter 2 and analysed in chapter 3.

1-2-3 Fatigue Analysis Methodology & Conservatism

Fatigue life is essentially defined as the number of cycles of stress or strain a structure or structural element can sustain before failure of the material occurs. In practice fatigue life often refers to the number of years for which safe operational conditions are ensured.

To ensure a fatigue life larger than the desired service life, the industry accepted fatigue analysis methodology is used. This is a three-step procedure:

1. Dynamic analysis to couple metocean conditions and riser motions. The fatigue critical zone/cross-section is detected for further analysis in the second step.
2. Quasi-static analysis to couple motions and stresses.
3. Fatigue life calculation transforms stresses to fatigue damage and includes additional safety.

Figure 1-4 shows a concise overview of the input data or source required for each process step, usually a calculation, and the output parameters subsequently used in the next step.

The accuracy of calculation methodology is a topic of discussion; this calculation is over-conservative. Checking the actual presence of cracks and other indicators of failure is challenging in operational conditions. New initiatives such as embedding strain sensing optical fibers or frequent wire inspection to identify wire break are promising developments in order to match calculations with the actual damage accumulating in the material throughout its service life.

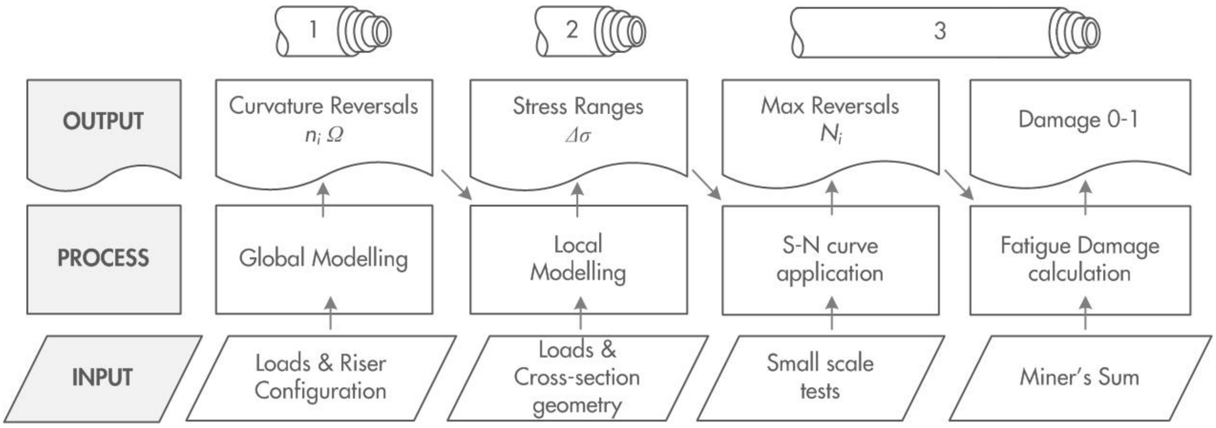

Figure 1-4: Overview of three-step fatigue analysis of flexible risers

Conservatism

Values that are highly variable or uncertain are generally overestimated to ensure safe margins between the actual capacity of a structural element and the engineering prediction. As a result, conservatism "builds up" in the calculation after each decision regarding input values; e.g. average load intensity, material deterioration, stochastic number of repetitions, changing utility rate, potential damage and so on. Secondly, the used software packages are never able to completely predict the mechanical responses hence conservatisms build up likewise in each step.

1-2-4 Local Modelling

This second fatigue analysis step couples motions (curvatures) and wire stress ranges and finds the fatigue critical helix element. For Shell this is currently the largest "black-box" hence their proposal was focused on development of an in-house local model.

All elements in the cross-section are individually modelled to determine their contributions to the riser axial, radial and bending stiffness.

Two assumptions can be made in the context of conservatism:

1. Local Models are completely able to model the response behaviour. What matters is the false input.
2. The methodology/algorithm is not correct; what matters is to revise the formulae and validate with experiments or operational data.

Under the first assumption, a local model can be used to study the influence of changed input parameters representing changed conditions. Does it matter that we were a bit wrong in the initial global analysis (curvature and tension levels), the planning of operational conditions (pressure) or the available friction between layers (friction coefficient and contact pressure)?

The second assumption questions the methodology and the model. Knowledge development and experimental or operational data generation are key to improve current algorithms of software models. Shell can play a role as they did in the past by initiating experiments but also by investing in new technologies able to extract response data from flexible risers during operation, something not possible in the past.

Both assumptions are worth studying, however this study will only focus on the first assumption, the local model (ABC Fatigue) is completely able to model the response behaviour.

1-3 Research Plan

The scope of present work focuses on integrity management of flexible riser systems currently operating in the North-Sea. An important method to ensure safe operation is the fatigue analysis methodology hence the second point of interest. Finally, the second step of this procedure is further investigated. These three research elements are hierarchical structured as shown in figure 1-2. This section elaborates on the research methods and report structure.

1-3-1 Methods

First a literature review was conducted to study the three main elements of present work: integrity management, fatigue analysis methodology & conservatism and local modelling.

Secondly, the impact of changed conditions on the fatigue analysis steps are analysed . This resulted in a guideline to support engineers responsible for taking adequate measures after sudden condition changes are detected in fatigue-critical flexible riser systems.

Thirdly, a local model was developed able to convert curvature ranges to stress ranges; main goal was to imitate state-of-art local model-techniques used by specialist companies and other industry players. The model algorithm and validation methodology are presented.

Finally, a benchmark case-study illustrates the purpose of an in-house pre-analysis and the usefulness of ABC Fatigue by analysing a typical flexible riser designed for North-Sea environmental conditions.

1-3-2 Report structure

- **Literature review**
  Chapter 2

  1. Industry vision on Integrity Management.
  2. Fatigue Analysis: Methodology & Conservatism.
  3. Local Modelling: Fundamental theory & industry development.

- **Analysis: Integrity Management, Fatigue Analysis and Local Modelling**
  Chapter 3

  1. Qualitative analysis of Integrity Management & Fatigue Analysis.
  2. Deliverable: New integrity management proposal (guideline).
  3. Deliverable: Fatigue Analysis steps and their relation to conservatism.

- **Model development: ABC Fatigue**
  Chapters 4 & 5

  1. Theory
  2. Algorithm steps.
  3. Model validation.
  4. Model capacity and limits.

- **Benchmark case-study**
  Chapter 6

  1. Research Questions and Methodology
  2. Background & Hypothesis based on literature
  3. Results: Impact of changed design conditions.

- **Conclusions & Recommendations**
  Chapter 7

  1. Deliverables and findings of present work.
  2. Recommended directions for Shell engineering focus.

Chapter 2

Literature Study

2-1 Integrity Management

From the early days ($\approx$ 1970—1992), fatigue life was based on the fatigue limit criterion; i.e. none of the occurring stress ranges were to exceed the given limit for non-welded, cold-formed, high yield stress steel used in a dry environment. For this type of steel the limit is $\approx$ 400-600 MPa. Cross-section reduction due to metallic wear between tensile armour layer ultimately caused to fail this criterion. Usually defined for 10^6 cycles for constant amplitude loading.

However, fatigue testing by Saevik showed the governing impact of fretting. The existence of this mechanism introduced the standardization of plastic anti-wear sheaths between the metallic layers, also eliminating the cross-section reduction due to wear.

The new fatigue limit, adopted from the mid-nineties, is based on the fatigue damage criterion. This new approach also takes into account non-dry conditions which is more likely to be present in the flexible riser annulus because of seawater ingress (outer sheath breach) and leakage of corrosive gasses from the inner-bore. These are demonstrated regularly during maintenance operations.

2-1-1 Corrosion fatigue

Corrosion of armour wires has been thoroughly studied for the last 10-15 years. Currently the assumed dry-annulus conditions are usually not present during the service-life of the riser. A couple of serious failures of flexible risers were caused by corrosion of armour wires which were found on risers with breaches in the top section near the splash zone or above sea level. Four risers failed with loss of containment (1 in Africa and 3 in the North Sea region) and at least 3 near misses were reported (2 in Norway and 1 in Africa). Also the influence of H2S has presumably caused failure of high strength steel wires in at least 7 flexible flowlines in the North Sea, West Africa and Arabian Gulf. All surprising failures as flowlines do not suffer from large dynamic motions hence the suspicion of governing deterioration from H2S.

The most important observation has been that all failed risers suffered from damaged outer sheaths hence the best way to avoid corrosion fatigue is to prevent breaches. As this is not a feasible target, a second important observation were cases of risers which survived long periods with breaches.

Unfortunately no clear correlations —only indicators such as breach location, type of damage and riser configuration— have been found explaining this difference. (4Subsea)

To date no corrosion failures have been reported from risers with intact annuli. Multiple risers were retrieved —e.g. a BP West-of-Shetland Gas Injection Riser replaced in 2008 (Charlesworth et al., 2011)— and dissected to complete the life-cycle showing no damage up to the expected level.

2-1-2 Operational data

Improvement of integrity management hence judgements of changed in-field conditions is an industry focus. In 2009, Oil and Gas UK decided to extend their information of riser failures to a worldwide pipe integrity database instead of focusing solely on the North-Sea. Statistics are now available showing damage and failure covering 130 field developments across the world (Obrien et al., 2011).

Manufactures of flexible risers highly recommend monitoring techniques able to deliver in-field data. Strain monitoring, by embedding strain sensing optical fibers, continuously measures strain rates in multiple wires around the circumference. The remaining fatigue life capacity is subsequently obtained from rainflow-counting the number of load cycles and strain amplitudes. At the end of a design life it is easy to evaluate life time extension options. Also this information can act as a solid basis to when unexpected conditions are encountered such as other bore conditions but also loads on the tensile armour wires. (Dahl et al., 2011)

Design specifications should be very specific and continuously evolve to account for unexpected mechanisms where application are used under new conditions. Verification of the riser system design assumptions is expected to evolve into monitoring the following:

- Metocean conditons (design input parameter)
- Vessel motions, especially heave and translational movement at tie-in location (design input parameter)
- Bend stiffener deflection for high risk applications (response parameter).
- Integrity of the annulus (design versus actual condition).

(Out, 2012)

2-2 Fatigue Analysis Methodology & Conservatism

Fatigue analysis is defined as research that encompasses global dynamic motions and local stress in the tensile armour wires. Existing methodologies lack the consistency and level of transparency that is required to independently demonstrate the level of safety and conservatism in new flexible riser designs. The Fatigue Analysis Methodology Guidelines were a major step into reaching industry accepted methodology. This document is the main deliverable from the Real Life Joint Industry Project, managed by MCS. Their approach generally starts with simpler conservative calculations that can be safely applied to a riser designed far below the fatigue critical limit. For fatigue critical designs, more accurate and comprehensive methods are advised. Paragraph 2-2-1 and 2-2-2 cite the most important steps and assumptions associated to global and local analyses (Smith and Grealish).

This industry accepted design verification philosophy was not enough to completely resolve the technology protection issue. Propriety of knowledge and models still characterizes the industry. Universally recognized API Spec 17J and API Spec 17B are continuously updated to commingle consensus on minimum requirements between operators, suppliers and regulators. Technology evolves; new materials and new design design scenarios (deep water) introduce new failure mechanisms (Loback et al., 2010).

2-2-1 Global Analysis

The key steps in the global analysis are as follows.

1. Collate the external environmental conditions for the fatigue loading.
2. Assemble a global structural analysis model of the flexible pipe system.
3. Simulate the global motions or load response of the flexible pipe system.
4. Collate the global responses for input to the local analysis stage.

The above steps should be subject to sensitivity and calibration checks in relation to the fatigue life of the flexible pipe. The last step involves the transposition from the global to local analysis and is listed here to convey continuity of the fatigue design procedure.

Pipe tension and measures of pipe bending —which may comprise of angular motions relative to an interface or components of bending curvature or moment— are required for local analysis of the armour wires:

The global load response is required at potential fatigue-critical locations where the pipe motion is comparatively high. Locations include the following:

1. Topside interface between the flexible pipe and Floating Production Unit.
2. Hog and sag bends of a wave riser configuration.
3. Seabed touchdown of a catenary riser.
4. Other locations merited by the design of the flexible pipe system.

(Smith and Grealish).

2-2-2 Local Analysis

The local fatigue analysis converts the global loading at selected hotspots to stress in the armour wires. The analysis requires a numerical model of the flexible pipe cross-section and an interface that is compatible with the global to local transposition procedures. The general requirements for LA models are outlined as follows:

1. Verified against full-scale measurements.
2. Capable of modelling tension and curvature ranges.
3. Preferably account for hysteresis effects, if not already addressed in the global or intermediate analysis.
4. Take into account the effects of external pressure.

5. Stresses to be calculated at the four corners of the rectangular shaped wires normally used for tensile armour.
6. Preferably output stresses at eight points around the circumference, so that directionality effects can be considered.

There are significant uncertainties in the selection of the friction coefficient to be used in the local analysis. This can be affected by issues such as temperature in annulus, wire/sheath surface condition (new versus aged), lubricant condition (whether lubricants applied in fabrication are still active), wire corrosion, annulus environment (wet or dry), variations between internal and external surface of wires.

Friction coefficients may be derived from small scale tests, though more typically they are derived from full scale tests. The results from full scale tests can be used to calibrate friction coefficients in local analysis models. Representative values of the friction coefficient vary between 0.1 and 0.2, although higher values can be applicable under adverse conditions. Due to the uncertainties associated with the friction coefficient it is recommended that an upper bound conservative value be applied. Use of a higher value of friction coefficient will always be conservative.

(Smith and Grealish)

2-2-3 Fatigue Life Calculation

Mean stress correction

The mean stress level σ_m is incorporated by correcting the stress range $\Delta\sigma$ to $\Delta\sigma^*$ with the Goodman, see 2-1, or Gerber relation.

$$\Delta\sigma_i^* = \frac{c_2}{1 + c_1 \cdot c_2} \tag{2-1}$$

$$c_1 = \frac{(1+R)}{2(1-R)\sigma_u} \tag{2-2}$$

$$c_2 = \frac{\Delta\sigma_i}{1 - (\frac{\bar{\sigma}_i}{\sigma_u})} \tag{2-3}$$

$$R = \frac{\sigma_{min}}{\sigma_{max}} \tag{2-4}$$

(Larsen et al., 2014)

S-N Curves

Small-scale experiments are carried out to construct the S-N curve typical for a single helix wire under the apparent load and environmental (annulus) conditions.

Basquins equation 2-5 is the log-log relationship constructed by obtaining constants a and m from small-scale experiments. With this relation, the number of allowable cycles can be derived from evaluated stress ranges without testing.

$$\log N_i = \log a - m \log (\Delta\sigma^*) \tag{2-5}$$

(Larsen et al., 2014)

Important characteristics are:

1. Variability of stress reversals to failure
    - Low variability for high stress ranges thus short lives
    - High variability for low stress ranges and long lives
2. Environment
    - Dry environment: infinite fatigue life for low stress ranges (knee in S-N curve).
    - Corrosive: all cycles count (no knee) and increased significance of frequency.

The right S-N curve should represent both the correct material and the predicted annulus conditions. Small-scale test conditions are generally split into two categories: fully reversed and pulsating tension. The first based on zero mean stress and constant amplitude tension-compression reversals, the second being pre-tensioned resulting in tension-tension reversals.

The tension-tension method is often used to simulate the friction-stress cycles. Combining the ever tensioned condition, caused by the self-weight induced tension and inner-bore pressure, and the friction stress reversals experienced axially by the individual wires. However, this method does not include local bending stress.

Another experimental method of cyclic bending reversals is required to simulate local bending stresses. This method is based on a pre-tensioned wire subjected to uni-axial lateral displacement reversals. Industry focus on this type of fatigue testing has increased, joint industry project funding is used to expand the variation of load and annulus conditions. (Fatemi)

The changed vision on annulus environment (corrosive instead of dry) particularly influences this calculation. An issue with long-term fatigue is that some S-N curves are generated over a few days, weeks or months were the some corrosion processes develop slowly. It is known from literature in other industry fields that surface irregularities can lower the fatigue life with as much as one order of magnitude (4Subsea).

Fatigue Damage

Fatigue damage is the quantity used to determine the service-life of a structure subjected to cyclic loads. Corresponding to all relevant load conditions i two parameters are used to calculate the fatigue damage:

- The number of reversals n obtained in the global dynamic analysis.
- The allowable cycles N derived in step 3.

The total damage accumulation per year is calculated with Miner's Sum, see equation 2-6.

$$\text{Fatigue Damage} = \sum_{i=1}^{N} \frac{n_i}{N_i(\Delta\sigma^*)} \tag{2-6}$$

Fatigue Life

The fatigue life (in years) is derived from the total fatigue damage, a number between 0 and 1, and a safety factor of minimal 10.

$$\text{Fatigue Life} = \frac{1}{\text{Fatigue Damage} \cdot (10 + \text{Additional Safety})} \tag{2-7}$$

If the fatigue life is more than the design life of the riser system, the outcome justifies a safe design. Whereas the calculation should be revised for situations where the fatigue life is shorter than the design life.

$$\text{Fatigue Life} > \text{Design Life} \tag{2-8}$$

(Larsen et al., 2014)

2-3 Local Modelling

This study focuses on local modelling: fundamental theories, theory development and state-of-art algorithms. This to understand and apply contemporary local modelling techniques for the development of the new in-house model ABC Fatigue.

The industry-accepted approach splits flexible riser stress-analysis into two independent calculations: Firstly an axisymmetric analysis (riser response to pressure and tension) and secondly a bending analysis (response to uni-axial bending). Several relations and theories have been developed and published separately hence considered likewise in present work.

Section 2-3-1 and section 2-3-2 sequentially present literature findings from different angles:

- Fundamental theory to explain the main characteristics of pressure, helix wires and global bending.
- Summary of theory development in the research area's of flexible risers and analogous structures.

2-3-1 Axisymmetric Analysis

Fundamental theory

A **parametric description of the helix wire** (Stewart, 2007) is required to couple the riser axis-system with the individual wire axis-system. Lancret's Theorem states that a curve is a helix when the ratio between curvature and torsion is a constant. As the tensile and pressure armour wires are modelled as helices, this theorem relates the longitudinal riser axis to the local helix position as well as the initial curvature of the helix wires.

The theory of a **thin-walled pressure vessel** (Hibbeler, 2013) can predict the radial and axial deformation of a single-layer thin-walled cylinder subjected to internal pressure, external pressure and axial tension. This theory is used to predict the equilibrium state after pressurizing and tensioning all composite layers of the flexible riser.

Theory development

First modelling of steel helix wires under axial loading was developed for cables, wire ropes and curved rods. Initially, only rigid core models were used, later enhanced with compliant cores proportional to an empirical factor (Oliveira et al., 1985).

Flexible riser theory development was initiated following the same fundamentals and introduced the helix wires around a compliant core based on a measurable factor (Goto et al., 1987). Simultaneously, studies emerged treating radial deformation as an independent factor based on material and geometry parameters: equilibrium and continuity relations of all layers were now modelled as individual elements with orthotropic stiffness (Feret and Bournazel, 1987). Also, a Finite Element based method was developed with combined stiffness matrices for thin-walled tubes (plastic pipe) and bonded and non-bonded helical layers (metal helix) (Lotveit and Often, 1990). A fourth method focused on constitutive relations for thick-walled cylinders (plastic pipe) and three dimensional curved beams (metal helix) (Witz and Tan, 1992).

To summarize, four different approaches have been developed to predict the axisymmetric behaviour of flexible risers. The biggest challenge for all of them was to relate radial deformation to pressure and axial tension. Due to inaccurate measurement results, the first approach by Goto et al. was rejected. The final three approaches were based on the same key feature: radial deformation is an unknown variable. Despite their fundamental differences, responses of these three approaches converged to similar outcomes and were (and still are) all able to produce satisfying wire stresses, interlayer contact pressures and gap formation (Witz, 1995), (Larsen et al., 2014).

2-3-2 Bending Analysis

Fundamental Theory

Quasi-static bending of beams considers a slender structure with constant cross section subjected to lateral loading not changing over time. Initially, the flexible riser responds according to a perfect elastic-plastic material characteristic; i.e. linear stress-strain responses in the strength governing elements. **Euler-Bernoulli Beam Theory** describes a perfect distribution of load according to the position of this element (tensile armour wire) with respect to the neutral bending axis (Hibbeler, 2013). Hereafter, slip is initiated hence releasing the load increment.

Theory Development

The assumption of proportionality between axial forces and wire sliding-distance was firstly applied on a marine cable bent over a drum subjected to axial loads (Luchansky, 1969).

The sliding criterion based on interlayer friction was first introduced for helically reinforced cables by Lanteigne (1985). The assumption of in-line layers was a major shortcoming of his work. Knapp (1987), leading investigator of reinforced cables, introduced frictionless slipping to study bending of the wire about its own axis and accumulated shear due to torsion. Circular wires were assumed, this was a major deviation from the rectangular wires used in flexible risers. In a second study by Knapp, friction prevents all movement and the assumption of plane sections remain plane was introduced resulting in a simple analysis of wire-strain and the deformed helical path. A useful insight for flexible riser modelling. From the early nineties, research steered towards a different mathematical model and diffraction from cables research.

Various researchers —all dedicated to local modelling of flexible risers— were keen to find the governing wire-deformation and wire-displacement as a response to global riser bending. Their ultimate goal was to formulate a reliable general model for the prediction of wire stress.

Curved rods subjected to axial, banding and torsional loading including linear (Leclair and Costello, 1987) or non-linear (Out, 1989) constitutive relations were studied. Also the first general model for wire-stress and wire-slip prediction was proposed assuming constant riser curvature and geodesic slip direction (Feret and Bournazel, 1987). This model was enhanced numerous times (Feret and Momplot, 1991), (McIver, 1992), (Witz and Tan, 1992). A generic summary of all previous work was presented by Berge and Olufsen (1992). This work states that all the commingled generic formulae can be used for design purposes but with caution and preferably cross-verified with multiple models.

Further theory development introduced layer interaction (Feret and Leroy, 1995), changed layer interactions due to anti-wear layers (Out and von Morgen, 1997), a new model with coupled movements and stresses of helical layers (Leroy and Estrier, 2001) and stress range diversion due to hysteresis (Leroy et al., 2010).

Generic models for flexible pipes —i.e. umbilicals and risers— were developed in-house by flexible pipe manufacturers NOV (Flexpipe), Technip (Life6)(Leroy et al., 2010) and Wellstream (no name). But also by specialist consultants 4Subsea (no name) and MCS Kenny (Layercom) and by regulators DNV (Helica) (Skeie et al., 2012) and research institutes Marintek (BFLEX) and the University of Rio De Janeiro (no name) (Vargas-Londono et al., 2014). The latter being a new player in flexible riser analysis considering deep-water flexible risers subjected to small curvature values and large tension values.

A second generic handbook was made possible through the Joint Industry Project: Safe and Cost Effective Operation of Flexible Pipes, 2011-2013 (Larsen et al., 2014) commingling state-of-art theories.

Chapter 3

Conservatism Indicators and Engineering Guideline

Three types of fatigue analysis are distinguished for further analysis:

1. New design - All variables can be changed iteratively until fatigue life criterion is met.
2. Sudden operational hazard - Monitoring and Inspection detected a significant condition change and measures are required to keep risk within acceptable limits.
3. Life time extension - Service life is altered and thorough check of operational conditions is required to ensure sufficient fatigue life.

Focus of present work is on sudden operational hazards and life time extensions. Both events require a fatigue life re-assessment within the limits of the initial design.

After identification of a changed condition a quick decision on a safe but cost-effective approach (definition of integrity management present work) is required. In this chapter, the fatigue analysis methodology steps are analysed to identify assumptions which alter the level of conservatism. Furthermore, two hazardous scenario's and their impact on fatigue life are illustrated. A new approach is advised to support in-field flexible risers currently operated in the North-Sea region.

3-1 Fatigue Assessment Analysis: Conservatism Indicators

Table 3-2 presents an overview of all conservatism indicators used in the three-step fatigue analysis. To define these critical elements, literature on current methodology and local analysis techniques was studied in a literature review. The local analysis has been deeply investigated hence analysis elements are more detailed.

It is expected that simple model techniques result in conservative analysis results: i.e. elaborate techniques can potentially solve an event of insufficient fatigue life.

Two events are likely to happen within the service life of the riser: outer sheath breach and gas diffusion from the inner bore (literature review 2). Both resulting in a major change of the initial conditions hence quick and adequate measures by the operator are evident after detection. For both hazards table 3-1 presents (from left to right): a description of the condition change, the impact on the re-assessment of fatigue life and conservatism indicator corresponding to table 3-2.

Table 3-1: Two common scenario's: conditions and corresponding conservatism indicator jeopardising fatigue life after re-assessment

Detected event (Hazard)	Changed condition	Impact on Fatigue Life	No.
Outer sheath breach	Non-dry annulus	**Corrosion fatigue S-N curve**	27
(Seawater in annulus)	Self-weight increases	Changed dynamic behaviour	5-8
	Interlayer contact pressure	Changed friction conditons	19-22
	Increased uncertainty	Additional safety factor	31
Diffusion from inner bore	Sour-service (H2S + H2O)	**Corrosion fatigue S-N curve**	27
(H2S/H2O in annulus)	Increased uncertainty	Additional safety factor	31

Fatigue life reduction is a certainty after the introduction of corrosion fatigue. Whether the other changed conditions have a positive or negative effect in this context is case dependent and should be investigated likewise.

Life-time extension re-assessments are preferably carried out in accordance with updated operational and inspection data. If no major changes are present compared to the design condition (proven with up to data from monitoring and inspection activities), the service life can be stretched to its new value.

A case-study is presented in chapter 6 to show the impact of variable load parameters on the stress-range experienced by the local wires. A 6" production riser recently re-assessed by a specialist consultant was used for benchmark load and geometry parameters (Kenny).

3-2 Advice: Engineering Guideline

Currently, Shell's actions after detection of a sudden hazard heavily rely on the advice given by specialist consultants. Their advice and expertise are essential however the following initial actions are advised to change the collaboration environment.

1. Collate and neatly store design conditions - i.e. all input values and model assumptions which were used for the initial fatigue analysis prior to riser installation.
2. Rate all conservatism indicators with "simple" or "elaborate" (table 3-2)to determine the extensiveness of the initial fatigue analysis.
3. Determine the current and desirable quality of load data obtained from monitoring and inspection activities. Collate and have them readily available in case a re-assessment is triggered.
4. Pro-actively analyse high-risk riser systems and strive for optimal input through monitoring, inspections and data management.

In case of a sudden hazard, fatigue life can be enhanced by implementing actual conditions instead of initial predictions (loads) and by elaborating the model (formats and responses) where possible. Pre-analyses and model runs can be done in-house, a verified model combined with recent operational data can quantify the impact of changed input data. Subsequent collaboration with specialist consultant is advised. ABC Fatigue's suitability for in-house pre-analyses is analysed in chapter 5 trough model cross-validation and verification.

Table 3-2: Overview of Analysis Elements in the Global Analysis (1-11), Local Analysis (12-24) and Fatigue Life calculation (25-31).

Fatigue Analysis Step	Conservatism Indicator	Simple	Elaborate	No.
Loads	Critical sections: end/sag-bend/touchdown	No difference from catenary	Special treatment (mesh/non-linearities)	1
	Wave Loadings	Regular	Irregular	2
	Directionality incoming waves	unidirectional	multidirectional	3
	Operational conditions	Averaged over lifetime	Variable	4
Responses	Frequency responses	wave-riser	wave-FPU-riser	5
	Damping	no damping	with damping	6
	Moment-curvature response	linear	non-linear	7
	Hysteresis	no	yes	8
Transposition	Format	Histogram	Full timetrace	9
	Directionality	2D	3D	10
	Tension/Curvature responses	independent	correlated	11
Model	Model verification	Full-scale measurements	Model cross-validation	12
	Cross-section model	Helical layers only	All layers	13
Loads	Variable loads	Curvature	Curvature/Tension	14
	Variable load format	Ranges	Time-domain	15
	Directionality	Dominant bending direction only	Mean bending direction	16
	Constant loads	Internal pressure only	Internal + External pressure	17
	Input parameters	Averaged for life time	Variable	18
Responses	Stress accumulation	Friction only	Friction and Local bending	19
	Circumferential wire stress	Averaged	Variations	20
	Maximum stress location	Outer fiber	Monitoring all wires	21
	Wire slip	No	Yes	22
	Lateral contacts	No	Yes	23
	Stress range measurement	After one cycle	After 10 cycles	24
Mean stress correction	Relation	Goodman (linear)	Gerber (non-linear)	25
	R-value	standard tension-tension	incorporate bending	26
S-N curve	Annulus environment	Dry	Corrosive	27
	Small scale test method	tension-tension (R=0.1-0.5)	tension-tension + uni-axial bending	28
	Design curve	margin of 2 standard deviations	case-specific margin	29
Fatigue Damage	Miner's sum	Single load-case	Multiple load-cases	30
Risk assessment	Safety factors	10 + large safety margin	10 + additional risk assessment	31

Chapter 4

ABC Fatigue: From Fundamental Theory to Algorithm

This chapter elaborates on a new analytical software model developed to study the major sources of conservatism in local fatigue analysis: ABC Fatigue. Through this model a local fatigue analysis can be carried out studying a section along the flexible catenary. In practice, this small riser section is showing the highest average stress levels in the global dynamic analysis, this model-part of the fatigue analysis not within the scope of present work.

ABC refers to a composition of three local fatigue analysis elements:

Axisymmetric Analysis (Model A)
Bending Analysis (Model B)
Cyclic Analysis (Model C)

By combining Models A and B, stress dependence is signified by circumferential location only. Secondly, a "time-dependent" analysis is possible by combining Models A and C. Now response values are dependent on both "time" and circumferential location.

First, section 4-1 explains the purpose and interdependence of the three models. Secondly, sections 4-2 to 4-4 elaborate on the response behaviour, fundamental theories and algorithms behind Model A, Model B and Model C. The purpose and structure of these three paragraphs is defined as follows:

Paragraph 1: Fundamental Theory - References

- Exact assumptions and limitations described in general theory.
- All formulae used as a basis for the algorithm are stated in original composition but with parameter naming corresponding to present work.

Paragraph 2: Response behaviour - Interpretation of theory

- Explains geometry, loads and responses by introducing parameters and corresponding figures.
- Describes the complete response behaviour, regardless the ability to model it.

Paragraph 3: Algorithm - Application of theory and development of new model

- List of algorithm steps.
- Paragraphs elaborating on all steps including justification of the enhanced formulae and assumptions.
- Model response predictions based on formulae.

A complete overview of the geometry, load and response parameters required to run ABC Fatigue and their relation with Models A, B or C are listed in appendix A.The validated algorithms of Model A and B are presented in B. Model C is not validated but used for indicative study only. This algorithm is presented in appendix D.

4-1 Introduction to ABC Fatigue

The general function of a software model is to imitate the mechanical behaviour of a structure under imposed loading in order to predict stress levels hence capacity and life-time of a (steel) structure. Local fatigue analysis of flexible risers, scope of present work, focuses on predicting the armour wire stress-levels as these wires are signifying the riser strength. Assuming contemporary global analyses are capable of relating wave loads and riser motions and local models correctly match the global output curvatures to local wire stress responses, two aspects still compromise the accuracy of this calculation:

1. Input parameters are not correct: design conditions deviate from actual in-field measurements.
2. The methodology and/or algorithm is not correct.

ABC Fatigue should be capable to run a reasonably accurate local fatigue analysis with a main purpose to study parameter impact on wire-stress for pre-analysis and feed studies. Modelling the influence of hysteresis and irregular waves is desired. Furthermore, ABC Fatigue is based on analytical formulae, a preferred feature to search for linkages between load and response parameters for different riser cross-sections and load-cases.

Model A and B assess multiple wire-locations around the circumference and along the helix wire assuming constant loading characteristics, i.e. constant axisymmetric loading and constant curvature.

Hysteresis is incorporated in Model C; extending the algorithm of Model B by including periodic curvature to simulate regular and irregular wave patterns. This study is signified by diligent tracking of wire positions and superposing the responses from curvature cycles.

Figure 4-1 shows the main elements and input parameters of ABC Fatigue. Paragraph 4-2 to 4-4 will elaborate on each individual part.

MATLAB by Mathworks is used for all response behaviour simulations by running the mathematical relations as presented in appendix A.

4-2 Model A: Axisymmetric Analysis

4-2-1 Fundamental Theory

The general model presented by Feret and Bournazel (1987) is incorporated in most analytical models to determine axisymmetric responses. For design purposes, analytical software models are preferred

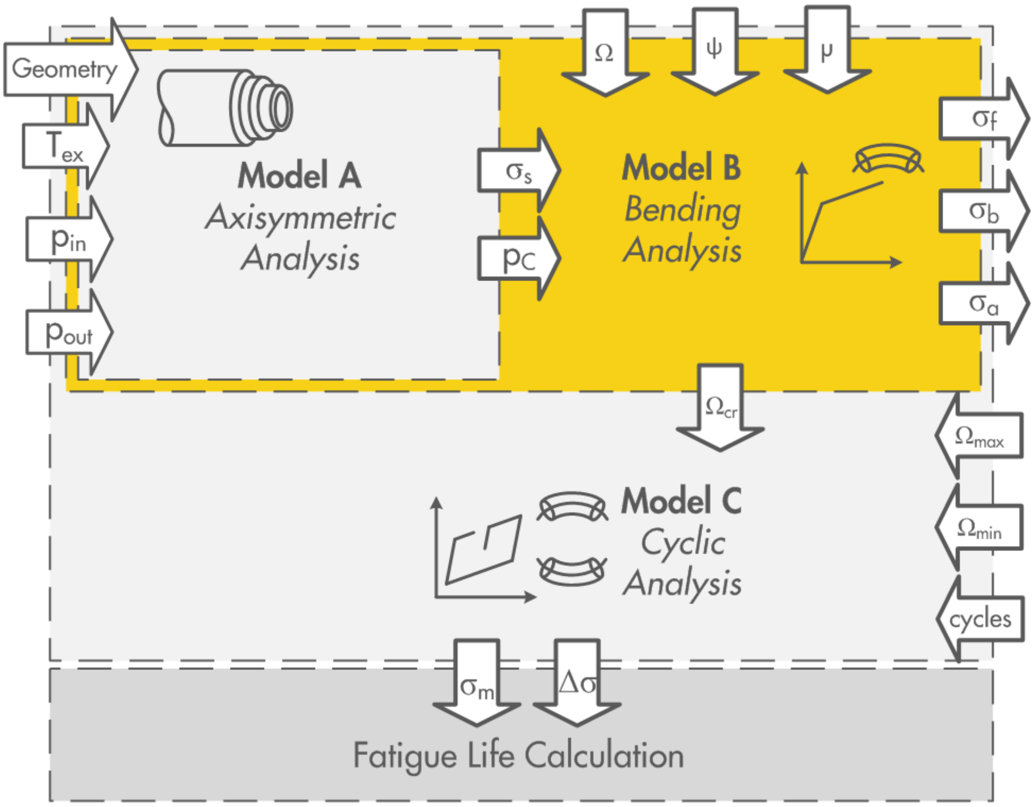

Figure 4-1: ABC Fatigue: Local Fatigue Analysis

over Finite Element software models due to their ability to incorporate various assumptions considering the layered structure of the composite riser as well as their computation time benefit (Larsen et al., 2014).

The **general method** to describe the mechanical behaviour of a composite flexible pipe consisting of N helical and N′ plastic layers is based on the following assumptions and altogether resulting in a system of 6N+6N′ + 2 equations.

1. Continuity of the radii
2. Continuity of the contact pressures
3. Equilibrium of the axial forces

A **simplified approach** only considers the participation of N helical armour layers and the following assumptions:

1. Participation of plastic sheath is negligible $N' = 0$.
2. Constant material and geometry parameters; symmetric cross-section.
3. Initial stress-free, helically curved wires.
4. No initial interlayer contact pressure.
5. Geometrical deformations $\Delta L, \Delta a$ and $\Delta\theta$ are small.
6. All layers remain in contact.

The three equations of equilibrium between stresses and axial forces 4-1, radial forces 4-2 and moment (torsion) 4-3 defined as follows:

$$\sum_{i=1}^{N} n_i \sigma_i A_i \cos\alpha_i = T_{ex} + \pi p_{in}^2 a_{in}^2 - \pi p_{out} a_{out}^2 = F_0 \tag{4-1}$$

$$\sum_{i=1}^{N} \frac{n_i \sigma_i A_i \sin\alpha_i \tan\alpha_i}{2\pi a_i} = p_{in} a_{in} - p_{out} a_{out} = p_0 \tag{4-2}$$

$$\sum_{i=1}^{N} n_i \sigma_i A_i \sin\alpha_i a_i = M \tag{4-3}$$

The continuum equations to link pipe deformations and axial stresses in the armour wires:

$$\frac{\sigma_i}{E_i} = \cos^2\alpha_i \frac{\Delta L}{L} + \sin^2\alpha_i \frac{\Delta a}{a_i} + a_i \sin\alpha_i \cos\alpha_i \frac{\Delta\theta}{L} \tag{4-4}$$

$$p_i = \frac{n_i \sigma_i A_i \sin\alpha_i \tan\alpha_i}{2\pi a_i^2} \tag{4-5}$$

Equation 4-2 then being equivalent to

$$\sum p_i a_i = p_0 \tag{4-6}$$

Resulting in a mean contact pressure $p_{C,i}$ between each layer by the recurrent formula

$$p_{C,i+1} = p_{C,i} - p_i \tag{4-7}$$

Linking operational pressures by $p_{C,1} = p_{in}$ and $p_{C,N+1} = p_{out}$.

(Feret and Bournazel, 1987).

4-2-2 Response behaviour

The imposed loads in this analysis are internal pressure p_{in}, external pressure p_{out} and external tension T_{ex}. The expected physical behaviour of the flexible riser in this axisymmetric analysis is signified by:

1. Stress in the metallic armour wires σ_i for N helical layers i.
2. Contact pressures $p_{C,i}$ and $p_{C,i+1}$ pressing inside and outside of layers i.
3. Symmetric deformation of the riser cross section: elongation ΔL, expansion Δa and torsion $\Delta\theta$.

The load is shared among the N metallic layers according to wire laying angle and helix radius. A process of load transmission, based on the stress-strain constitutive relation for linear materials, introduces contact pressure transmission trough the armour layers. The model response is based on finding the radial, circumferential and longitudinal equilibrium and to define the load distribution among each metallic layer. The correct calculation of stress in the wires in this axisymmetric analysis is mainly challenged by the helical shape of the armour layers and the composite character of the flexible riser.

The main geometry parameters used for subsequent evaluations are depicted in figure 4-2. The load and response parameters used in the Axisymmetric Analysis, or Model A of the ABC Fatigue model, are shown in figure 4-3. All geometry, load and response parameters used in Model A are summarized in appendix A.

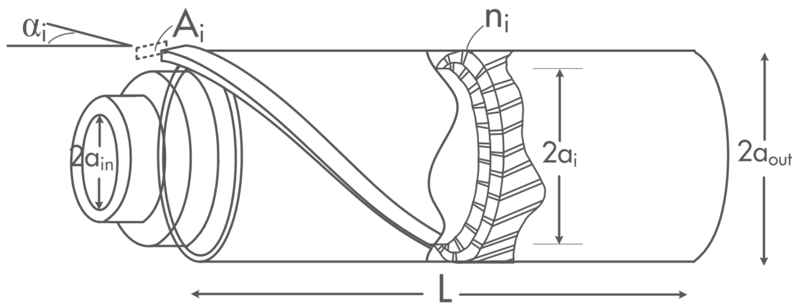

Figure 4-2: Axisymmetric Analysis - Geometry parameters

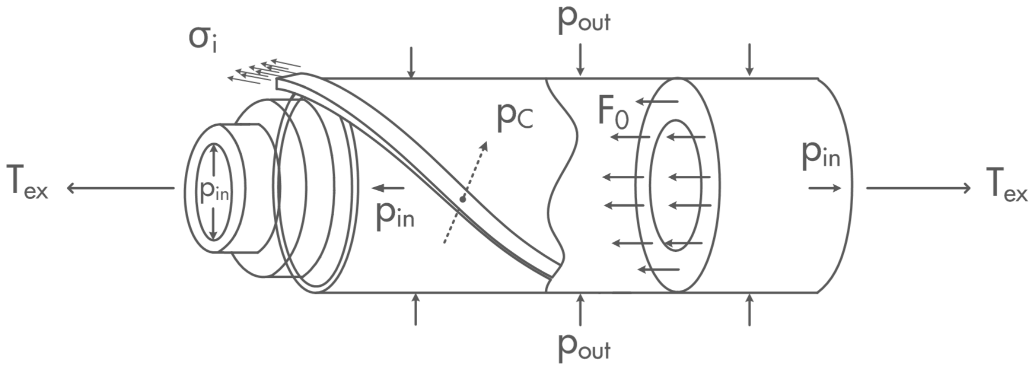

Figure 4-3: Axisymmetric Analysis - Load and Response parameters

4-2-3 Model A Algorithm

The approach by Feret and Bournazel (1987) still holds as the basis for most contemporary axisymmetric analyses. Parameters, relations and assumptions proposed in this theory are also the fundamental basis of Part A. The influence of torsion $\Delta\theta$ is assumed to be negligible and is not taken into account.

Methodology

The algorithm of Model A can be summarized as follows:

1. An initial expansion Δa_0 and elongation ΔL_0 are assumed to simulate a constitutive response.
2. The wire-stress in each layer i as a response to the imposed deformation is calculated and the approximate values for wall tension $\sum F_{ap,i}$ and total pressure differential $\sum p_{ap,i}$ are derived from wire-stresses.
3. The total wall tension F_t and total pressure differential p_t are calculated from the initial load conditions.
4. Through an iterative approach the correct deformation, hence equilibrium, is determined by checking $F_t = F_{ap}$ and $p_t = p_{ap}$ after each iteration cycle.
5. The final wire stresses are subsequently used to calculate the pressure differential p_i through each layer from the inner bore to the outer layer. Finally, the layer pressure differentials are

subtracted from the inner-bore pressure p_{in} to calculate the net contact pressures $p_{C,i}$ between each concentric layer.

Wire stresses and contact pressures are subsequently used for Models B and C described in sections 4-4 and 4-4.

Step 1: Deformation simulation

An initial elongation ΔL_0 and expansion Δa_0 are assumed to simulate a constitutive response.

$$\begin{aligned} L &= L + \Delta L \\ a_i &= a_i + \Delta a \end{aligned}$$

Step 2: Constitutive wire-stress reaction

Wire-stresses are derived by using predictied initial deformations ΔL_0 and Δa_0 in equation 4-8. Wire-stresses are subsequently used to approximate the value for wall tension, see equation 4-9, and total pressure differential, see equation 4-10.

$$\sigma_i = E_i \cdot \left(\cos^2 \alpha_i \frac{\Delta L}{L} + \sin^2 \alpha_i \frac{\Delta a}{a_i} \right) \tag{4-8}$$

Wall tension

$$F_{ap} = \sum_{i=1}^{N} n_i A_i \cos \alpha_i \cdot \sigma_i \tag{4-9}$$

Rewritten

$$F_{ap} = \sum_{i=1}^{N} \frac{n_i A_i \cos \alpha_i E_i \cos^2 \alpha_i}{L} \cdot \Delta L + \sum_{i=1}^{N} \frac{n_i A_i \cos \alpha_i E_i \sin^2 \alpha_i}{a_i} \cdot \Delta a$$

Total Pressure differential

$$p_{ap} = \sum_{i=1}^{N} \frac{n_i A_i \sin \alpha_i \tan \alpha_i}{2\pi a_i} \cdot \sigma_i \tag{4-10}$$

Rewritten

$$p_{ap} = \sum_{i=1}^{N} \frac{n_i A_i \sin \alpha_i \tan \alpha_i E_i \cos^2 \alpha_i}{2\pi a_i L} \cdot \Delta L + \sum_{i=1}^{N} \frac{n_i A_i \sin \alpha_i \tan \alpha_i E_i \sin^2 \alpha_i}{2\pi a_i^2} \cdot \Delta a$$

Step 3: General load-response condition

Total wall tension, equation 4-11, and total pressure differential, equation 4-12, are calculated from the initial load conditions.

$$F_t = T_{ex} + \pi p_{in}(a_{in} + \Delta a)^2 - \pi p_{out}(a_{out} + \Delta a)^2 \tag{4-11}$$

$$p_t = p_{in}(a_{in} - \Delta a) - p_{out}(a_{out} - \Delta a) \tag{4-12}$$

Step 4: Equilibrium iteration using Newton-Raphson

The riser cross-section will elongate and contract from tensioning and external pressure. Inner bore pressure is a counteracting mechanism and both expands and shortens the riser. The elongation and expansion corresponding to the equilibrium state are derived by solving this 2-dimensional, non-linear system of equations using Newton-Raphson method. In general, this method is used to successively find better approximations for the zero value of a function $f(x)$ by using equation 4-13.

$$x_{n+1} = x_n + \frac{f(x_n)}{f'(x_n)} \tag{4-13}$$

For a linear equation, this method uses 1 iteration to find the correct value for x. The real strength of this method becomes apparent when solving non-linear equations and systems of non-linear equations.

Equations 4-15 and 4-18, non-linear and dependent on the deformation variables ΔL and Δa, are approximated by using the Newton Raphson method. For a system f of 2 non-linear equations vector and matrix denotations are required as follows:

$$f\begin{bmatrix} x \\ y \end{bmatrix} = \begin{bmatrix} f_1(x,y) \\ f_2(x,y) \end{bmatrix}$$

the derivative is replaced by the Jacobian matrix J, see equation 4-14.

$$\boldsymbol{F_{n+1}} = \boldsymbol{F_n} - \boldsymbol{F_n} \times \boldsymbol{J^{-1}} \tag{4-14}$$

or

$$\begin{bmatrix} x_{n+1} \\ y_{n+1} \end{bmatrix} = \begin{bmatrix} x_n \\ y_n \end{bmatrix} - \begin{bmatrix} x_n \\ y_n \end{bmatrix} \times \begin{bmatrix} f_1'^x & f_1'^y \\ f_2'^x & f_2'^y \end{bmatrix}^{-1}_{(x_n,y_n)}$$

The first function $f_1(\Delta L, \Delta a)$ defines the wall tension equilibrium as shown in equation 4-11. Derivatives are taken with respsect to ΔL, see equation 4-16, and Δa see equation 4-17.

$$f_1(\Delta L, \Delta a) = F_{ap} - F_t \tag{4-15}$$

$$f_1 = \sum_{i=1}^{N} \frac{n_i A_i \cos\alpha_i E_i \cos^2\alpha_i}{L} \cdot \Delta L + \sum_{i=1}^{N} \frac{n_i A_i \cos\alpha_i E_i \sin^2\alpha_i}{a_i} \cdot \Delta a$$
$$-T_{ex} - \pi p_{in}(a_{in} + \Delta a)^2 + \pi p_{out}(a_{out} + \Delta a)^2$$

$$f_1'^{\Delta L} = \sum_{i=1}^{N} \frac{n_i A_i \cos\alpha_i E_i \cos^2\alpha_i}{L} \tag{4-16}$$

$$f_1'^{\Delta a} = \sum_{i=1}^{N} \frac{n_i A_i \cos\alpha_i E_i \sin^2\alpha_i}{a_i} - 2\pi(p_{in} - p_{out}) - 2(p_{in} - p_{out})\Delta a \tag{4-17}$$

Similar procedure is used to find the pressure differential equilibrium and the two derivatives. See equations 4-18 to 4-20.

$$
\begin{aligned}
f_2(\Delta L, \Delta a) &= p_{ap} - p_t && (4\text{-}18)\\
f_2 &= \sum_{i=1}^{N} \frac{n_i A_i \sin\alpha_i \tan\alpha_i E_i \cos^2\alpha_i}{2\pi a_i L} \cdot \Delta L + \sum_{i=1}^{N} \frac{n_i A_i \sin\alpha_i \tan\alpha_i E_i \sin^2\alpha_i}{2\pi a_i^2} \cdot \Delta a \\
&\quad - p_{in} a_{in} + p_{out} a_{out} - p_{in} + p_{out} \\
f_2'^{\Delta L} &= \sum_{i=1}^{N} \frac{n_i A_i \sin\alpha_i \tan\alpha_i E_i \cos^2\alpha_i}{2\pi a_i L} && (4\text{-}19)\\
f_2'^{\Delta a} &= \sum_{i=1}^{N} \frac{n_i A_i \sin\alpha_i \tan\alpha_i E_i \sin^2\alpha_i}{2\pi a_i^2} - p_{in} + p_{out} && (4\text{-}20)
\end{aligned}
$$

Now equation 4-14 is applied to find $\boldsymbol{F_{n+1}}$.
Where **F** is:

$$
\begin{bmatrix} f_1(\Delta L, \Delta a) \\ f_2(\Delta L, \Delta a) \end{bmatrix}
$$

And **J** is:

$$
\begin{bmatrix} f_1'(\Delta L, \Delta a)^{\Delta L} & f_1'(\Delta L, \Delta a)^{\Delta a} \\ f_2'(\Delta L, \Delta a)^{\Delta L} & f_2'(\Delta L, \Delta a)^{\Delta a} \end{bmatrix}
$$

A satisfactory approximation is found when subsequent iteration cycles converge to a single value, i.e. the error approaches zero.

Step 5: Post-processing

The final wire stress is used to calculate the layer pressure differential through equation 4-21.

$$
p_i = \frac{n_i \sigma_i A_i \sin\alpha_i \tan\alpha_i}{2\pi a_i} \qquad (4\text{-}21)
$$

The interlayer contact pressure, used as input value for Model B, is obtained by the recurrent formula 4-22 and $i = 1..N$.

$$
\begin{aligned}
p_{C,i+1} &= p_{C,i} - p_i && (4\text{-}22)\\
p_{C,1} &= p_{in} \\
p_{C,N+1} &= p_{out}
\end{aligned}
$$

4-3 Model B: Bending Analysis

For axisymmetric loads, analytical stress calculations are highly accurate. For a-symmetric deformation, or bending, a tenuous and non-linear stiffness characteristic compromises the stress-response calculation. Hence, bending analysis did not converge to a general analytical model as presented for axisymmetric analysis by Feret and Bournazel.

However, an acceptable approach has been developed. This method is based on the friction induced axial shear stress and local bending of the individual wire induced by riser curvature. To evaluate both responses, the riser section is viewed from the global (cross-section) perspective and the local wire perspective.

4-3-1 Fundamental Theory

The response behaviour as described in Larsen et al. (2014) is generally accepted but formulations to accurately describe and interpret stress and wire slip are not totally converged. The comparison of different theories is compromised by deviating axis systems and sign conventions, slip direction assumptions and tenuous descriptions of the stick-slip behaviour.

Generally accepted assumptions used in the generic theory (Larsen et al., 2014) are as follows:

1. A constant curvature Ω_2 is applied to a local section with length L; local section is bent into a torus.
2. No end effects; i.e. model of section along the riser catenary away from end-terminations.
3. Stress level of helically wrapped wires is zero without the influence of global curvature.
4. For stick conditions, the condition 'plane sections remain plane' ensures a constant stress-change of tensioned and compressed bounds according to Euler-Bernoulli beam theory.
5. Material friction characteristics defined by μ are equal for all layers.

All formulations required to determine relevant values regarding wire geometry and bending stresses are now summarized and subsequently used to construct the algorithm presented in section 4-3-3. Figure 4-4 illustrates all load and response characteristics of both the global and local axis system.

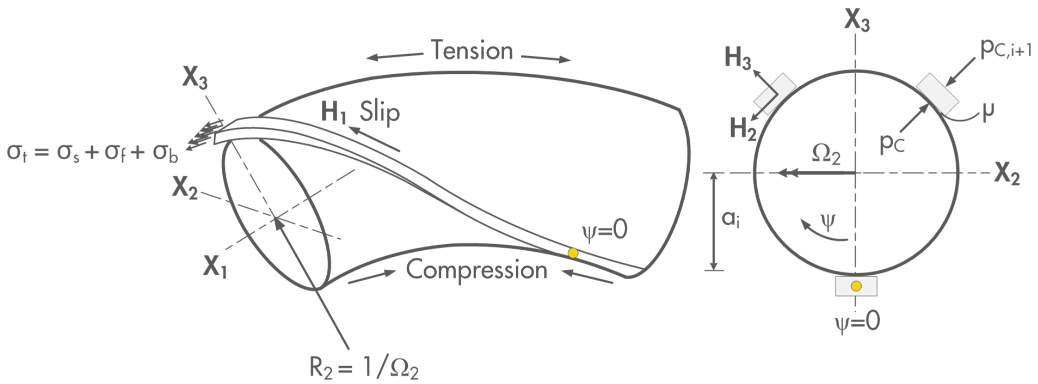

Figure 4-4: Bending Analysis - Wire geometry and local curvatures

Friction Stress

An axial shear force emerges prior to wire slip given by equation 4-23

$$Q_1 = -EA\cos^2\alpha a\cos\psi\cdot\Omega \tag{4-23}$$

The associated shear force per unit length which fulfils the rigid pipe condition (plane surfaces remain plane) is obtained by applying equation 4-24 and differentiating 4-23 with respect to the length coordinate H_1.

$$\psi = \frac{\sin\alpha}{a}\cdot H_1 \tag{4-24}$$

As a result equation 4-25 is derived where the maximum shear stress is found at $\psi = 90°$ i.e. the neutral axis of global bending. This force increases until the maximum possible shear has been reached: i.e. the available friction as formulated in equation 4-26 where q_3 is defined as the lateral line load imposed by adjacent layers on a single helix wire.

$$q_1 = EA\cos^2\alpha\sin\alpha\sin\psi\cdot\Omega \tag{4-25}$$

$$q_{1,f} = \mu(q_3^i + q_3^{i+1}) \tag{4-26}$$

The critical global curvature results from the equilibrium situation where $q_1 = q_{1,f}$ formulated in equation 4-27.

$$\Omega_{cr} = \frac{\mu(q_3^i + q_3^{i+1})}{EA\cos^2\alpha\sin\alpha} \tag{4-27}$$

From this, the maximum shear stress on the outer fibers is derived, either with a positive sign on the outrados ($\psi = \frac{\pi}{2}$) or negative sign on the intrados ($\psi = -\frac{\pi}{2}$), see equation 4-28.

$$\sigma_{f,max} = +/-\frac{\mu(q_3^i + q_3^{i+1})a}{\sin\alpha A}\psi \tag{4-28}$$

Local Bending stress

Wires are cold formed and thus stress free for zero curvature Ω. Local curvature of wires in stick condition is defined by equations 4-29 to 4-31 for all three orthogonal directions H_1, H_2 and H_3 of the local helix system.

$$\omega_1 = \sin\alpha\cos\alpha^3\cos\psi\cdot\Omega \tag{4-29}$$

$$\omega_2 = -\cos^4\alpha\cos\psi\cdot\Omega \tag{4-30}$$

$$\omega_3 = (1+\sin^2\alpha)\cos\alpha\sin\psi\cdot\Omega \tag{4-31}$$

According to Larsen et al. (2014), wire slip changes the curvature formulation around the H_2 axis, often referred to as weak axis as the wire thickness is always small compared to the wire width, into equation 4-32. However, Skeie et al. (2012) does not include this change and holds on to equation 4-30 for all conditions.

$$\omega_{2,slip} = -\cos^2\alpha\cos 2\alpha\cos\psi\cdot\Omega \tag{4-32}$$

Theory again diverges by considering a second slip contribution or not; i.e. either the loxodromic or geodesic slip direction is assumed. The former assuming displacement H_1 in axial direction only, the latter also considering lateral displacement H_2. The geodesic assumption introduces different curvature formulations ω_1 and ω_2 and ω_3 is zero for all global curvatures.

Based on experimental evidence of governing axial slip, the present work assumes the loxodromic slip direction.

Stick-slip condition

A two zoned cross-section is present after slip is initiated at the neutral axis of global curvature. The angle defining the stick-slip boundary is defined by equation 4-33 and changes non-linearly with increased curvature with a magnitude depending on the parameters defining the moment slip is initiated, i.e. critical curvature Ω_{cr}.

$$\psi_0 = \cos^{-1} \frac{\Omega_{cr}}{\Omega} \tag{4-33}$$

As a result of this stick-slip boundary, stress accumulation develops differently around the circumference as axial shear stress is already constant for the wires within the slip region and still increasing for wires in the stick region further away from the global bending axis. Friction stress for the full slip, see equation 4-34, shows a linear relationship with circumferential position ranging from $\psi = 0$ at the global bending axis to $\psi = \frac{\pi}{2}$ on the outrados.

Stress in the sticking wires is superposed from from the maximum shear stress present in the stick-slip boundary ψ_0 and the additional accumulation dependent on the circumferential location ψ of the assessed wire from the boundary towards the outrados, see equation 4-35.

$$\sigma_{f,slip} = \frac{\mu(q_3^i + q_3^{i+1})a}{\sin \alpha A}\psi \tag{4-34}$$

$$\sigma_{f,stick} = E\cos^2 \alpha a_i(\sin\psi - \sin\psi_0) \cdot \Omega + \frac{\mu(q_3^i + q_3^{i+1})a}{\sin \alpha A}\psi_0 \tag{4-35}$$

Global bending stiffness

By integration, the bending moment contribution of each layer can be determined. A tri-linear curvature-bending moment relationship results from successive phases stick, stick-slip and full slip as described in previous paragraph. Following a perfect elastic-plastic material characteristic (seen by initial and full yield bending moments for normal steel pipes, i.e. rigid pipes) the difference between $M_{stickslip}$ and M_{slip} is dependent on a constant value $\frac{4}{\pi}$ as shown by equation 4-36

$$M_{slip} = \frac{4}{\pi} \cdot M_{stickslip} \tag{4-36}$$

In general, the intermediate stick-slip phase is neglected and a bi-linear curvature-bending moment relationship is established. Implementation of this assumption results in a corrected value for the critical curvature as shown in 4-37

$$\Omega_{cr*} = \frac{4}{\pi} \cdot \Omega_{cr} \tag{4-37}$$

$$\Omega_{cr*} = \frac{4}{\pi} \cdot \frac{\mu(q_3^i + q_3^{i+1})}{EA\cos^2\alpha \sin\alpha} \tag{4-38}$$

(Larsen et al., 2014)

4-3-2 Response behaviour

The physical behaviour as a response to a curvature Ω_2, or curvature radius R_2 is signified by:

1. Friction stress σ_f; an axial shear stress emerging during the wire stick-condition, reaching a constant maximum value after reaching the full slip-condition.

2. Local bending stress σ_b in two orthogonal directions H_2 and H_3, dependent global curvature.
3. Total alternating stress σ_a resulting from the superposition of friction and local bending stress.

Compressive and tensile forces emerge from bending the riser cross-section as shown in figure 4-4. A thin-walled steel cylinder would show linear shortening of the compressive side and similarly elongation on the tensile side as a response to curvature Ω.

However, the layered and helical character of the flexible riser introduces non-linear strain behaviour for each concentric layer i when following helix wire wrapped around the layer circumference. Friction stress σ_f and bending stress σ_b are superposed with the static stress σ_s calculated by Model A to find the total wire stress σ_t. The global axis-system is labelled $X_{1,2,3}$ and the local (helix-wire) axis-system as $H_{1,2,3}$. All main geometry, load and response parameters used in the bending analysis of Model B are summarized in appendix A.

Friction conditions

Wire slip has a major influence on the riser stiffness and is the main reason for its flexible character. Prior to wire slip, the stick condition, elongation at the riser tension side and the shortening at the lower compression side is fully counteracted by the helix stiffness. The accumulation of friction stress around the circumference is shown in figure 4-5. As the wires start to slip, further increase of stress is

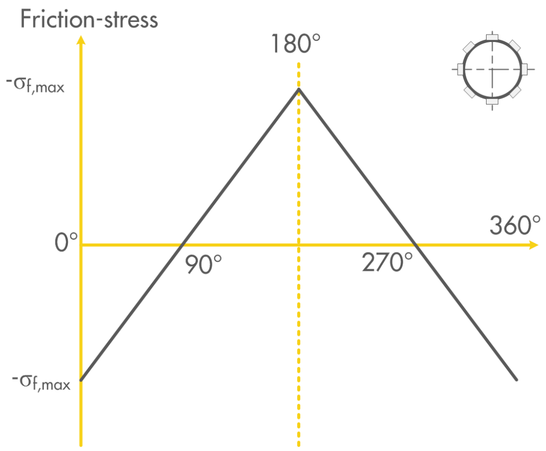

Figure 4-5: Friction stress accumulation around circumference for constant curvature level; linear slope.

stopped and the material is slowly redistributed towards the outrados; all wires slip to a new position in axial direction. This uni-directional slip follows the loxodromic assumption of keeping the initial path of each wire.

To summarize, three conditions can be distinguished:

1. Stick condition: Curvature is very small and no slip is initiated.
2. Stick-slip condition: Axial shear force is higher than available friction force and wire slip is initiated at the riser neutral axis.
3. Full-slip condition: Wires are slipping for al circumferential angles ψ.

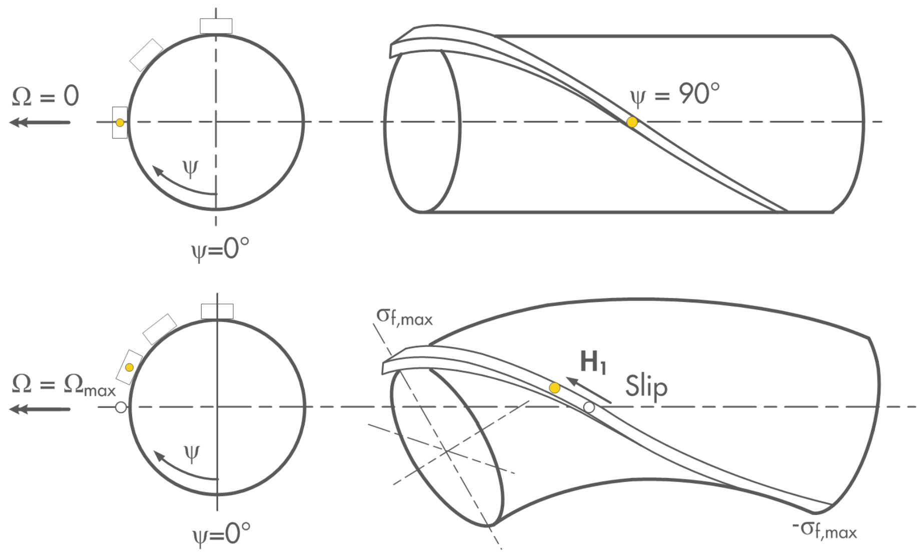

Figure 4-6: Slip path of the wire

The stick-slip is not taken into account in the algorithm of this model: condition of slip (stick or full slip) is always equal for all positions around the circumference.

For condition 3, the axial shear forces of wires located on the outer fibers $\psi = 0°$ and $\psi = 180°$ are equally loaded in opposite directions and slip is never initiated. This is as a result of vertical symmetry of the cross-section.

The relationship between curvature and slip distance is shown for three different locations around the circumference, see figure 4-7 As expected, slip is never initiated at the outer fiber (blue line), maximum at the outrados (green line) and 70% of maximum at the the north-east position (red line). This indicates a non-linear relationship between slip distance and circumferential position.

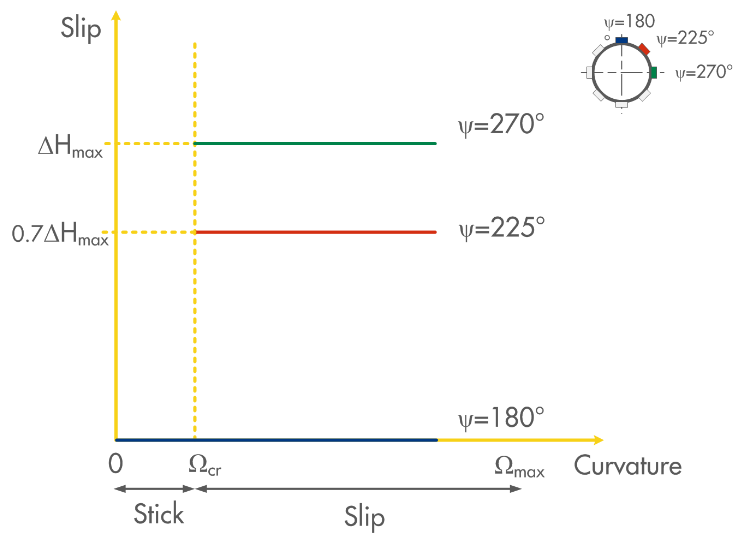

Figure 4-7: Friction stress accumulation; linear increase up to critical curvature and linearly increasing with distance from neutral bending axis X_2

Local wire curvature

The local bending stress depends on the local wire-curvature and wire dimensions. The deformation of the wire after curvature increments is dependent on its circumferential position.

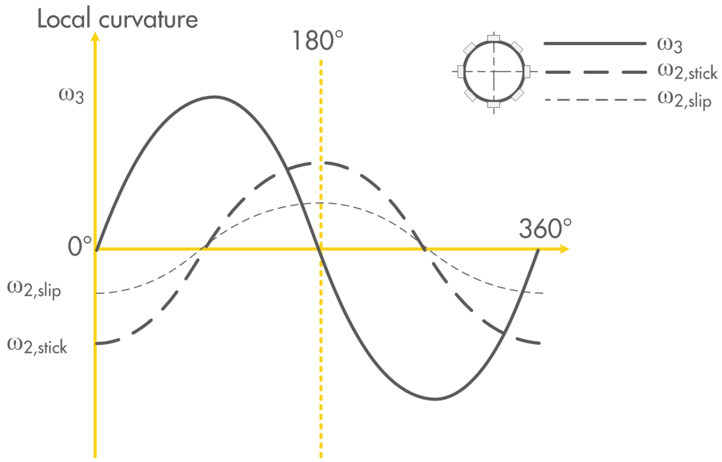

Figure 4-8: Curvature distribution around circumference for constant curvature level

The stress is not uniformly distributed over the wire cross-section. The bending moment thus bending stress linearly increases towards the edges of the wire. The wire hotspot-locations are top left and right with respect to the helical axis system $H_{2,3}$.

Total stress

Static pre-tension and friction shear forces are uniformly distributed over the wire-cross section and define the minimum total stress level. The stress-increment results from additional wire curvature.

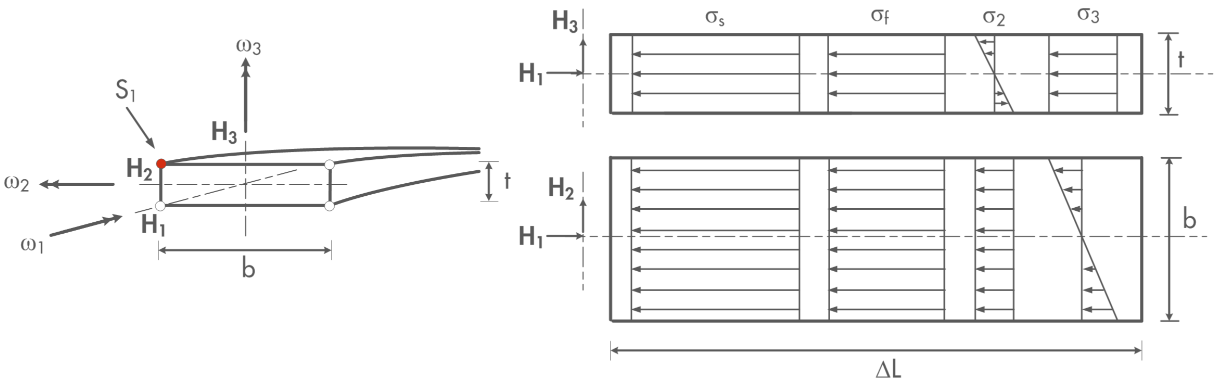

Figure 4-9: Hotspot stress (left) S_1 at upper left corner of the wire. Side view (top right) and top-view (bottom right) showing all 4 stress contributions.

4-3-3 Algorithm

For the present work, a publication of generic theory (Larsen et al., 2014) was used to define the algorithm of Model B. Subsequent cross-validation was carried out by comparing response values to values generated by local flexible riser model Helica, described and evaluated in Skeie et al. (2012). Their analytical model is generally based on similar generic formulations. Also this model is validated according to international standards hence the accuracy is assumed to be satisfactory for future in-house calculations using ABC Fatigue.

For this analysis, the riser is subjected to a constant curvature Ω around the X_2 axis.

Assumptions ABC fatigue in addition to general bending assumptions stated in 4-3-1.

1. Pressure armour stiffness is negligible for bending analysis
2. The inner tensile armour is governing the riser fatigue life.

Methodology

The algorithm of Model B can be summarized as follows:

1. Define additional geometry and curvature loading b, t and Ω_{max}.
2. Define friction coefficient and calculate critical curvature and
3. Calculate friction stresses by extending the domain of a quarter pitch to all 360 circumferential locations.
4. Calculate lateral and transverse bending and superpose to find total bending stress for all circumferential positions ψ.
5. Superposition of friction and bending stress to find total stress σ_a for all circumferential positions ψ.

Step 1: Additional geometry, local wire hotspot and constant curvature

Model A geometry only requires a definition of the total wire area A whereas Model B specifies the wire width b and thickness t to find hotspots S_1 to S_4 at the outer fibers of the individual wire. Transverse direction H_2 corresponds to the wire strong axis and the lateral direction to the lateral or weak axis H_3. Wires are always rectangular but dimensions are highly variable. Some typical width x thickness values are:

- 6" Production Riser (Technip): 12x5 (Cook)
- 6" Riser (Technip): 20x3 (Leroy)
- 6" Dynamic Umbilical (Unknown manufacturer): 10x5 (Skeie)
- 8" Gas Re-injection Riser (NOV): 15x6 (Pierce)
- 10" Production Riser (Wellstream): 12x7 (Pierce)
- 12" Riser (NOV): 15x6 (JIP)

The local hotspot S is defined as the upper right corner for each individual wire around the circumference: $H2 = \frac{1}{2}b$ and $H3 = \frac{1}{2}t$. Curvature is usually defined in 1/m, however calculations are preferably in 1/mm hence Ω is divided by 1000. Typical curvature values for a production riser in North Sea environmental conditions and a water-depth of approximately 80 meters are ranging between -0.04 and 0.04.

Step 2: Friction coefficient and critical curvature

The friction factor is a critical but also highly discussed computational value. Typical values are deviating between 0.11-0.13 (BFLEX), 0.15 (Flexpipe), 0.20 (Helica). The influence of the friction factor directly influences the axial shear stress level governing the maximum stress values accumulating in the wires. An incentive to further investigate the major difference between Helica and BFLEX.

To find the critical curvature, equation 4-27 is used and adapted to fit Model A output value contact pressure p_C instead of contact pressure line-load q_3 by multiplying the overall pressure value by the wire width b, the new formula is shown in equation 4-39.

$$\Omega_{cr} = \frac{\mu(p_C(i) + p_C(i+1)}{Et\cos^2\alpha\sin\alpha} \cdot \frac{4}{\pi} \tag{4-39}$$

Step 3: Friction stress

Friction stresses are linearly dependent on the circumferential location ψ defined for a range of 0 to $\frac{\pi}{2}$ by equation 4-34. for full cross-section application, i.e. input values ranging from $\psi = 0 - 360°$, circumferential locations left from the vertical symmetry axis $\psi = 0 - 180°$ are evaluated with equation 4-40.

$$\begin{aligned} \sigma_{f,slip}(\psi) &= \frac{\mu(p_C(i) + p_C(i+1)a}{t\sin\alpha} \cdot \psi_{left} \\ \sigma_{f,slip}(\psi) &= \frac{\mu(p_C(i) + p_C(i+1)a}{t\sin\alpha} \cdot \left(\frac{\psi\pi}{180} - \frac{\pi}{2}\right) \end{aligned} \tag{4-40}$$

On the right side, $\psi = 180 - 360°$, equation 4-41 is applied.

$$\begin{aligned} \sigma_{f,slip}(\psi) &= \frac{\mu(p_C(i) + p_C(i+1)a}{t\sin\alpha} \cdot \psi_{right} \\ \sigma_{f,slip}(\psi) &= \frac{\mu(p_C(i) + p_C(i+1)a}{t\sin\alpha} \cdot \left(\frac{\pi}{2} - \frac{\pi(\psi - 180)}{180}\right) \end{aligned} \tag{4-41}$$

Note that for both formulations, contact pressures were transformed into line loads by a multiplication of reference equation 4-34 with the wire width b.

Friction stress will linearly increase with curvature. From the moment slip is induced, the friction stress remains constant at the level reached at Ω_{cr}. The critical curvature is 0.0002 1/m for a 6" production riser in normal operational conditions in the North-Sea and a curvature load of 0.01 1/m ($\Omega_{cr} = 2\%$ of Ω_{max}).

Step 4: Local Bending stress

Local wire curvatures ω_2 and ω_3 were multiplied with elastic modulus E to find elastic stress relations accumulating with larger distances along the respectively H_3 axis and H_2 axis. Transverse bending σ_{b2} on the outer fiber is defined by equation 4-42.

$$\begin{aligned} \sigma_{b2}(\psi) &= \omega_3 \cdot EH_2 \\ \sigma_{b2}(\psi) &= -(1 + \sin^2\alpha)\cos\alpha\sin\psi \cdot \Omega \cdot EH_2 \end{aligned} \tag{4-42}$$

Lateral bending stress σ_{b3} on the outer fiber calculated with equation 4-43.

$$\begin{aligned} \sigma_{b3}(\psi) &= \omega_2 \cdot EH_3 \\ \sigma_{b3}(\psi) &= -\cos^4\alpha\cos\psi \cdot \Omega \cdot EH_3 \end{aligned} \tag{4-43}$$

Note that the formulation for lateral bending derived from equation 4-30, and the generic theory states that this formulation corresponds to wires in stick condition. As the maximum curvature is much larger than critical, a full slip condition is present. However, validation response values matched with Helica conform the stick formulation hence the decision was made to carry on likewise.

Total stress values for hotspot location $H2 = \frac{1}{2}b$ and $H3 = \frac{1}{2}t$ are derived by superposing the contributions of transverse and lateral bending shown by equation 4-44. All wires are evaluated for the same hotspot location; i.e. "top-right" for reference case of horizontally positioned wires at $\psi = 0°$ and $\psi = 180°$.

$$\sigma_b(\psi) \quad = \quad \sigma_{b2}(\psi) + \sigma_{b3}(\psi) \tag{4-44}$$

Step 5: Total bending stress

The total bending stress σ_a (alternating) is derived by a summation of friction and bending stresses. Diligent superposition of $\sigma_f(\psi)$ and $\sigma_b(\psi)$ for all positions around the circumference results in an overview of the stress distribution around the circumference, see equation 4-45.

$$\sigma_a(\psi) \quad = \quad \sigma_f(\psi) + \sigma_b(\psi) \tag{4-45}$$

Friction stress accumulates linearly and local bending non-linearly indicating a non-linear total stress distribution. However, the influence of friction stress governs the shape of this curve for small curvature values hence the total stress response is linearly shaped accordingly.

4-4 Model C: Cyclic Analysis

In Model C cyclic curvature is introduced. Extreme response values are measured at cycle top and crest to define the maximum stress range experienced in the numerous wires around the circumference. A crucial uncertainty regards the direction and magnitude of wire slip and the relation with curvature. Wire slip results in a major change of riser stiffness and non-linear stress accumulation in the wires around the circumference.

4-4-1 Fundamental Theory

The bending theory as described in section 4-3-1 is continuously repeated for each curvature level $\Omega(t)$ at $t_{i+1} = t_i + \Delta t$ for $i = 0 - 2\pi$.

The assumed conditions used in this generic theory are as follows

1. A cyclic curvature $\Omega(t)$ is applied to a local section with length L; the riser is repetitively bent into a torus with up and downward orientation.
2. Quasi-static frequency domain: no dynamic acceleration and incorporation of mass.
3. Wire-slip only in longitudinal direction H_1: no change of wire laying angle in the bent state according to loxodromic assumption.

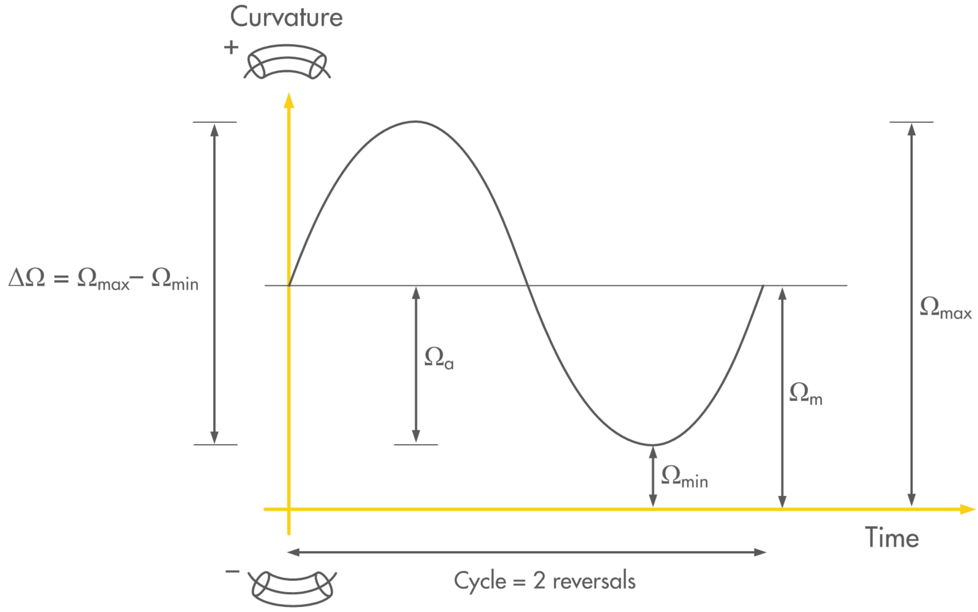

Figure 4-10: Cyclic curvature: characteristics

Cyclic Curvature

The cyclic curvature formulation is shown in equation 4-46 and figure 4-10.

$$\Omega(t) = \Omega_a \sin t \tag{4-46}$$

Main cyclic curvature relations are described in 4-47.

$$\begin{aligned} \Delta\Omega &= \Omega_{max} - \Omega_{min} \\ \Omega_a &= \frac{1}{2}\Delta\Omega \\ \Omega_m &= \frac{\Omega_{max} + \Omega_{min}}{2} \end{aligned} \tag{4-47}$$

For rigid riser bending, the response graph looks identical and stresses can be derived directly after determination of a factor c_{rigid} as shown in 4-48.

$$\sigma(t) = c_{rigid} \cdot \Omega_a \sin t \tag{4-48}$$

$$\Delta\sigma = c_{rigid} \cdot \Delta\Omega \tag{4-49}$$

Stress minimum and maximum values will lead towards stress ranges accordingly to the relations described by 4-47, however no direct translation via a constant $c_{flexible}$ is possible due the stick-slip behaviour.

Periodicity of the riser curvature is assumed to be very low frequent and can be approximated by the helix pitch length, equation 4-50, and corresponding frequency by equation 4-51.

$$L_p = \frac{2\pi a}{\tan \alpha} \tag{4-50}$$

$$f = \frac{1}{L_p} \tag{4-51}$$

Wire position and slip

Position along the helix and corresponding circumferential location are related by the laying angle and layer radius, see equation 4-52.

$$\psi = \frac{\sin\alpha}{a} \cdot H_1 \tag{4-52}$$

Assuming no axial friction is present, i.e. full slip condition, the longitudinal relative displacement follows equation 4-53.

$$H_1 = a^2 \frac{\cos\alpha^2}{\sin\alpha} \sin\psi \cdot \Omega \tag{4-53}$$

This indicates that local bending also depends on the character of preceding load-cycles as wire slip changes the initial positions of the wire.

4-4-2 Response behaviour

The response behaviour resulting from one curvature cycle $\Omega(t = 0 - 2\pi, \psi_w)$ for wires w_1 to w_n excited with a constant amplitude Ω_a is signified by:

1. Axial wire slip $\Delta H_1(t, \psi_w)$ after overcoming the available friction hence critical curvature Ω_{cr}.
2. Maximum stress σ_{max} corresponding to $\Omega_{max}(\frac{\pi}{2}, \psi_w)$.
3. Minimum stress σ_{min} corresponding to $\Omega_{min}(\frac{3\pi}{2}, \psi_w)$.
4. Stress range $\Delta\sigma(\psi_w)$ defined as the distance between the maximum wire stress and the minimum wire stress.

The curvature period of a flexible riser in North-Sea conditions can be approximated by one helix pitch length. For a 6" production riser this results in a frequency of 0.00078 which is in the quasi-static frequency domain and excludes the influence of dynamic mass-dependent accelerations.

Curvature reversals within quasi-static frequency domain result in slow and continuous wire slip and after one period all wires have returned to their initial positions.

4-4-3 Algorithm full slip

1. Modelling one curvature load-cycle with constant curvature amplitude in the quasi-static frequency domain.
2. Linear relationship between curvature increment $d\Omega$ and slip distance ΔH.
3. Wires are immediately in full-slip condition in the first time-step after curvature sign change thus $d\Omega = 0$.

The initial circumferential points are ψ_0. After application of a first curvature load, the wire will slip axially to a new position along the wire longitudinal axis H_1. Slip distance ΔH is also dependent on the current location.

Overview of procedure

1. Determination of initial wire locations ψ_{c0} and H_{c0}.
2. Definition of Ω_{max} and Ω_{min} values and derivation of Ω_a for one sinusoidal wave $\Omega(t)$.
3. Linear curvature-wire slip relation determines wire displacements thus and changed circumferential helix positions ψ and H for each time-step Δt.
4. Friction stress is calculation; sign dependent on (preceding) slip-direction and magnitude on circumferential location. No influence of curvature after Ω_{cr}.
5. Local bending stress calculation; dependent on circumferential (updated) position and magnitude of Ω.
6. Total stress maxima an minima measured at top and crest $d\Omega = 0$, prior to sign change of axial shear force.

4-4-4 Algorithm stick-slip

1. Stick-condition pertains until axial shear force is higher than available friction force. At initiation of first curvature increment and at maxima and minima of curvature reversals, wire slip is zero.
2. The stick region is delineated by the critical curvature; stick condition emerges as $d\Omega < \Omega_{cr}$ and pertains after sign change of $d\Omega$ until the sum of curvature increments is larger than the critical curvature.
3. Ten cycles c_c are modelled;
   - Constant or Irregular Ω_a.
   - Instead of 2 reversals for a full cycle, reversals range between 1.75-2.25.
4. First cycle is identical to tenth cycle regarding amplitude and reversals.

Overview of procedure

1. Determination of initial wire locations ψ_{c0} and H_{c0}.
2. Calculation of critical curvature Ω_{cr}.
3. Definition of ten random Ω_{max} values.
4. Define the relation between Ω_{max} and Ω_{min} to determine the wave character (regular/irregular) and calculate Ω_a for ten sinusoidal waves $\Omega(t)$.
5. One cycle $\neq$ 2 reversals. Define range and assign random number of reversals to each load cycle c.
6. Set $\Omega_{c1} = \Omega_{c10}$.
7. Monitor wave-train $c1$ to $c10$ and find σ_{max} and σ_{min} for each cycle c. For each $|\sigma_{max}|$, determine responses $\Delta\sigma_{c1}$, $\Delta\sigma_{c10}$, ψ_{c1} and H_{c1}.
8. Compare responses of first cycle to tenth cycle.

Chapter 5

ABC Fatigue: Validation & Verification

A clear distinction exists between the "Physical response" and the "Model response". The former being the real response seen under operational conditions and/or experiments, the latter obtained from mathematical relations. Minimal differences are desired as model predictions hence fatigue life estimates are consequently reliable and operational safety judgements —based on a fatigue life re-assessment including updated conditions— can be made without hesitation.

Response parameters of Model A were cross-validated with Flexpipe, an industry accepted model used and owned by Technip (Technip). Model B was cross-validated with Helica, a newly developed (Skeie et al., 2012) and also industry accepted model by DNV.

The verification criterion relates to its suitability for pre-analysis; incorporating in-field environmental and operational conditions to study their impact on stress range hence their potential to raise the fatigue life of the flexible riser.

5-1 Case-study selection: Experiments or Cross-Validation

5-1-1 Prime experimental source: Deepwater Flexible riser JIP

The Deepwater Flexible riser JIP was initiated in 1994 to encourage the development of new riser designs and to optimize the current theoretical models. The participating companies were five European operators, Shell among others. Five full-scale dynamic 'service life' tests of five different pipe designs were carried out from 1996 to 2000. Based on the results obtained from these tests, numerous design and manufacturing changes have been recommended and implemented by suppliers.

As a participating company, Shell is authorized to use experimental and analysis data as presented in the reports. Experimental data was processed by analytical contractor Seaflex and for the 10" riser tested by Shell in 1995 all experimental data and a very extensive analysis is available. However, this riser showed atypical tensile armours, four instead of two armour layers, hence not suitable. Other test combinations also showed to be unsuitable caused by numerous reasons:

- The lack of corresponding load-response data (10" Wellstream).
- Very large diameter, almost never used, and four tensile armour layers (16" Technip).

- Perfect geometry, no strain measurements but curvature calibrations carried out (12" NOV).
- Carbon fiber tensile armours, not withinn the scope of present work (9" Technip).

Table 5-1 displays the main particulars of the Deepwater flexible riser JIP.

Table 5-1: Deepwater flexible riser JIP: overview of case-study experiments

Inner bore diameter	10"	10"	16"	12"	9"
Manufacturer	Technip	Wellstream	Technip	NOV	Technip
Dynamic testing	Shell	Shell	Shell	SINTEF	SINTEF
Analytical	Seaflex	Seaflex	Seaflex	Seaflex	Seaflex
Start date	1995	1995	1997	1999	2000
Finish date	1995	1996	1998	2000	2000
Test rig	FSCTF	FSCTF	FSCTF	Marintek	Marintek
Location	Rijswijk	Rijswijk	Rijswijk	Trondheim	Trondheim
Suitable	no	no	no	no	no
Reason	armour	data	armour diameter	measurements	carbon fiber

Consequently, no experimental data was used for validation purposes.

5-1-2 Other validation sources

Numerous research programs have studied the local behaviour of flexible risers. Publications either include elaborate and numerical descriptions of geometry, load and response parameters or present only concise riser details and graphical responses. The following publications all focused on an analytical local analysis model complete with full-scale experiments to validate their model; i.e. suitable for validation of ABC Fatigue.

- Hans Out —Service Life Prediction of Flexible Pipe Parts 2 and 4 (1986-1990)
- Svein Saevik —On Stresses and Fatigue in Flexible Pipes (1992)
- Tatiana Vargas-Londono and Jose Renato M. De Sousa and Carlos Magluta and Ney Roitman —A theoretical and experimental analysis of the bending behaviour of unbonded flexible pipes (2014)
- Carl Martin Larsen and Svein Saevik and Jacob Qvist —Handbook on Design and Operation of Flexible Pipes; B1 Design Analysis (2014)
- Jean-Marc Leroy and Timothee Perdrizet and Vincent Le Corre and Pascal Estrier —Stress assessment in armour layers of flexible risers (2010)
- Geir Skeie and Nils Sodahl and Oddrun Steinkje —Efficient Fatigue Analysis of Helix Elements in Umbilicals and Flexible Risers: Theory and Applications (2012)

The research published by Skeie/DNV (Skeie et al., 2012) describes the process of building and validating their in-house analytical model Helica. This output is used to validate the friction and bending stress contributions of the inner tensile armour only.

The research published by Leroy/Technip (Leroy et al., 2010), describes three different model tests based on different methodologies. Firstly their in-house analytical model Life6 is used hereafter compared to FEM approaches using Abaqus software. All three models are compared to full-scale experimental data. The relation and difference between stress distributions of the inner and outer tensile armour is studied with all three models.

5-2 Model A

The algorithm of model A follows from the theory as described in section 4-2 and is shown in appendix A.

5-2-1 Validation

Manufacturers always include a design report complete with axisymmetric analysis for the governing load-cases, hence available for flexible risers owned and operated by Shell. Consequently, the parameters of Model A are cross-validated with an industry accepted model.

The required load, geometry and response parameters are presented in appendix A. All geometry and response parameters are layer specific, this is denoted by the subscript indicator "i" for each individual layer. A typical flexible riser consists of four metallic layers; two pressure armours and two reverse-oriented tensile armours and a carcass.

Wire Stress

In this research, axisymmetric validation is carried out according to five relevant load-cases defined by the manufacturer. It should be noted that validation according to other software model output can not justify the hundred percent accuracy of ABC Fatigue as these reference figures are possibly over-conservative. However, for the purpose of studying fatigue analysis methodology and influencing parameters, this validation is assumed to be sufficient.

Five load-cases are addressed as presented in table 5-2. In this overview the static inner-layer stress response is compared to the values as stated in the design report of a 6 inch production riser currently used in North Sea conditions. All but load-case 3 are within the 1% deviation, thus a satisfying validation. A 8.89% deviation of the no-pressure load-case indicates that the tension-stress response is not accurate.

Table 5-2: Validation inner tensile armour according to design load-cases

		p_{in}	T_{ex}	Design	ABC	Error
		[MPa]	[kN]	[MPa]	[MPa]	[%]
LC1	Design pressure	46.2	0	314	316	0.64
LC2	Maximum tension	46.2	220.6	359	357	-0.56
LC3	No pressure	0	220.6	45	41	-8.89
LC4	Offshore leak test	50.8	131.1	372	372	0.00
LC5	Factory Acceptance Test	72.1	0	490	494	0.82

Comparison of all four metallic layers of the 6 inch production riser are presented in table 5-3. The response values of the first three layers all correspond to the design calculation by the manufacturer. Contrasting results are present in the outer tensile layer, showing large errors around 25%.

Clearly the manufacturer uses a different relation to define load-sharing among the two tensile armours. A stress distribution linearly dependent on layer radius and number of wires—wire elastic modulus, area and laying angle are equal for both tensile armours— is applied by ABC Fatigue. Hence the load bearing capacity of the outer armour is almost similar to the inner armour. Flexipipe presumably includes torque unbalance and

For the purpose of this research, the investigation of the inner tensile armour is sufficient. Firstly because the mechanical stick-slip behaviour in bent condition is not dependent on the static wire stress. Secondly because the contact pressure is higher for the inner tensile layer and this has a significant influence on the stress accumulation in bending. Higher contact pressures defer the moment of wire slip and this results in (much) higher axial stresses.

Table 5-3: Validation of axial stress levels four metallic layers: Design(left) ABC(right)

	Pressure Armor 1			Pressure Armor 2			Inner tensile			Outer tensile		
	[MPa]		[%]	[MPa]		[%]	[MPa]		[%]	[MPa]		[%]
LC1	347	345	-0.58	329	330	0.30	314	316	0.64	229	311	26.37
LC2	338	337	-0.30	321	323	0.62	359	357	-0.56	271	353	23.23
LC3	-9	-9	0.00	-8	-8	0.00	45	42	-8.89	42	40	-5.00
LC4	376	375	-0.27	357	358	0.28	372	372	0.00	277	368	24.73
LC5	542	540	-0.37	514	516	0.39	490	494	0.82	357	487	26.69

Contact Pressure

The second output parameter from this analysis is the pressure existing between adjacent layers. This parameter has a major influence on the response behaviour of the curved cross-section hence on model B. The validation results are presented in table 5-4.

Table 5-4: Validation of contact pressures between four metallic layers: Design(left) ABC(right

	Layer 1 in			Layer 1-2			Layer 2-3			Layer 3-4		
	[MPa]		[%]	[MPa]		[%]	[MPa]		[%]	[MPa]		[%]
LC1	45.49	45.13	-0.80	14.70	14.99	1.93	5.15	6.09	15.44	2.10	2.97	29.29
LC2	45.46	45.04	-0.93	15.33	15.59	1.67	6.02	6.89	12.63	2.48	3.36	26.19
LC3	0.00	0.00	0.00	0.64	0.62	-3.23	0.83	0.81	-2.47	0.38	0.40	5.00
LC4	50.00	49.58	-0.85	16.54	16.84	1.78	6.20	7.17	13.53	2.54	3.49	27.22
LC5	70.99	70.50	-0.70	22.95	23.41	1.96	8.11	9.50	14.63	3.28	4.62	29.00

The model is very reliable for determination of the contact pressure between the two pressure armour layers. However, a significant error emerges as the expansion moves outward towards the outer tensile layer. The expansion rates of the design tool and ABC Fatigue are similar, two of the previously described load-cases are shown in figures 5-1a and 5-1b, however ABC Fatigue is more conservative.

Higher contact pressures are the result of a lower pressure differential through each layer, this is potentially caused by the simplification of neglecting the plastic layers. This has no major impact on

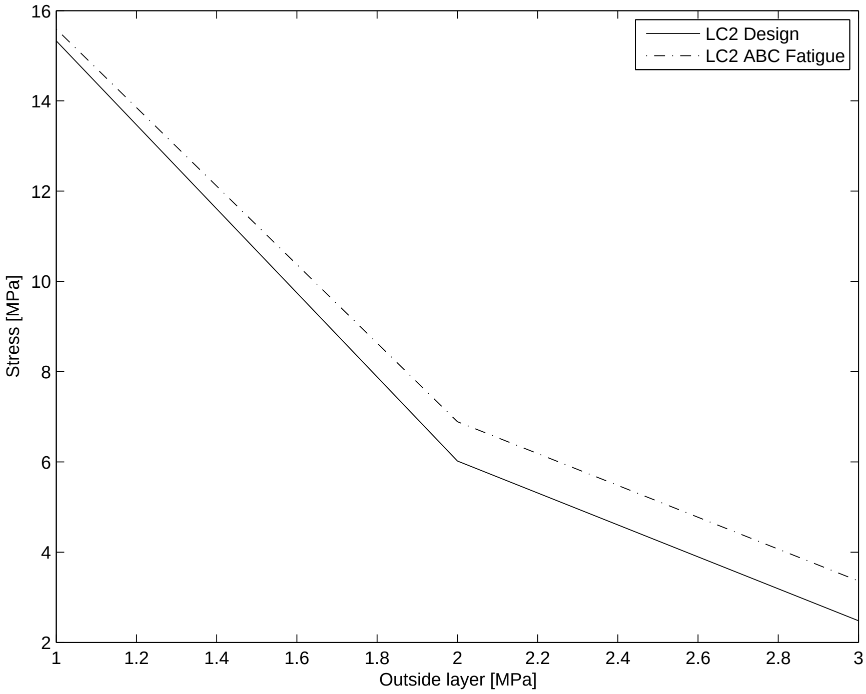

(a) Load-case 2

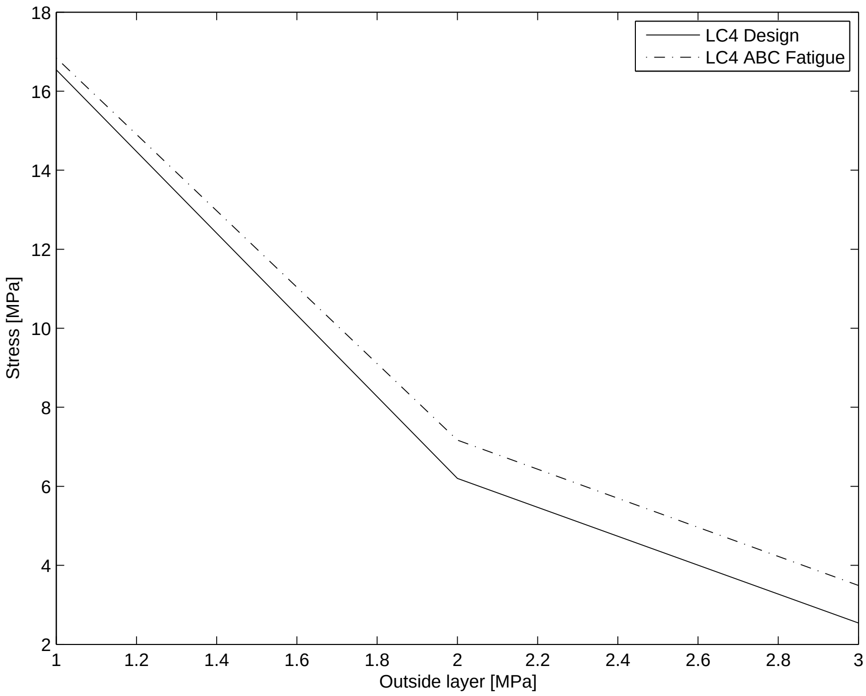

(b) Load-case 4

Figure 5-1: Contact pressure between first and second pressure armour (layer 1), on to the first tensile armour(layer 2) and on to the second tensile armour (layer 3) the expanding behaviour of the pressure armours, helically wound with an angle of almost 90 degrees, as the wires are perfectly oriented to counteract the hoop-stress causing the radial expansion hence contact pressure. Tensile armours, generally with a laying angle of 25-30 degrees, are much more sensitive to radial expansion and this influences the relative load bearing influence of the plastic layers.

High contact pressures will induce higher stress values in the bending analysis. This influence is taken into consideration in the validation-process of Model B as well as the study of conservatism in chapter 3.

5-2-2 Capacity & Limits

The following validation statements can be made with regard to axisymmetric analysis:

- The model can accurately calculate the axial wire stresses from constant pressure and tension existing in the first three metallic layers, i.e. for both pressure and tensile oriented armour, within relevant operational domains.
- The response of the outer tensile armour is not validated. Load sharing relations defined for the two tensile armours are tenuous, also in literature.
- Contact pressure between the first and second pressure armour is aligned with the design calculations.
- Contact pressures between second pressure armour, inner tensile armour and outer tensile are over-conservative. However the slope of the curves are aligned, indicating a correct method. High values calculated by ABC Fatigue are presumably related to the the omission of plastic layers.

5-3 Model B

For the validation of the bending model, a new set of parameters is required in addition to the model A input. Meaning that a suitable validation case-study should describe all parameters of the two models described in A. As with the axisymmetric validation, a case-study showing both experimental and validated-model data would be preferred. A-typical cross-sections, tenuous experiment descriptions and data confidentiality resulted in a laborious process to obtain satisfying data-sets.

Two complementary validation-cycles are carried out for the following purposes:

- Helica, DNV: Validation of friction and bending stress of the inner tensile armour (governing the riser fatigue life).
- Life6, Technip: Validation of friction stress distribution around circumference of inner and outer tensile armour.

The ABC Fatigue algorithms, imitating the flexible pipes as presented in these two publications, are shown in appendix B.

5-3-1 Validation B1: Helica

The model is validated with a two-step approach. Assumptions are made to match the geometry since some parameters are missing in the research article. However, available geometry of another 6 inch riser and matching mean stresses of the inner tensile armour justify these assumptions. In the second step, matching of response parameters is presented.

The recentness of this research, published in 2012, and clear presentation of the underlying algorithm and load-response graphs produced by Helica are main reasons to validate ABC Fatigue accordingly.

Step 1: Match geometry

Table 5-5 gives an overview of required loads, geometry and responses. Main issues influencing

Table 5-5: Overview of input/output variables; "X" indicates missing from dataset

	Model A			Model B		
Loads	T_{ex}	1000	kN	Ω	0.3	1/m
	p_{in}	0	MPa			
	p_{out}	0	MPa			
Geometry	E_i	210E3	MPa	ψ	180/225	deg
	α_i	35/37	deg	$1/2b$	5	mm
	a_i	X	mm	$1/2t$	2.5	mm
	n_i	38/42	-	μ	0.2	-
	A_i	50	mm^2			
Responses	σ_m	graph	MPa	σ_f	graph	MPa
	$p_{C,i}$	X	MPa	σ_b	graph	MPa
				σ_a	graph	MPa

imitation of this case-study are summarized as follows:

- Helica analyses an umbilical and not a riser. This influences the character of the inner-bore pressure as smaller diameter tubes are present instead of a main core carrying hydrocarbons. In addition, pressure armour particulars are not included.
- The radii of the tensile armours are not mentioned. Instead the central core value is given: 76.2mm or 6 inches.
- Response graphs can correspond to the inner or outer tensile armour, this is not stated.
- The contact pressure between adjacent tensile armour layers is unknown.

The following approach resulted in a satisfactory match between Helica and ABC Fatigue:

- The radius of the first pressure armour layer is scaled down to match the inner bore diameter (scale factor 0.72) with a single wire of nearly zero, the second armour is removed by setting the number of wires to zero.
- A fill fraction of 0.9 (commonly used, see ref handbook) is used in equation 5-1 to calculate the radii of the inner and outer tensile armours.

- The mean wires stresses are traced from the Helica response graph, this value is matched with the axisymmetric wire stress output from Model A. Near match with inner tensile armour is confirmed.
- Axisymmetric validation of ABC Fatigue in section 5-2-1 showed accurate results for the contact pressures of load-case 3: tensioned riser with zero inner-bore pressure. Therefore contact pressures from model A are assumed to be acceptable in for this load-case. This assumption is evaluated in section 5-3-3.

$$a_i = \frac{nb}{F_f 2\pi \cos \alpha_i} \tag{5-1}$$

Step 2: Validate friction/bending stresses

Friction and Local bending stresses are evaluated conform the following criteria:

1. Sign convention check at two circumferential locations: the outrados ψ=180 degrees and north-east ψ=225 degrees.
2. Circumferential stress distribution for all four corner-hotspot locations.
3. Exact values of friction and bending stress at two circumferential locations and the character of mismatch.

The stick-slip transition phase is not modelled by both ABC Fatigue and Helica [ref to paper]: i.e. after reaching the critical curvature, friction stress is constant for all locations around the circumference. Incorporating the stick-slip behaviour, thus a phase of slipping wires at the neutral axis and sticking wires at the outer fibers, will result in a non-linear friction-stress distribution around the circumference. The influence of this simplification is assumed to be very small, this is confirmed in a small experiment described in chapter 6.

Firstly, ABC Fatigue models positive friction stress for positive curvature values on both circumferential locations, similar to Helica. Figure B-2 displays the total stress accumulation of both models at two circumferential locations. The graphs confirm correct sign conventions for both $\psi = 180°$ and $\psi = 225°$.

Secondly, the default corner hotspot location is top right. At this location, the total stress range, being the summation of bending stress and friction-stress, matches Helica results. At other corner positions, maximum stress values are found at other circumferential locations. The top right circumferential stress distribution is shown in figure B-8. Similar graphs for all four corners are shown in B-2-1. Maximum stress ranges are equal for all hotspot locations, i.e. corners of the individual wire, however located at different positions around the circumference.

Conform the third criterion, table 5-6 shows the comparison of response values by Helica and ABC Fatigue for two circumferential positions. All Helica values are approximations, limited to zero digits as they are measured from a graph. Hence, small errors are probable.

An underestimation of mean stress corresponds to the validated response values of Model A; i.e. underestimating the axisymmetric stress response for load-cases with axial tension and no inner-bore pressure. Furthermore, ABC fatigue slightly overestimates the alternating stress response. This is an acceptable deviation, given the probability of Helica measurement errors.

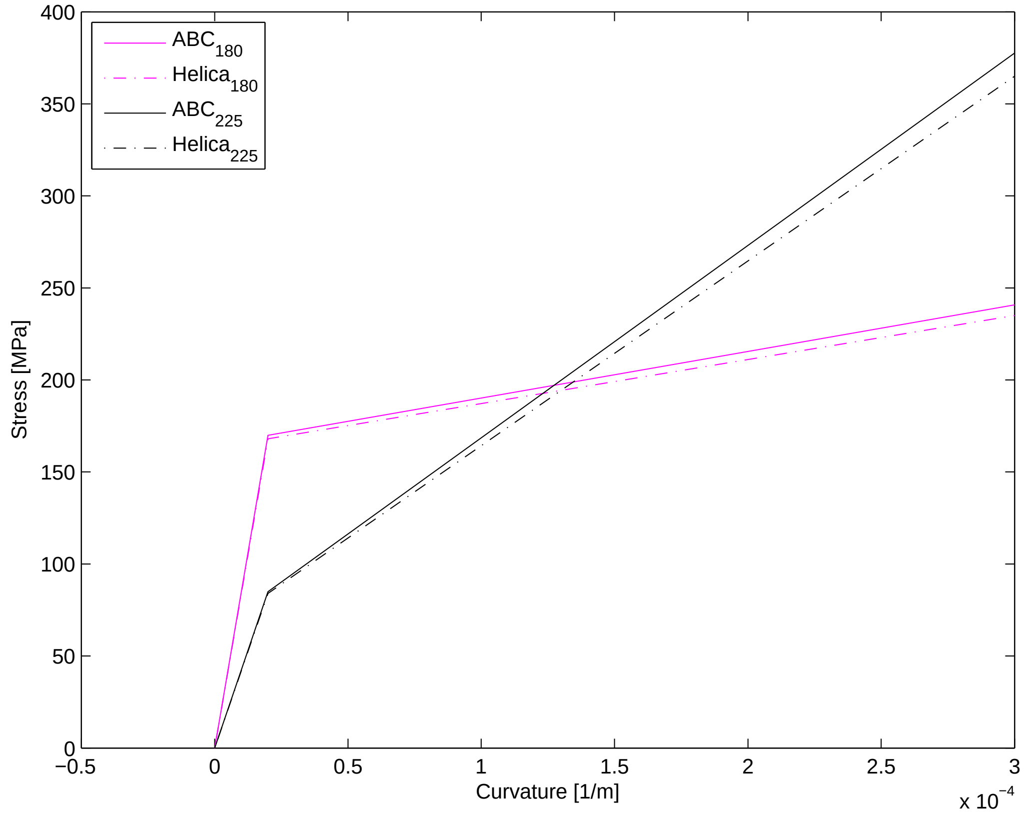

Figure 5-2: Total wire stress @ inner tensile armour

Table 5-6: Validation results showing comparison between Helica and ABC Fatigue Results

		ψ = 180 deg			ψ = 225 deg		
		Helica	Model B		Helica	Model B	
		[Mpa]	[Mpa]	[%]	[Mpa]	[Mpa]	[%]
Mean stress	σ_m	326	315	-3.37	320	315	-1.56
Friction stress	σ_f	168	170	1.19	84	85	1.19
Bending stress	σ_b	66	71	7.58	281	293	4.27
Alternating stress	σ_a	234	241	2.99	365	378	3.56

Step 3: Model full cycle

A complete load-cycle with an amplitude of 0.3 1/m is imitated. The general shape of a full cycle is compared. Figure 5-4 shows a clear correspondence. Mean stress and stress range values are compared in table 5-7.

The general shapes of both curves is correct, shown in figure 5-4.

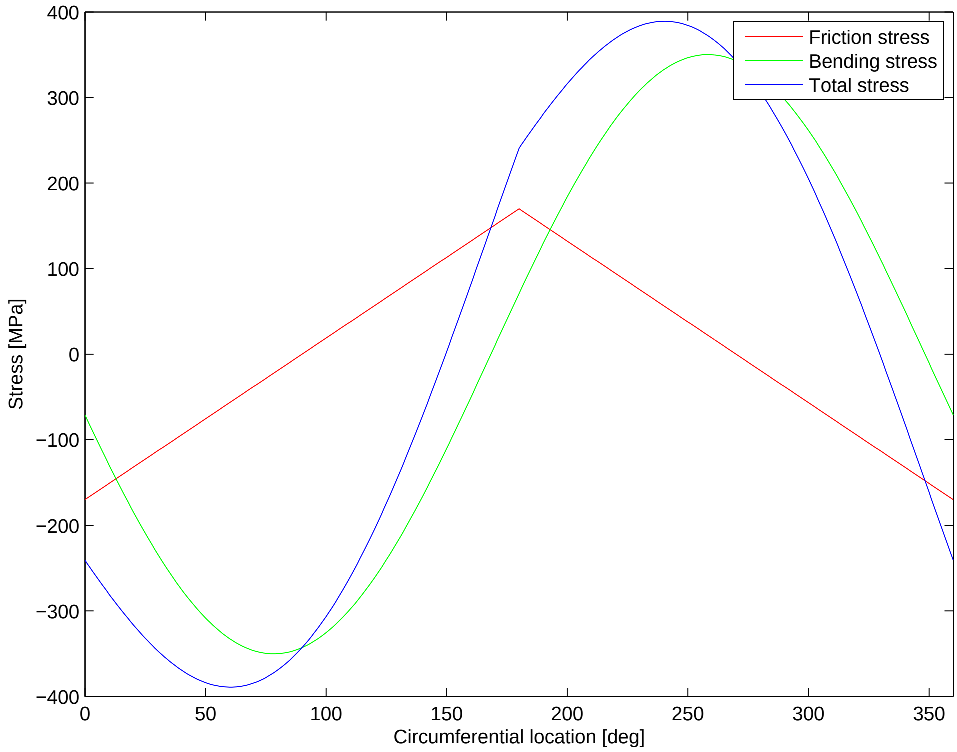

Figure 5-3: Circumferential stress distribution, top right $\Omega = 0.3$ 1/m

Table 5-7: Validation results showing results and comparison of Helica and ABC Fatigue model B results

		$\psi = 180$ deg			$\psi = 225$ deg		
		Helica	Model B		Helica	Model B	
		[Mpa]	[Mpa]	[%]	[Mpa]	[Mpa]	[%]
Mean stress	σ_m	326	315	-3.37	320	315	-1.56
Friction stress	σ_f	181	170	-6.08	84	82	-2.38
Bending stress	σ_b	67	71	5.97	281	298	6.05
Alternating stress	σ_a	248	241	-2.82	365	380	4.11
Friction stress range	$\Delta\sigma_f$	362	340	-6.08	168	164	-2.38
Bending stress range	$\Delta\sigma_b$	134	142	5.97	562	596	6.05
Total stress range	$\Delta\sigma$	496	482	-2.82	730	760	4.11

5-3-2 Validation B2: Life6

This publication shows elaborate graphical and numerical response data. Many geometrical variables are unknown. However, the inner-bore diameter is similar to the design case used for validations A and B1. Also the manufacturer is equal to validation B1, justifying the assumption of relatively minor changes to the riser design.

Similarly to validation B1, a two-step method is used to first optimize the algorithm of ABC Fatigue for a reliable case-study imitation and secondly to compare response values.

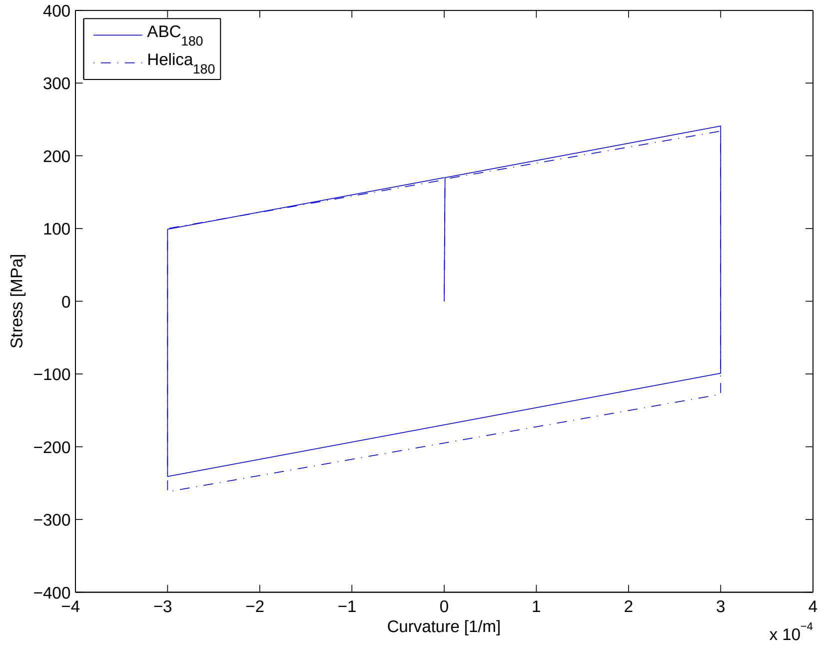

(a) Hysteresis curve at $\psi = 180°$

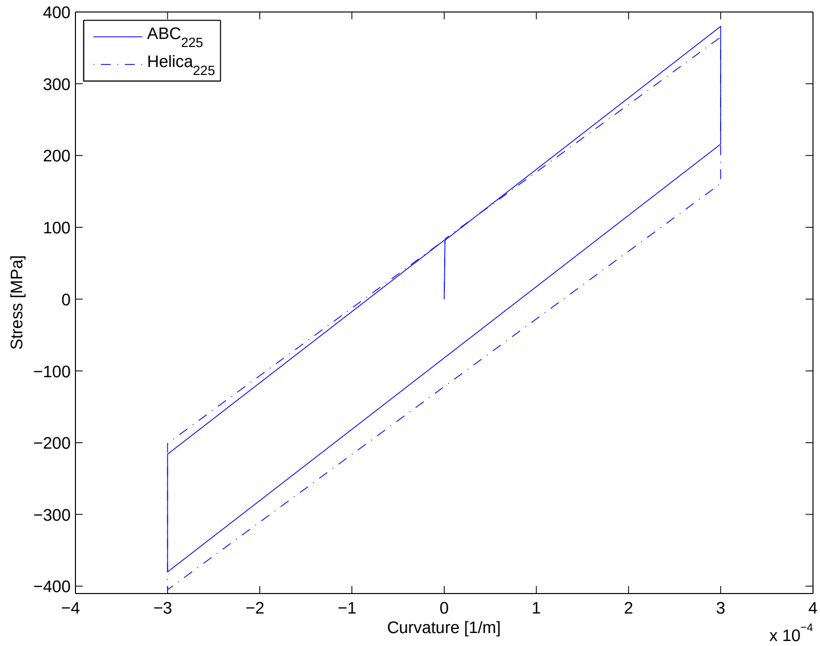

(b) Hysteresis curve at $\psi = 225°$

Figure 5-4: Total stress hysteresis curve for one cyclic curvature reversal

Extensiveness of response data and a study of both the inner and outer tensile armour layer raised the potential this publication. Also, presented response values correspond to the tenth load cycle instead of the first. This introduces the significance and influence of hysteresis, investigated by Model C.

Step 1: Match geometry

Table 5-8 indicates a major shortage of information. The following assumptions are made:

- Laying angles are similar to the 6" riser used for validation A: assumption based on similarity of riser inner-bore and manufacturer.
- Layer radii of pressure armour layers are equal, tensile armour layers are smaller due to smaller wire thickness.
- Number of wires dependent on fill fraction of 0.9 and equation 5-1.
- The friction factor is changed to match inner and outer tensile armour friction stresses. With a very small value of $\mu = 0.113$ as a result. The width of the wires, $b = 20$, justifies this value.
- For the representation of friction stress distribution of the outer tensile armour, a corrected mean stress value is used. Mean stress values for the outer tensile armour are known to be severely overestimated by ABC Fatigue. Correction will not influence the friction stress calculation.
- Load cycles influence the response values, this is taken into account in the evaluation of validation results.

The 10th stress cycle is used in Life6 calculations, this possibly influences the friction stress range thus impeding the significance of this validation.

Table 5-8: Overview of input/output variables; "X" indicates missing from dataset

	Model A			Model B		
Loads	T_{ex}	0	kN	Ω	0.2/0.3	1/m
	p_{in}	50	MPa			
	p_{out}	0	MPa			
Geometry	E_i	210E3	MPa	ψ	variable	deg
	α_i	X	deg	b	20	mm
	a_i	X	mm	t	3	mm
	n_i	X	-	μ	X	-
	A_i	50	mm^2			
Responses	σ_m	variable	MPa	σ_f	variable	MPa
	$p_{C,i}$	X	MPa	σ_b	variable	MPa
				σ_a	variable	MPa

Step 2: Validate friction stresses

The following criteria are evaluated:

1. Mean stress check to ascertain correct geometrical assumptions.

2. Slope of the friction stress distribution; linear or non-linear.
3. Sign convention of the friction stress distribution around the circumference.
4. Exact values of friction stress for inner and outer tensile armour.

The mean stress value of the inner (validated) armour matches the value generated by Life6. This confirms correct geometry thus boundary conditions for the bending analysis. The mean value of the outer tensile armour is corrected to show clear correspondence of the friction stresses.

Slope directionality, thus sign conventions are correct for both the inner and outer tensile armour. The inner tensile armour shows large deviations of minimum and maximum friction stresses. This is clearly shown in figure 5-5. Results are summarized in table 5-9.

The stress range differences and mean values are clearly shown in figure 5-6. The outer tensile armour is subjected to lower mean values and stress ranges indicating that the inner tensile armour governs fatigue analysis calculations for friction dominated load conditions.

Table 5-9: Validation of friction stress around circumference

		Inner Armour			Outer Armour			Outer Armour		
		Life6	ABC		Leroy	ABC		Life6	ABC*	
		[Mpa]	[Mpa]	[%]	[Mpa]	[Mpa]	[%]	[Mpa]	[Mpa]	[%]
Mean stress	σ_m	585	587	0.34	475	583	22.74	475	475	0.00
Stress range	$\Delta\sigma$	310	318	2.58	110	104	-5.45	110	104	-5.45
Friction stress	σ_a	155	159	2.58	55	52	-5.45	55	52	-5.45
Min stress	σ_{min}	430	428	-0.47	420	531	26.43	420	423	0.71
Max stress	σ_{max}	740	746	0.81	530	635	19.81	530	527	-0.57

To conclude, the large amount of assumptions required to fit this analysis rules out a full validation since the magnitudes of radii and friction coefficient are dominating the friction stress levels. However, equal friction coefficients are used for the inner and outer tensile armour and the difference between the inner and outer radius is known.

ABC fatigue correctly models the linear slope, the correct sign and the relative difference between the inner and outer tensile armour.

5-3-3 Capacity & Limits

In general, the sign of friction stress is correct for all circumferential locations and both inner and outer tensile armour. However, assumptions were made to match the riser geometry and case-study data was presented in graphical forms. Hence, data-quality of the case-study compromise the reliability of both validations. Based on data quality, the validation cycle of Model B-Helica is more trustworthy than the second scheme used for Model B-Life6. Consequently, the latter does not influence model validation statements.

The following statements can be made

- Response data presented by (Skeie et al., 2012) studied the inner tensile armour thus no possible comparison for outer tensile armour.
- The values of friction stress and total stress are within a 1-4% deviation range.

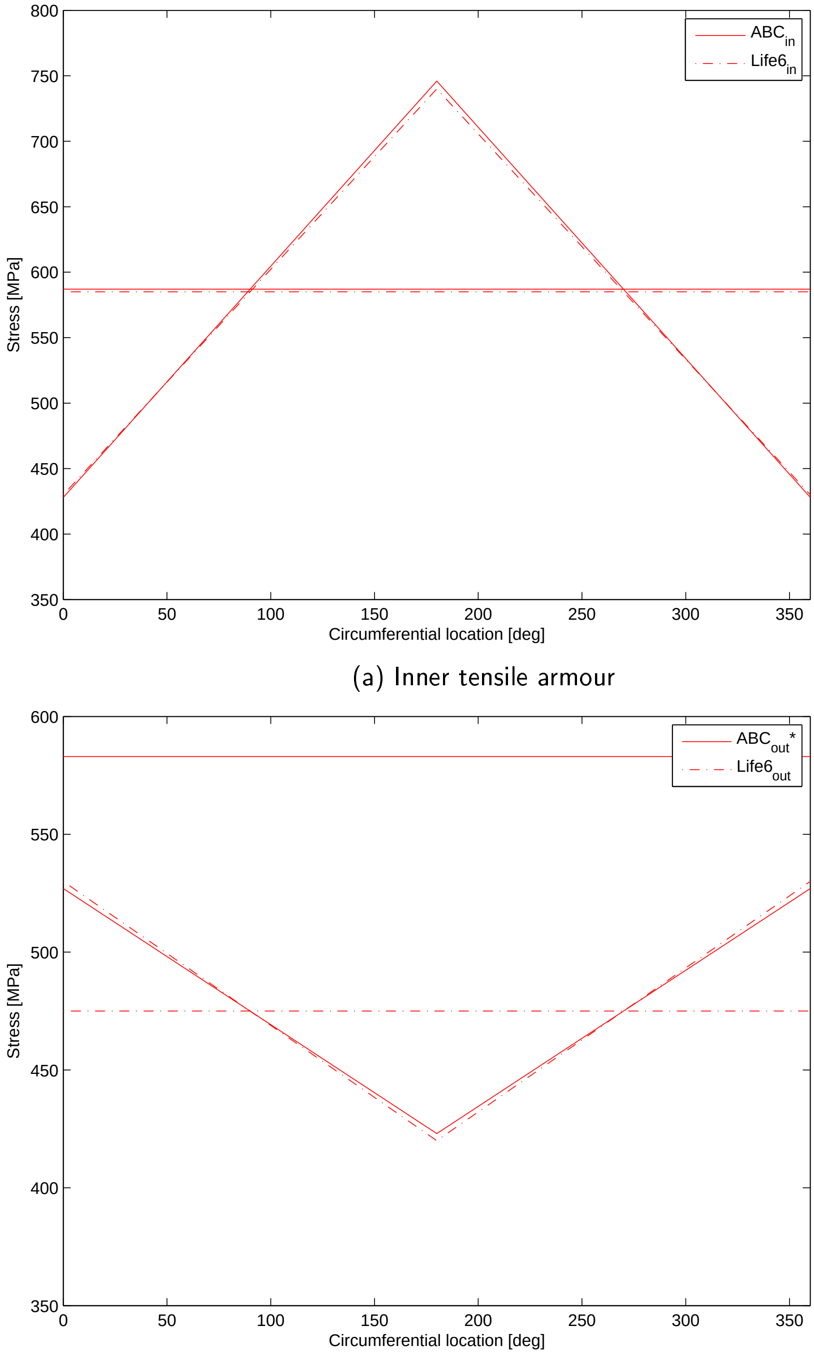

(a) Inner tensile armour

(b) Outer tensile armour

Figure 5-5: Friction stress around circumference

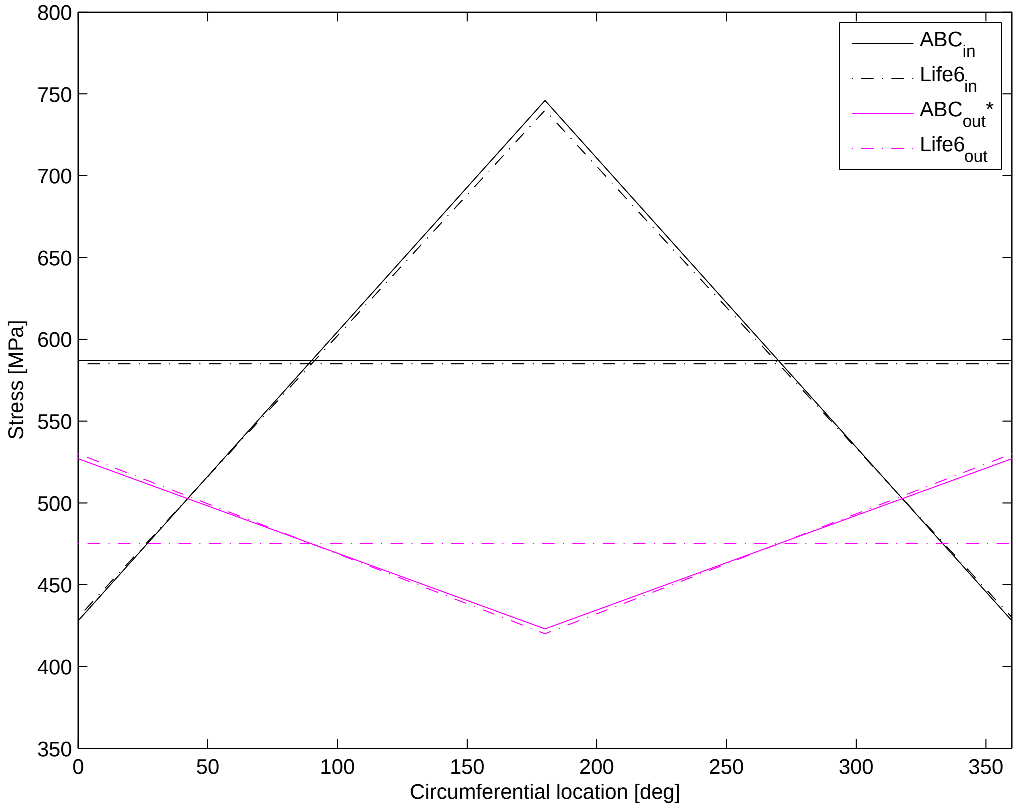

Figure 5-6: Friction stress around circumference with mean value correction for the outer tensile armour

5-4 Verification

Based the six general requirements for a local model (Grealish et al., 2006), the current capability of ABC Fatigue and advice in the context of model development is presented in table 5-10.

Tension domain enhancement

ABC Fatigue —a superposition of Model A and Model B— is currently not suitable for elaborate in-house local analysis. Three out of six criteria are not satisfied. In theory, follow-up on the third action presented in table 5-10 is sufficient to finalize a local model which is ready for data comparison, e.g. with specialist consultants and riser manufacturers. This relatively simple enhancement would enable in-house pre-analyses within the limit of the inner tensile armour. In addition, information exchange is advised to design the post-processing application.

Also ABC Fatigue can be extended to allow for in-house FEED studies next to in-field condition changes. A relatively cheap hence independent model is convenient as flexible riser analyses are not frequently carried out by Shell engineers. The model should be readily available in case of a sudden operational hazard.

Table 5-10: Six general local model requirements, ABC Fatigue capacity and action advice.

No.	Criterion	ABC Fatigue	Action
1	Validated against full-scale measurements.	No	Collaborate with insitution and/or specialist to obtain new data
2	Capable of modelling tension and curvature ranges.	No	Simple enhancement can include tension ranges
3	Preferably account for hysteresis effects, if not already addressed in the global or intermediate analysis.	No	Validation of Model C procedure
4	Take into account the effects of external pressure.	Yes	
5	Stresses to be calculated at the four corners of the rectangular shaped wires normally used for tensile armour.	Yes	
6	Preferably output stresses at eight points around the circumference, so that directionality effects can be considered.	Yes	

Full-scale validation experiments

Experimental data is required to validate ABC Fatigue up to industry standards. Currently, all three manufacturers of flexible pipe own a private test rig hence data is potentially generated and exchanged. However there should be a clear incentive, such as JIP involvement, to retrieve test data. Manufacturers are hesitant to disclose data other than presented in the JIP wrap-up report and have full rights over all data even managed by independent test facilities such as Marintek in Norway (Laksafoss and , NOV).

A full-scale validation strives for alignment between experiment and model load-response variables. Present work clearly presents an overview of all model variables, see A, hence relatively little effort is required to design an experiment and to validate ABC Fatigue accordingly.

Hysteresis Effects: Model C

Model C extension is recommended to fully benefit from ABC fatigue when dealing with sudden hazardous operational conditions. A full time-trace of tension and curvature and subsequent rainflow-counting generates more realistic stress-ranges by including wire position changes and corresponding friction and bending stresses. Full-scale measurements of curvature loads versus wire-slip responses of the (inner) tensile armour required.

Outer tensile armour

Although the inner tensile armour is assumed to be fatigue critical, it is strongly recommended to introduce a new relation for the axisymmetric response of the outer tensile armour. Cross-model validation would be sufficient however full-scale validation experiments are advised.

Chapter 6

Benchmark Case-Study

This chapter elaborates on the model experiment signifying the impact of changing design loads. This is evident as in-field measurements —i.e. monitoring of operational and metocean conditions and inspections of sudden and accumulated riser damage— prove deviations from initial predicted values used for flexible riser design and corresponding fatigue life calculation.

Present work advises imitation of this experiment (or then called pre-analysis) by Shell engineers to study the fatigue life margins of their flexible riser portfolio and to determine positive and negative fatigue life contributions from various input parameters. Also the relative impact of each input parameter is important to determine highly influential parameters which can potentially alter the fatigue life. Elaborate analysis by specialist consultants should subsequently investigate these predictions by generating accurate values —i.e. within the limits of current state-of-art model technology— resulting in a strategy to alter the fatigue life in case of critical fatigue life.

The influence of environmental loads is studied by deviation of the curvature and tension ranges. Operational load is signified by the inner-bore pressure. Parameter domains are derived from a 6 inch production riser operated by Shell in the North-Sea. Wire-stress accumulation, or stress-range, is relevant as this parameter is proportional to fatigue life.

6-1 Research Questions and Methodology

Research Objective: Signify the impact of changing design loads.

Four research questions were formulated to study the influence of environmental and operational conditions:

Question 1: What is the relative influence of pressure, tension and wire dimension on the magnitude of friction stress?

Question 2: What is the influence of the bi-linear response behaviour, i.e. wire-slip?

Question 3: Which circumferential location governs the stress calculation?

Question 4: Is the maximum stress range always acting at the same circumferential location?

Six experiments were carried out:

1. Pressure range - Stress range
2. Tension range - Stress range
3. Wire width range - Stress range
4. Curvature range - Stress range (Benchmark pressure/tension)
5. Curvature range - Stress range (High pressure)
6. Curvature range - Stress range (High tension)

An overview of of the six experiments and corresponding parameter deviations (compared to the benchmark level BM) is shown in table 6-1.

Table 6-1: Overview of six experiments and the deviations from benchmark values in each experiment

Experiment				Model A					Model B
				p	T	b	t	n	Ω
No.	Var	BM	Δ_{var}	[MPa]	[kN]	[mm]	[mm]	[-]	[1/m]
1	p	25	5	5-50					
2	T	100	20		20-200				
3	b	118.2	1.778			8-24	7.5-2.5	76-25	
4	Ω	0.01	0.004						0-0.04
5	Ω_p	0.01	0.004	60					0.0001-0.04
6	Ω_T	0.01	0.004		200				0.0001-0.04

To scale the cross-section with the wire-dimensions, a fraction filled ratio is usually around 0.9 for the tensile armour defined by equation 6-1.

$$F_f = \frac{nb}{\cos \alpha 2\pi a} \tag{6-1}$$

(Larsen et al., 2014)

For this experiment, Models A and B are identical to the validation algorithm "Model B Helica" described in appendix A.

6-2 Background: Realistic conditions

Parameters either fluctuate constantly with each environmental load cycle (curvature and tension) or more gradually over the entire lifetime (pressure and friction) or are assumed to be constant like the structural dimensions. Either way, it is evident that parameters are studied within a realistic domain to find realistic evidence in the context of over-conservatism. Two questions are answered with a background study to determine what parameters should be studied and for which values.

1. What parameters are likely to change throughout the riser lifetime?
2. What parameter domains should be studied for a flexible riser in North-Sea conditions?

Variable and constant parameters

To simulate with realistic ranges for load and geometry parameters it is important to acknowledge the following indicators of environmental and operational conditions corresponding to the North-Sea region.

- Wave loads: Dynamic top-tension and curvature
- Water depth/riser length: Static top-tension and curvature distribution
- Field lay-out: individual riser capacity (diameter), purposes (pressure) and risks (damage).
- Production plan: maximum production rate and utilization plan (pressure change)

Load ranges are based on the following categorisation of input values:

Constants: Wire width, thickness, area - number of wires, radius

Averaged: Inner bore pressure, Outer (hydrostatic) pressure, Tension (self-weight)

Ranged: Tension, Curvature

Computational constants: Friction coefficient, Critical curvature (based on experimental evidence)

Parameter domains

An elaborate fatigue analysis was done in 2014 to assess the riser fatigue integrity for flooded annulus conditions (Kenny). The 6" production riser was supplied by Technip and installed to the Anasuria FPSO in 2000, with a design life of 8 years. Geometry and loads are based on this riser and analysis.

The selection of realistic parameter domains is based on the following:

Variable 1: Pressure 5-50 MPa
Within realistic operational limits presented in design report.

Variable 2: Tension 20-200 kN
Based on operational values presented in recent riser analysis by MCS Kenny and design report.

Variable 3: Wire width 8-24 mm
Atypical values noticed, high variety and seemingly unrelated to load-conditions and riser diameter; values based on other case-studies and wire area remains constant.

Variable 4: Curvature -0.04-0.04 1/m
Based on range shown in recent riser analysis by MCS Kenny.

Table 6-2 summarizes the benchmark riser characteristics. Variations of inner bore pressure and external tension (averaged parameters), the wire dimensions (design constant) and curvature (ranged) will be cross-varied in 6 model-runs.

Table 6-2: Benchmark case-study characteristics; geometry and design load-cases (also used for validation of Model A)

Design PR 6"		i=1	i=2	i=3	i=4		
Geometry	E_i	200	200	200	200		GPa
	α_i	-86.6	87.6	30	-30		deg
	a_i	108.1	113	118.2	124.6		mm
	n_i	2	2	50	53		-
	A_i	218.7	45.3	60	60		mm^2
		LC1	LC2	LC3	LC4	LC5	
Loads	T_{ex}	0	220.6	220.6	131.1	0	kN
	p_{in}	46.2	46.2	0	50.8	72.1	MPa
	p_{out}	0	0	0	0	0	MPa

6-3 Hypothesis

6-3-1 Relative influence

Pressure and tension both increase the interlayer contact pressure hence delays the stress-releasing slip mechanism. A proportional relationship between pressure and stress range is expected.

A clear proportional relationship is expected between curvature and stress range. The multiplication factor c ($\Delta\Omega = c \cdot \Delta\sigma$) expected to dependent on pressure and tension levels.

6-3-2 Wire-slip

Initiation

The critical curvature (a computational constant dependent on interlayer contact pressure and friction coefficient) predicts the initiation of wire slip. This constant is a measure for the accumulation of friction stress. Pressure and tension both stimulate the interlayer contact pressure hence alter friction stress.

Various width/thickness ratios are studied to find unexpected relations between riser types and slip initiation which governs the wire-stress.

Impact

The impact of slip distance on the stress level can be studied when following the wire while re-calculating the bending-stresses at these new locations. This mechanism is not studied with Models A and B as the wire positions are not continuously updated while the curvature is increased. Furthermore, the relationship between riser curvature and slip distance is assumed to be linear. Consequently, studying position changes due to wire-slip is only relevant in assessments incorporating stick-slip behaviour and (irregular) cyclic loading.

6-3-3 Maximum stress location

As described in section 4-1, alternating stress contributions are superposed from axial shear stress (uniform) and local bending stress (linearly increasing towards outer fibers of the wire).

Figure 6-1 shows the expected stress increments for three different locations around the circumference: on the riser outrados $\psi = 180$, north-east position $\psi = 225$ and on the east neutral axis $\psi = 270$. The relations between curvature and wire-stress are all linear. However, stress increases non-linearly around the circumference.

The maximum stress is initially perceived at the outrados of the cross section because of the governing friction stress (blue line). The wires located at the neutral axis (green line) are subjected to the largest local bending stresses, this as a result of the rectangular shaped wires and variable wire orientation around the circumference (horizontal on the outrados and vertical at the neutral axis). All (normalized) local bending stress increments are shown in figure 6-1. After a certain curvature threshold Ω_b, the maximum stress is no longer perceived at the outrados.

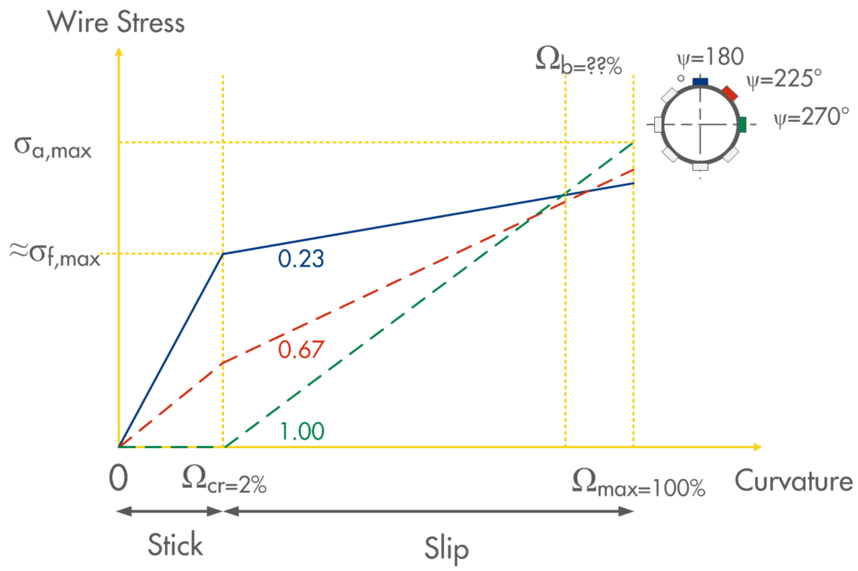

Figure 6-1: Expected curvature slopes monitored at three different positions around the circumference

Pressure and tension values are influencing the critical curvature hence the initial friction stress level. Wire dimensions determine the slope and thus location of the bending threshold; i.e. the curvature level Ω_b where the contribution of local bending dominates the maximum stress alternation.

Table 6-3 shows the slope of lateral and transverse curvature contributions respective to three circumferential locations. Because of its horizontal positioning on the outrados, $\omega_{3,180} = 0$ accordingly, the vertical orientation on the neutral axis results in $\omega_{2,90} = 0$.

6-4 Results

Parameter impact

Friction, bending and total stress were monitored at four constant locations around the circumference for all load conditions. Table 6-4 shows all stress range values σ_a and that wires at the outrados were

Table 6-3: Expected contributions from local bending

	$\frac{\delta\omega}{\delta\Omega}$			Moment	
Location	180°	225°	180°	b/t=2.4	Axis
ω_2	0.6	0.8	0	$\frac{1}{2}t$	H_3
ω_3	0	0.4	1.1	$\frac{1}{2}b$	H_2
$\Delta\sigma_b$	0.3	0.88	1.32		

experiencing the highest stresses $\sigma_{a,max}$ for all maximum load conditions Var$_{max}$. For each load-step Δ_{var} the wire stress increases with $\Delta_{\sigma var}$. These increments are normalized to show the relative influence of each parameter. Pressure is most influential within this domain with a stress increment of 12.85 MPa for each load-step of 5 MPa.

Linear curvature-stress relationships are established in experiments 1.4 to 1.6; The benchmark case shows a that for each curvature increment of 0.004 1/m, the stress increases with 1.58 MPa. The stress-increments $\Delta\sigma_{\Delta\Omega}$ are significantly higher at circumferential locations ψ_{225} and ψ_{270} compared to ψ_{180}.

Also, high pressure significantly increases the maximum stress level. Pressure increases with a factor 2.4 (25 to 60 MPa) while the maximum stress increases with 2.21 (71 to 157 MPa). The multiplication factor $c = 0.88$.

This compared to the tension which increases with a factor 2 (100 to 200 kN) while the stress increase is only 1.06 (71 to 75 MPa). The multiplication factor $c = 0.53$.

Both pressure and tension alter the interlayer contact pressure thus critical curvature and accordingly the friction stress can accumulate for a longer period before overcoming the available friction. Within this range, the expanding behaviour induced by inner-bore pressure is clearly more dominant than the contracting behaviour induced by increased tension.

Table 6-4: Experiment 1: Comparison of alternating stress at three positions around circumference

				$\psi = 180°$			$\psi = 225°$			$\psi = 270°$		
				$\sigma_{a,max}$	$\Delta\sigma_{\Delta var}$		$\sigma_{a,max}$	$\Delta\sigma_{\Delta var}$		$\sigma_{a,max}$	$\Delta\sigma_{\Delta var}$	
No.	Var	Var$_{max}$	Δ_{var}	[MPa]	[MPa]	[%]	[MPa]	[MPa]	[%]	[MPa]	[MPa]	[%]
1	p	50	5	117.93	12.85	100	67.49	6.29	100	10.54	-0.26	-5
2	T	200	20	61.26	1.40	11	38.87	0.60	10	12.20	0.02	0
3	b	24	1.778	104.81	7.60	59	74.42	5.31	84	29.44	2.32	41
4	Ω	0.04	0.004	64.77	1.58	12	70.63	4.98	79	50.69	5.60	100
5	Ω_p	0.04	0.004	153.87	1.58	12	114.41	5.00	80	49.03	5.63	100
6	Ω_T	0.04	0.004	71.37	1.58	12	73.88	4.99	79	50.56	5.61	100

6-4-1 Critical curvature and Wire-slip

Pressure, tension and wire dimensions all positively influence the critical curvature value resulting in higher friction stresses accordingly. Critical curvatures are calculated and constant for each load-case as shown in table 6-5. Pressure is dominating the critical curvature as expected and the 90%

difference with tension can be seen as another justification that tension is not dominating in North-Sea conditions due to shallow water hence low self weight induced pre-tension and tension domain.

6-4-2 Circumferential location of σ_{max}

As expected, under the influence of curvature highest stresses are no longer perceived by the outer fiber. For a maximum curvature of 0.04 1/m, the wire at $\psi = 225°$ shows highest stress responses for the benchmark load-case (experiment 4). However, in the high-pressure load-case this mechanism is not induced. Clearly high pressure significantly alters the friction stress and the threshold value Ω_b as described in section 6-3 is never reached.

Table 6-5 summarizes the maximum stress values at the outrados and the new maximum stress position ψ_{max}. This study is not relevant for the first three experiments as the curvature is constant and clearly the benchmark value $\Omega_{BM} = 0.011$/m is below threshold Ω_b.

The maximum stress alternation has moved right in experiment 4. High pressure delays or completely stops this mechanism showed by experiment 5. High tension delays Ω_b from 0.027 1/m to 0.031 1/m as showed in experiment 6.

For experiment 4, high pressure, the maximum stress is 9.9% higher than the stress in the outer fiber. For experiment 6, high tension, this value is 5.4%.

Table 6-5: Experiment 1: Comparison of alternating stress at outrados $\psi = 180°$ and maximum stress position around circumference

				$\psi = 180°$			$\psi = \sigma_{max}$				
				$\sigma_{a,max}$	$\Delta\sigma_{\Delta var}$		σ_{max}		ψ_{max}	Ω_b	Ω_{cr}
No.	Var	Var$_{max}$	Δ_{var}	[MPa]	[MPa]	[%]	[MPa]	[%]	[deg]	[1/m]	[%]
1	p	50	5	117.93	12.85	100	117.93	100	180	-	100
2	T	200	20	61.26	1.40	11	61.26	100	180	-	10
3	b	24	1.778	104.81	7.60	59	104.81	100	180	-	2
4	Ω	0.04	0.004	64.77	1.58		71.10	110	220	0.027	BM
5	Ω_p	0.04	0.004	153.87	1.58		153.87	100	180	-	BM
6	Ω_T	0.04	0.004	71.37	1.58		75.25	105	213	0.031	BM

6-4-3 Irregular wave conditions

A second small experiment was executed with Models A and C. Now the stick-slip algorithm was used, see 4-4-4. Irregular waves were simulated by variation of cycle length and curvature alternation to study change of stress ranges and wire slip after a wave train of 10 irregular waves.

Initial observation: due to low frequency of cyclic curvature, all wires return to initial circumferential position after a cull cycle. No stress range difference after 10 cycles, suspect wire slip is not properly defined.

After multiplication of slip with 1000, satisfactory slip-levels were established (20-30cm). Stress ranges of the tenth identical load cycle vary between 76 and 127 with a reference value of 121 MPa (first load cycle) for 5 identical runs with arbitrarily chosen wave amplitudes and cycle completions.

The following queries are currently not part of the pre-analysis objective but would be interesting to study after validating Model C:

1. Does a precedence of load cycles with an irregular character influence the relationship between curvature and maximum stress range?
2. Can computational uncertainties seriously impact the reliability of model results?

6-5 Conclusions

6-5-1 Observations

Influence of changing input parameters (pre-analysis)

Firstly, increasing pressure, tension and wire width all result in larger stress alternations for equal curvature levels. Pressure has the largest influence followed by wire width and tension.

Secondly, curvature-wire stress relations are linear and positive for all wire locations and three load conditions (Benchmark, high pressure, high tension) ψ, the slope of this relation increases for circumferential positions ψ towards the neutral axis at $\psi = 270$ as expected according to initial friction stress dominance and accumulating bending stresses for increasing curvature levels.

Thirdly, for this riser a pressure variation has a large impact on the curvature response compared to tension. The low pressure curvature - high pressure curvature multiplication factor is $c = 0.88$ and the low tension curvature - high tension curvature multiplication factor is $c = 0.53$.

Governance of friction stress

Increasing pressure, tension and wire width all result in a higher critical curvature value; i.e. wire slip is delayed. Pressure is clearly dominating this mechanism. However, tension also contributes and for other tension domains (deep water) this influence could become governing.

Circumferential maximum stress position

For a curvature value of Ω=0.01 1/m (benchmark), the maximum stress is always located at the outer fiber of the riser cross-section. The threshold value Ω_b indicating local bending dominance is not reached.

The threshold curvature is $\Omega_b = 0.027$ 1/m for the benchmark conditon. High pressurizing delays wire slip and maintains the highest stress range in the wire located at the outer fiber. High tension brings the threshold value Ω_b to 0.031 1/m.

Circumferential max moves to $\psi_{max} = 220°$ and the stress level is 10% higher than in the outer fiber at $\psi = 180°$. This is only 5% for the high-tension load-case. In high pressurized condition there is no difference.

This mechanism raises the question: What wires eventually govern fatigue life?

Irregular waves

Model C is not properly cross-validated. However, the impact of hysteresis was modelled indicatively; a precedence of load-cycles definitely influences the relationship between curvature magnitude and wire stress-range as expected.

6-5-2 Impact of changing design conditions

Each pre-analysis should incorporate an investigation of the load parameters pressure and tension cross-evaluated with an array of significant curvature domains. The study of this riser showed a predominant influence from pressure. Diligent study of pressure logs and the reformulation of one or multiple pressure load-cases can result in longer fatigue life.

Similarly the influence of friction coefficient is advised. The determination of this parameter is often tenuous but the impact can be large (proportional to the critical curvature hence initial friction stress.

A full time-trace of tension and curvature and subsequent rainflow-counting generates more realistic stress-ranges by including wire position changes and corresponding friction and bending stresses. If wire-slip and hysteresis are properly introduced by validating Model C, this mechanism probably redistributes the maximum stress among the circumferential wires hence lowering decisive stress ranges.

Chapter 7

Conclusions

The following research objective was formulated to guide this thesis work:

Studying Conservatism in Flexible Riser Fatigue Analysis and Development of an Engineering Model to Study Influencing Parameters of Local Wire Stress

First a literature review was conducted to study the three main elements of present work: integrity management, fatigue analysis methodology & conservatism and local modelling.

Secondly, the impact of changed conditions on the fatigue analysis steps are analysed . This resulted in a guideline to support engineers responsible for taking adequate measures after sudden condition changes are detected in fatigue-critical flexible riser systems.

Thirdly, a local model was developed able to convert curvature ranges to stress ranges; main goal was to imitate state-of-art local model-techniques used by specialist companies and other industry players. The model algorithm and validation methodology are presented.

Finally, a benchmark case-study illustrates the purpose of an in-house pre-analysis and the usefulness of ABC Fatigue by analysing a typical flexible riser designed for North-Sea environmental conditions.

State-of-Art knowledge

Current knowledge development in the context of fatigue analysis of flexible risers is focused on monitoring of operational data and incorporation of corrosion fatigue. The former can potentially reduce conservatisms from the global and local analysis steps. The latter mechanism inevitably diminishes the fatigue life however incorrect annulus environment predictions induce over-conservatisms.

A big step towards industry consensus and transparency of Fatigue Analysis Methodology was established in the Real Life JIP (2006). However, propriety of software models is still the main compromiser of model development and methodology consensus .

In the context of local modelling, three model theories can be used to simulate axisymmetric load-response behaviour. Pioneering work published in 1987 still hols as the state-of-art analytical method. Theory to simulate the rigourous bending behaviour is not converged and clearly published. Various analytical models are used by manufacturers, research institutes and regulators for design and research purposes. Their publications commonly refer to similar basic formulations with minor enhancements. Most studies conclude with a satisfactory model-validation through full-scale experiments and/or reference models. However fundamental differences regarding slip direction, stick-slip mechanism and cycle repetition are blurring true model fundaments, capabilities and limits.

To conclude, industry investigations are focused on stimulating data monitoring and management, small-scale testing and stimulating tranparency of hysteresis formulations applied in the bending model.

Flexible Riser Integrity Guideline

Currently, Shell's actions after detection of a sudden hazard heavily rely on the advice given by specialist consultants. Four actions are advised to change the collaboration environment. These actions are based on implementing actual conditions instead of initial predictions (loads) and elaborations of the local and global analysis models (formats and responses) where possible by determining the extensiveness of fatigue analyses through a rating system based on 31 conservatism indicators.

Pre-analyses and model runs can be done in-house, a verified model combined with recent operational data can quantify the impact of changed input data. Subsequent collaboration with specialist consultant is advised.

ABC Fatigue: in-house local model

ABC Fatigue —a superposition of Model A and Model B— is currently not suitable for elaborate in-house local analysis. Three out of six criteria are not satisfied. In theory, a tension domain enhancement is sufficient to finalize a local model ready for data comparison, e.g. with specialist consultants and riser manufacturers. This relatively simple enhancement would enable in-house pre-analyses within the limit of the inner tensile armour.

Model C incorporates wire-slip and the stick-slip behaviour. However, this application is not validated hence the study of irregular waves and hysteresis was not possible in present work.

Case-study

The study of a 6 inch case-study riser showed a predominant influence from pressure. Diligent study of pressure logs and the reformulation of one or multiple pressure load-cases can result in longer fatigue life.

Chapter 8

Recommendations

Restore balance

Currently, Shell's actions after detection of a sudden hazard heavily rely on the advice given by specialist consultants. Their advice and expertise are essential however a new action plan is advised to change the collaboration environment.

In addition, Shell can boost industry knowledge development by good data management, currently a company focus point. Documenting all operational load, response and condition parameters stimulates in-house model development and also enables a mutually beneficial collaboration with specialist consultants. This simultaneously restores the balance of knowledge reliability on external expertise. The specialist consultant averages the total stress around the circumference. Find out what averaging assumption are being used.

Pre-analyses

Imitation of the case-study experiment is advised to study the fatigue life margins of Shell's flexible riser portfolio and to determine positive and negative fatigue life contributions from various input parameters. Each pre-analysis should incorporate an investigation of the load parameters pressure and tension cross-evaluated with an array of significant curvature domains. In addition, information exchange is advised to design the post-processing application.

Similarly, the study of friction coefficient impact is advised. The determination of this parameter is often tenuous but the impact can be large (proportional to the critical curvature hence initial friction stress).

Also a pre-analysis for the given curvature ranges can point out the location of maximum wire-stresses and the position of this maximum. If wire-slip and hysteresis are properly introduced by verifying Model C, this mechanism can be studied. Ideally, this would redistribute the maximum stress among the circumferential wires hence lowers stress ranges and fatigue life.

Model development

Model C extension is recommended to fully benefit from ABC fatigue when dealing with sudden hazardous operational conditions. A full time-trace of tension and curvature and subsequent rainflow-counting generates more realistic stress-ranges by including wire position changes and corresponding friction and bending stresses. Full-scale measurements of curvature loads versus wire-slip responses of the (inner) tensile armour required.

Although the inner tensile armour is assumed to be fatigue critical, it is strongly recommended to introduce a new relation for the axisymmetric response of the outer tensile armour. Cross-model validation would be sufficient however full-scale validation experiments are advised.

Full-scale validation

A full-scale validation strives for alignment between experiment and model load-response variables. Present work clearly presents an overview of all model variables hence relatively little effort is required to design an experiment and to validate ABC Fatigue accordingly.

Furthermore, experimental data is required to validate ABC Fatigue up to industry standards. Currently, all three manufacturers of flexible pipe own a private test rig hence data is potentially generated and exchanged. However there should be a clear incentive, such as JIP involvement, to retrieve test data. Manufacturers are hesitant to disclose data other than presented in the JIP wrap-up report and have full rights over all data even when tests are managed by independent test facilities such as Marintek in Norway.

Appendix A

Model variables

Table A-1: My caption

Model A			
Geometry	For each layer i		
	Elastic modulus of metallic wires	E_i	MPa
	Laying angle	α_i	deg
	Radius	a_i	mm
	Number of wires	n_i	-
	Wire area	A_i	mm^2
Loads	External tension	T_{ex}	kN
	Wall tension	F_0	kN
	Inner bore pressure	p_{in}	MPa
	Outer pressure	p_{out}	MPa
Responses	Static stress	σ_s	MPa
	Pressure inside inner tensile layer	$p_{C,3}$	MPa
	Pressure outside inner tensile layer	$p_{C,4}$	MPa

Model B			
Loads	Curvature	Ω	1/m
Geometry	Circumferential position	ψ	deg
	Wire width	b	mm
	Wire thickness	t	mm
	Friction coefficient	μ	-
Responses	Critical curvature	Ω_{cr}	1/m
	Friction stress	σ_f	MPa
	Local bending stress	σ_b	MPa
	Total wire stress	σ_a	MPa

Model C			
Loads	Minimum curvature	Ω_{min}	1/m
	Maximum curvature	Ω_{max}	1/m
	Curvature frequency	f	1/s
	Number of cycles	n_c	-
	Time-step	Δt	s
Geometry	Helix pitch length	L_p	mm
	Initial circumferential wire location	$\psi_{w,0}$	deg
	Initial wire location along the helix	$H_{w,0}$	mm
Responses	Wire slip	ΔH	mm/s
	Final circumferential wire location	ψ_w	deg
	Final wire location along the helix	H_w	mm
	Friction stress range	$\Delta\sigma_f$	MPa
	Bending stress range	$\Delta\sigma_b$	MPa
	Total stress range	$\Delta\sigma$	MPa
	Mean wire stress	σ_m	MPa

Appendix B

Validation

B-1 Matlab Code

B-1-1 Model A

Design report 6" production riser

```
clear all
clc
close all
format loose

%+++++++++++++++++++++++++++++++++++++++++++++++++++++++++++++++++++++++
%               VARIABLE INPUT
    T_ex    = 0;      %[N] External tension
    p_in    = 46.2;   %[MPa] Inner bore pressure
    p_out   = 0.1;      %[MPa] Outer (hydrostatic) pressure
%
%+++++++++++++++++++++++++++++++++++++++++++++++++++++++++++++++++++++++

%%%%%%%%%%%%%%%%%% GEOMETRY RISER %%%%%%%%%%%%%%%%
%input riser geometry
a_in    = 108.1;    %[mm] Inner bore radius
a_out   = 124.6;   %[mm] Outer pipe radius
L       = 15000;  %[mm] Length local pipe section
N       = 4;      %[-] Number of metallic layers

%%%%%%%%%%%%%%%%%% MATERIAL LAYERS %%%%%%%%%%%%%%%%
%Elastic modulus
E1 = 200E3;
E2 = 200E3;
E3 = 200E3;
E4 = 200E3;

```

```
%%%%%%%%%%% GEOMETRY LAYERS %%%%%%%%%%%%%%%%%%
%Wire laying angle
alpha1 = -86.1*(pi/180); %[rad]
alpha2 = 87.6*(pi/180);
alpha3 = 30*(pi/180);
alpha4 = -30*(pi/180);

%Layer radius
a1 = 108.1;
a2 = 113;
a3 = 118.2;
a4 = 124.6;

%Layer number of wires
n1 = 2;
n2 = 2;
n3 = 50;
n4 = 53;

%Layer Area of wire
A1 = 218.7;
A2 = 45.3;
A3 = 60;
A4 = 60;

% Wire geometry
b = 12; %width
t = 5 ; %height

%
    ============================================================================
% Part A
%=========================================================================
sigma1_L = (E1*cos(alpha1)^2)/L;
sigma1_a = (E1*sin(alpha1)^2)/a1;

sigma2_L = (E2*cos(alpha2)^2)/L;
sigma2_a = (E2*sin(alpha2)^2)/a2;

sigma3_L = (E3*cos(alpha3)^2)/L;
sigma3_a = (E3*sin(alpha3)^2)/a3;

sigma4_L = (E4*cos(alpha4)^2)/L;
sigma4_a = (E4*sin(alpha4)^2)/a4;

F_1 = n1*A1*cos(alpha1);
F_2 = n2*A2*cos(alpha2);
F_3 = n3*A3*cos(alpha3);
F_4 = n4*A4*cos(alpha4);

%Summation for F_i and i=1:N
F_L = F_1*sigma1_L+F_2*sigma2_L+F_3*sigma3_L+F_4*sigma4_L;

F_a = F_1*sigma1_a+F_2*sigma2_a+F_3*sigma3_a+F_4*sigma4_a;
```

```
F_0c = T_ex + pi*p_in*a_in^2-pi*p_out*a_out^2;
F_0lin = (pi*p_in-pi*p_out)*2;
F_0nl = (pi*p_in-pi*p_out);

p_1 = (n1*A1*sin(alpha1)*tan(alpha1))/(2*pi*a1);
p_2 = (n2*A2*sin(alpha2)*tan(alpha2))/(2*pi*a2);
p_3 = (n3*A3*sin(alpha3)*tan(alpha3))/(2*pi*a3);
p_4 = (n4*A4*sin(alpha4)*tan(alpha4))/(2*pi*a4);

%Summation for p_i and i=1:N
p_L = p_1*sigma1_L+p_2*sigma2_L+p_3*sigma3_L+p_4*sigma4_L;
p_a = p_1*sigma1_a+p_2*sigma2_a+p_3*sigma3_a+p_4*sigma4_a;

p_0c = p_in*a_in - p_out*a_out;
p_0lin = p_in-p_out;

% Newton Raphson solution of two nonlinear algebraic equations
% set up the iteration
error1 = 1.e8;
xx(1) = 1; % Da (radial expansion)
xx(2) =10; %DL (elongation)
iter=0;
itermax=30;

% begin iteration
while error1>1.e-12
iter=iter+1;
x = xx(1); % Da expansion
y = xx(2); % DL elongation
% calculate the functions
f(1)= F_L*y +F_a*x - F_0c -F_0lin*x -F_0nl*x^2;
f(2)= p_L*y +p_a*x - p_0c -p_0lin*x;
% calculate the Jacobian
J(1,1) = F_a - F_0lin -2*F_0nl*x;
J(1,2) = F_L;
J(2,1) = p_a - p_0lin;
J(2,2) = p_L;
% solve the linear equations
yy = -J\f ;
% move the solution, xx(k+1) - xx(k), to xx(k+1)
xx = xx + yy ;
% calculate norms
error1=sqrt(yy(1)*yy(1)+yy(2)*yy(2));
error(iter)=sqrt(f(1)*f(1)+f(2)*f(2));
ii(iter)=iter;
if (iter > itermax)
error1 = 0.;
s=sprintf('****Did not converge within %3.0f iterations.****',itermax);
disp(s)
end
% check if error1 < 1.e-12
end
x = xx(1);
y = xx(2);
```

```
f(1)= F_L*y +F_a*x - F_0c -F_0lin*x -F_0nl*x^2;
f(2)= p_L*y +p_a*x - p_0c -p_0lin*x;
% print results
f;
xx;
iter;
% % plot results
% semilogy(ii,error)
% xlabel('iteration number')
% ylabel('norm of functions')
% clear ii
% clear error

% Wall tension
F_0deformed = F_L*y + F_a*x;
F_0load = F_0c +F_0lin*x + F_0nl*x^2;

%%%%%%%%%%%% OUTPUT PART A %%%%%%%%%%%%%%%%%%
%%%%%%%%%%% AXISYMMETRIC WIRE STRESS %%%%%%%%%%%%%%%%%%
sigma1 = sigma1_L*y + sigma1_a*x;
sigma2 = sigma2_L*y + sigma2_a*x;
sigma3 = sigma3_L*y + sigma3_a*x;
sigma4 = sigma4_L*y + sigma4_a*x;
sigma = [sigma1 sigma2 sigma3 sigma4];
display(sigma);

%Calculate pressure differential
Dp1= (n1*A1*sigma1*sin(alpha1)*tan(alpha1))/(2*pi*a1^2);
Dp2= (n2*A2*sigma2*sin(alpha2)*tan(alpha2))/(2*pi*a2^2);
Dp3= (n3*A3*sigma3*sin(alpha3)*tan(alpha3))/(2*pi*a3^2);
Dp4= (n4*A4*sigma4*sin(alpha4)*tan(alpha4))/(2*pi*a4^2);
Dp = [Dp1 Dp2 Dp3 Dp4];

%%%%%%%%%%% CONTACT PRESSURE %%%%%%%%%%%%%%%%%%
pC1 = p_in;
pC2 = pC1 - Dp1;
pC3 = pC2 - Dp2;
pC4 = pC3 - Dp3;
pC5 = pC4 - Dp4;
pC = [pC3; pC4; pC5];
pC_error = pC5-p_out ;
pC = pC - pC_error;
display(pC);
```

B-1-2 Model B: Maximum Curvature

Helica 6" umbilical

```
clear all
clc

close all
format loose
format shortg

%%%%%%%%%%%%%%%%%% LOADS %%%%%%%%%%%%%%%%%%%
%input axisymmetric loads
T_ex     = 1000000;      %[N] External tension
p_in     = -0.1;    %[MPa] Inner bore pressure
p_out    = 0.1;       %[MPa] Outer (hydrostatic) pressure

%%%%%%%%%%%%%%%%% GEOMETRY RISER %%%%%%%%%%%%%%%%
%input riser geometry
a_in     = 108.1;     %[mm] Inner bore radius
a_out    = 124.6;    %[mm] Outer pipe radius
L        = 15000;  %[mm] Length local pipe section
N        = 4;      %[-] Number of metallic layers

%%%%%%%%%%%%%%%%% MATERIAL LAYERS %%%%%%%%%%%%%%%%
%Elastic modulus
E1 = 210E3;
E2 = 210E3;
E3 = 210E3;
E4 = 210E3;

%%%%%%%%%%% GEOMETRY LAYERS %%%%%%%%%%%%%%%%%%
%Wire laying angle
alpha1 = -87.7*(pi/180); %[rad]
alpha2 = 87.7*(pi/180);
alpha3 = 35*(pi/180);
alpha4 = -36.7*(pi/180);

%Layer radius
%old radii
a1_0 = 108.1;
a2_0 = 113;
a3_0 = 118.2;
a4_0 = 124.6;
% radius scale factor
a_delta_p = 0.72

%new radii
a1 = a1_0*a_delta_p
a2 = a2_0*a_delta_p;
a3 = 82;
a4 = 93;
```

```
a_in = a1;
a_out = a4;

%%Layer number of wires
n1 = 1;
n2 = 0;
n3 = 38;
n4 = 42;

%Layer Area of wire
A1 = 2.5;
A2 = 30;
A3 = 50;
A4 = 50;
%
   ============================================================================

% Part A
%============================================================================
sigma1_L = (E1*cos(alpha1)^2)/L;
sigma1_a = (E1*sin(alpha1)^2)/a1;

sigma2_L = (E2*cos(alpha2)^2)/L;
sigma2_a = (E2*sin(alpha2)^2)/a2;

sigma3_L = (E3*cos(alpha3)^2)/L;
sigma3_a = (E3*sin(alpha3)^2)/a3;

sigma4_L = (E4*cos(alpha4)^2)/L;
sigma4_a = (E4*sin(alpha4)^2)/a4;

F_1 = n1*A1*cos(alpha1);
F_2 = n2*A2*cos(alpha2);
F_3 = n3*A3*cos(alpha3);
F_4 = n4*A4*cos(alpha4);

%Summation for F_i and i=1:N
F_L = F_1*sigma1_L+F_2*sigma2_L+F_3*sigma3_L+F_4*sigma4_L;

F_a = F_1*sigma1_a+F_2*sigma2_a+F_3*sigma3_a+F_4*sigma4_a;


F_0c = T_ex + pi*p_in*a_in^2-pi*p_out*a_out^2;
F_0lin = (pi*p_in-pi*p_out)*2;
F_0nl = (pi*p_in-pi*p_out);

p_1 = (n1*A1*sin(alpha1)*tan(alpha1))/(2*pi*a1);
p_2 = (n2*A2*sin(alpha2)*tan(alpha2))/(2*pi*a2);
p_3 = (n3*A3*sin(alpha3)*tan(alpha3))/(2*pi*a3);
p_4 = (n4*A4*sin(alpha4)*tan(alpha4))/(2*pi*a4);

%Summation for p_i and i=1:N
p_L = p_1*sigma1_L+p_2*sigma2_L+p_3*sigma3_L+p_4*sigma4_L;
p_a = p_1*sigma1_a+p_2*sigma2_a+p_3*sigma3_a+p_4*sigma4_a;
```

```
p_0c = p_in*a_in - p_out*a_out;
p_0lin = p_in-p_out;

% Newton Raphson solution of two nonlinear algebraic equations
% set up the iteration
error1 = 1.e8;
xx(1) = 1; % Da (radial expansion)
xx(2) =10; %DL (elongation)
iter=0;
itermax=30;

% begin iteration
while error1>1.e-12
iter=iter+1;
x = xx(1); % Da expansion
y = xx(2); % DL elongation
% calculate the functions
f(1)= F_L*y +F_a*x - F_0c -F_0lin*x -F_0nl*x^2;
f(2)= p_L*y +p_a*x - p_0c -p_0lin*x;
% calculate the Jacobian
J(1,1) = F_a - F_0lin -2*F_0nl*x;
J(1,2) = F_L;
J(2,1) = p_a - p_0lin;
J(2,2) = p_L;
% solve the linear equations
yy = -J\f ;
% move the solution, xx(k+1) - xx(k), to xx(k+1)
xx = xx + yy ;
% calculate norms
error1=sqrt(yy(1)*yy(1)+yy(2)*yy(2));
error(iter)=sqrt(f(1)*f(1)+f(2)*f(2));
ii(iter)=iter;
if (iter > itermax)
error1 = 0.;
s=sprintf('****Did not converge within %3.0f iterations.****',itermax);
disp(s)
end
% check if error1 < 1.e-12
end
x = xx(1);
y = xx(2);
f(1)= F_L*y +F_a*x - F_0c -F_0lin*x -F_0nl*x^2;
f(2)= p_L*y +p_a*x - p_0c -p_0lin*x;
% print results
f;
xx;
iter;
% % plot results
% semilogy(ii,error)
% xlabel('iteration number')
% ylabel('norm of functions')
% clear ii
% clear error

% Wall tension
```

```
F_0deformed = F_L*y + F_a*x;
F_0load = F_0c +F_0lin*x + F_0nl*x^2;

%%%%%%%%%%%% OUTPUT PART A %%%%%%%%%%%%%%%%%%
%%%%%%%%%%% AXISYMMETRIC WIRE STRESS %%%%%%%%%%%%%%%%%%
sigma1 = sigma1_L*y + sigma1_a*x;
sigma2 = sigma2_L*y + sigma2_a*x;
sigma3 = sigma3_L*y + sigma3_a*x
sigma4 = sigma4_L*y + sigma4_a*x

%Calculate pressure differential
Dp1= (n1*A1*sigma1*sin(alpha1)*tan(alpha1))/(2*pi*a1^2);
Dp2= (n2*A2*sigma2*sin(alpha2)*tan(alpha2))/(2*pi*a2^2);
Dp3= (n3*A3*sigma3*sin(alpha3)*tan(alpha3))/(2*pi*a3^2);
Dp4= (n4*A4*sigma4*sin(alpha4)*tan(alpha4))/(2*pi*a4^2);
Dp = [Dp1 Dp2 Dp3 Dp4];

%%%%%%%%%%% CONTACT PRESSURE %%%%%%%%%%%%%%%%%%
pC1 = p_in;
pC2 = pC1 - Dp1;
pC3 = pC2 - Dp2;
pC4 = pC3 - Dp3;
pC5 = pC4 - Dp4;
pC = [pC3; pC4; pC5]

%%%%%%%%%%%%% INNER TENSILE ARMOUR i=3 %%%%%%%%%%%

%%
%=======================================================
%                VARIABLE: CURVATURE
%                input values
                 Omega_min = -0.3; %1/m
                 Omega_max = 0.3; %1/m
%=======================================================
%Friction factor (equal for all layers)
mu = 0.2;

%Wire dimensions
b = 10; %mm
t = 5;  %mm

%Curvature range and amplitude
Omega_min = Omega_min/1000; %1/mm
Omega_max = Omega_max/1000; %1/mm
Omega_range = Omega_max - Omega_min;
Omega_ampl = Omega_range/2;

%Critical curvature
Omega_cr3 = (mu*(pC3 +pC4))/(E3*A3*cos(alpha3)^2*sin(alpha3))*(pi/2); %1/mm

% Circumferential position psi = psi(degrees +1)
% --> 0 degrees = intrados
points = 360;
PSI = points+1;
psi = linspace(0,360,PSI);
```

```
%Hotspot position
H2=0.5*b;
H3=0.5*t;

%pre-allocation friction stress
theta_left = zeros(1,PSI);
theta_right = zeros(1,PSI);
for i=1:PSI %range = outrados to right neutral axis
     if psi(i) <= 180 %LEFT SIDE OF CROSS SECTION
theta_left(i) =(psi(i)*pi)/(180)-pi/2;

% Friction stress
sigma_f(i) = ((mu*a3*(pC3 +pC4))/(t*sin(alpha3)))*theta_left(i);

    else %RIGHT SIDE OF CROSS SECTION
theta_right(i) = (pi/2-((pi/180)*psi(i-180)));

% Friction stress
sigma_f(i) = ((mu*a3*(pC3 +pC4))/(t*sin(alpha3)))*theta_right(i);
     end;

% Local bending Stress @ max curvature
sigma_b2_cr(i) = -E3*H2*cos(alpha3)*(1+sin(alpha3)^2)*sin(psi(i)*(pi/180))*
    Omega_cr3;
sigma_b3_cr(i) = -E3*H3*cos(alpha3)^4*cos(psi(i)*(pi/180))*Omega_cr3;
sigma_b_cr(i) = sigma_b2_cr(i) + sigma_b3_cr(i);

sigma_b2_max(i) = -E3*H2*cos(alpha3)*(1+sin(alpha3)^2)*sin(psi(i)*(pi/180))
    *Omega_max;
sigma_b3_max(i) = -E3*H3*cos(alpha3)^4*cos(psi(i)*(pi/180))*Omega_max;
sigma_b_max(i) = sigma_b2_max(i) + sigma_b3_max(i);

sigma_O_cr(i) = sigma_f(i)+ sigma_b_cr(i);
sigma_O_max(i) = sigma_f(i)+ sigma_b_max(i);
end

% ++++++++++++++++++++++++++++++++++++++++++++++++++++++++++++++
%                        POST PROCESSING
%                        INNER ARMOUR
% ++++++++++++++++++++++++++++++++++++++++++++++++++++++++++++++
figure
plot(psi,sigma_f,'r', psi,sigma_b_max,'b', psi,sigma_O_max,'g')
legend('Friction stress','Bending stress','Total stress')
axis([0,360,-400,400]);
xlabel('Circumferential location [deg]');
ylabel('Stress [MPa]');
print -depsc validationbft_psi.eps

% =========================================================
%               @ outrados  psi = 180 degrees
%               @ northeast psi = 225 degrees
%==========================================================
%response values
% @ outrados
```

```
sigma_f_180 = [0 sigma_f(181) sigma_f(181)];
sigma_b2_180 = [0 sigma_b2_cr(181) sigma_b2_max(181)];
sigma_b3_180 = [0 sigma_b3_cr(181) sigma_b3_max(181)];
sigma_b_180 = [0 sigma_b_cr(181) sigma_b_max(181)];
sigma_O_180 = [0 sigma_O_cr(181) sigma_O_max(181)];

%@ psi = 225 degrees
sigma_f_225 = [0 sigma_f(226) sigma_f(226)];
sigma_b2_225 = [0 sigma_b2_cr(226) sigma_b2_max(226)];
sigma_b3_225 = [0 sigma_b3_cr(226) sigma_b3_max(226)];
sigma_b_225= [0 sigma_b_cr(226) sigma_b_max(226)];
sigma_O_225 = [0 sigma_O_cr(226) sigma_O_max(226)];

%Curvatures
Omega3 = [0 Omega_cr3 Omega_max];

%plots
% friction-, total-stress @ psi = 180 deg, outrados
figure
plot(Omega3,sigma_f_180,'r',Omega3,sigma_O_180,'g')
legend('Friction stress', 'Total stress','location','northwest')
axis([0,0.0003,0,400]);
xlabel('Curvature [1/m]');
ylabel('Stress [MPa]');
print -depsc validationb180.eps

% friction-, total-stress @ psi = 225 deg
figure
plot(Omega3,sigma_f_225,'r',Omega3,sigma_O_225,'g')
legend('Friction stress', 'Total stress', 'location','northwest')
axis([0,0.0003,0,400]);
xlabel('Curvature [1/m]');
ylabel('Stress [MPa]');
print -depsc validationb225.eps

%VALIDATION
%Curvatures
Omega3 = [0 0.00002 Omega_max];
%validation psi = 180 degrees
sigmah_180 = [0 168 235];   %Helica
sigma_180 = [0 sigma_f_180(2) sigma_O_180(3)];    %ABC Fatigue

%%validation psi = 225 degrees
sigmah_225 = [0 84 365 ];   %Helica
sigma_225 = [0 sigma_f_225(2) sigma_O_225(3)];     %ABC Fatigue

%total-stress @ psi = 180,225 deg for Helica and ABC Fatigue
figure
plot(Omega3,sigma_180,'m',Omega3,sigmah_180,'m-.',Omega3,sigma_225,'k',
    Omega3,sigmah_225,'k-.' )
legend('ABC_{180}', 'Helica_{180}','ABC_{225}', 'Helica_{225}','location','
    northwest')
axis([-0.00005,0.0003,0,400]);
xlabel('Curvature [1/m]');
ylabel('Stress [MPa]');
```

```
print -depsc validationb180225.eps
```

Life6 6" riser

```
clear all
clc
close all
format loose
format shortg

%%%%%%%%%%%%%%%%%% LOADS %%%%%%%%%%%%%%%%%%%
%input axisymmetric loads
T_ex     = 0;       %[N] External tension
p_in     = 50;    %[MPa] Inner bore pressure
p_out    = -0.01;      %[MPa] Outer (hydrostatic) pressure

%%%%%%%%%%%%%%%%% GEOMETRY RISER %%%%%%%%%%%%%%%%
%input riser geometry
a_in     = 108.1;    %[mm] Inner bore radius
a_out    = 124.6-20;   %[mm] Outer pipe radius
L        = 15000;  %[mm] Length local pipe section
N        = 4;       %[-] Number of metallic layers

%%%%%%%%%%%%%%%%% MATERIAL LAYERS %%%%%%%%%%%%%%%%
%Elastic modulus
E1 = 200E3;
E2 = 200E3;
E3 = 200E3;
E4 = 200E3;

%%%%%%%%%%% GEOMETRY LAYERS %%%%%%%%%%%%%%%%%%
%Wire laying angle
alpha1 = -86.1*(pi/180); %[rad]
alpha2 = 87.6*(pi/180);
alpha3 = 30*(pi/180);
alpha4 = -30*(pi/180);

%Layer radius
a1 = 108.1;
a2 = 113;
a3 = 118.2-18;
a4 = 124.6-20;

%%Layer number of wires
n1 = 2;
n2 = 2;
n3 = 29;
n4 = 31;

%Layer Area of wire
A1 = 218.7;
A2 = 45.3;
A3 = 60;
A4 = 60;

```

```
%
    ===========================================================================
% Part A
%=========================================================================
sigma1_L = (E1*cos(alpha1)^2)/L;
sigma1_a = (E1*sin(alpha1)^2)/a1;

sigma2_L = (E2*cos(alpha2)^2)/L;
sigma2_a = (E2*sin(alpha2)^2)/a2;

sigma3_L = (E3*cos(alpha3)^2)/L;
sigma3_a = (E3*sin(alpha3)^2)/a3;

sigma4_L = (E4*cos(alpha4)^2)/L;
sigma4_a = (E4*sin(alpha4)^2)/a4;

F_1 = n1*A1*cos(alpha1);
F_2 = n2*A2*cos(alpha2);
F_3 = n3*A3*cos(alpha3);
F_4 = n4*A4*cos(alpha4);

%Summation for F_i and i=1:N
F_L = F_1*sigma1_L+F_2*sigma2_L+F_3*sigma3_L+F_4*sigma4_L;

F_a = F_1*sigma1_a+F_2*sigma2_a+F_3*sigma3_a+F_4*sigma4_a;

F_0c = T_ex + pi*p_in*a_in^2-pi*p_out*a_out^2;
F_0lin = (pi*p_in-pi*p_out)*2;
F_0nl = (pi*p_in-pi*p_out);

p_1 = (n1*A1*sin(alpha1)*tan(alpha1))/(2*pi*a1);
p_2 = (n2*A2*sin(alpha2)*tan(alpha2))/(2*pi*a2);
p_3 = (n3*A3*sin(alpha3)*tan(alpha3))/(2*pi*a3);
p_4 = (n4*A4*sin(alpha4)*tan(alpha4))/(2*pi*a4);

%Summation for p_i and i=1:N
p_L = p_1*sigma1_L+p_2*sigma2_L+p_3*sigma3_L+p_4*sigma4_L;
p_a = p_1*sigma1_a+p_2*sigma2_a+p_3*sigma3_a+p_4*sigma4_a;

p_0c = p_in*a_in - p_out*a_out;
p_0lin = p_in-p_out;

% Newton Raphson solution of two nonlinear algebraic equations
% set up the iteration
error1 = 1.e8;
xx(1) = 1; % Da (radial expansion)
xx(2) =10; %DL (elongation)
iter=0;
itermax=30;

% begin iteration
while error1>1.e-12
iter=iter+1;
x = xx(1); % Da expansion
```

```
y = xx(2); % DL elongation
% calculate the functions
f(1)= F_L*y +F_a*x - F_0c -F_0lin*x -F_0nl*x^2;
f(2)= p_L*y +p_a*x - p_0c -p_0lin*x;
% calculate the Jacobian
J(1,1) = F_a - F_0lin -2*F_0nl*x;
J(1,2) = F_L;
J(2,1) = p_a - p_0lin;
J(2,2) = p_L;
% solve the linear equations
yy = -J\f ;
% move the solution, xx(k+1) - xx(k), to xx(k+1)
xx = xx + yy ;
% calculate norms
error1=sqrt(yy(1)*yy(1)+yy(2)*yy(2));
error(iter)=sqrt(f(1)*f(1)+f(2)*f(2));
ii(iter)=iter;
if (iter > itermax)
error1 = 0.;
s=sprintf('****Did not converge within %3.0f iterations.****',itermax);
disp(s)
end
% check if error1 < 1.e-12
end
x = xx(1);
y = xx(2);
f(1)= F_L*y +F_a*x - F_0c -F_0lin*x -F_0nl*x^2;
f(2)= p_L*y +p_a*x - p_0c -p_0lin*x;
% print results
f;
xx;
iter;
% % plot results
% semilogy(ii,error)
% xlabel('iteration number')
% ylabel('norm of functions')
% clear ii
% clear error

% Wall tension
F_0deformed = F_L*y + F_a*x;
F_0load = F_0c +F_0lin*x + F_0nl*x^2;

%%%%%%%%%%%% OUTPUT PART A %%%%%%%%%%%%%%%%%%
%%%%%%%%%%% AXISYMMETRIC WIRE STRESS %%%%%%%%%%%%%%%%%%
sigma1 = sigma1_L*y + sigma1_a*x;
sigma2 = sigma2_L*y + sigma2_a*x;
sigma3 = sigma3_L*y + sigma3_a*x
sigma4 = sigma4_L*y + sigma4_a*x

%Calculate pressure differential
Dp1= (n1*A1*sigma1*sin(alpha1)*tan(alpha1))/(2*pi*a1^2);
Dp2= (n2*A2*sigma2*sin(alpha2)*tan(alpha2))/(2*pi*a2^2);
Dp3= (n3*A3*sigma3*sin(alpha3)*tan(alpha3))/(2*pi*a3^2);
Dp4= (n4*A4*sigma4*sin(alpha4)*tan(alpha4))/(2*pi*a4^2);
```

```
Dp = [Dp1 Dp2 Dp3 Dp4];

%%%%%%%%%%% CONTACT PRESSURE %%%%%%%%%%%%%%%%%
pC1 = p_in;
pC2 = pC1 - Dp1;
pC3 = pC2 - Dp2;
pC4 = pC3 - Dp3;
pC5 = pC4 - Dp4;
pC = [pC3; pC4; pC5];
%display(pC);

%%
%=====================================================
%               VARIABLE: CURVATURE
%               input values
                Omega_min = -0.3; %1/m
                Omega_max = 0.2; %1/m
%=====================================================
%Friction factor (equal for all layers)
mu = 0.113;

%Wire dimensions
b = 20; %mm
t = 3;  %mm

%Curvature range and amplitude
Omega_min = Omega_min/1000; %1/mm
Omega_max = Omega_max/1000; %1/mm
Omega_range = Omega_max - Omega_min;
Omega_ampl = Omega_range/2;

%Critical curvature
Omega_cr3 = (mu*(pC3 +pC4))/(E3*A3*cos(alpha3)^2*sin(alpha3))*(pi/2); %1/mm
Omega_cr4 = (mu*(pC4 +pC5))/(E4*A4*cos(alpha4)^2*sin(alpha4))*(pi/2); %1/mm

% Circumferential position psi = psi(degrees +1)
% --> 0 degrees = intrados
points = 360;
PSI = points+1;
psi = linspace(0,360,PSI);

%Hotspot position
H2=0.5*b;
H3=0.5*t;

%pre-allocation friction stress
theta_left = zeros(1,PSI);
theta_right = zeros(1,PSI);
for i=1:PSI %range = outrados to right neutral axis
     if psi(i) <= 180 %LEFT SIDE OF CROSS SECTION
        theta_left(i) =(psi(i)*pi)/(180)-pi/2;

% Friction stress
        sigma_f(i) = ((mu*a3*(pC3 +pC4))/(t*sin(alpha3)))*theta_left(i);

```

```
    else %RIGHT SIDE OF CROSS SECTION
        theta_right(i) = (pi/2-((pi/180)*psi(i-180)));

% Friction stress
        sigma_f(i) = ((mu*a3*(pC3 +pC4))/(t*sin(alpha3)))*theta_right(i);
      end;

% Local bending Stress
sigma_b2_cr(i) = -E3*H2*cos(alpha3)*(1+sin(alpha3)^2)*sin(psi(i)*(pi/180))*Omega_cr3;
sigma_b3_cr(i) = -E3*H3*cos(alpha3)^4*cos(psi(i)*(pi/180))*Omega_cr3;
sigma_b_cr(i) = sigma_b2_cr(i) + sigma_b3_cr(i);

sigma_b2_max(i) = -E3*H2*cos(alpha3)*(1+sin(alpha3)^2)*sin(psi(i)*(pi/180))*Omega_max;
sigma_b3_max(i) = -E3*H3*cos(alpha3)^4*cos(psi(i)*(pi/180))*Omega_max;
sigma_b_max(i) = sigma_b2_max(i) + sigma_b3_max(i);

sigma_0_cr(i) = sigma_f(i)+ sigma_b_cr(i);
sigma_0_max(i) = sigma_f(i)+ sigma_b_max(i);

%+++++++++++++++++++++++++++++++++++++++++++++++++++++
%               OUTER TENSILE ARMOUR
%+++++++++++++++++++++++++++++++++++++++++++++++++++++
      if psi(i) <= 180 %LEFT SIDE OF CROSS SECTION
        theta_left(i) =(psi(i)*pi)/(180)-pi/2;

        % Friction stress
        sigma_f4(i) = ((mu*a4*(pC4 +pC5))/(t*sin(alpha4)))*theta_left(i);

    else %RIGHT SIDE OF CROSS SECTION
        theta_right(i) = (pi/2-((pi/180)*psi(i-180)));

        % Friction stress
        sigma_f4(i) = ((mu*a4*(pC4 +pC5))/(t*sin(alpha4)))*theta_right(i);
      end;

sigma_b2_cr4(i) = -E4*H2*cos(alpha4)*(1+sin(alpha4)^2)*sin(psi(i)*(pi/180))*Omega_cr4;
sigma_b3_cr4(i) = -E4*H3*cos(alpha4)^4*cos(psi(i)*(pi/180))*Omega_cr4;
sigma_b_cr4(i) = sigma_b2_cr4(i) + sigma_b3_cr4(i);

sigma_b2_max4(i) = -E4*H2*cos(alpha4)*(1+sin(alpha4)^2)*sin(psi(i)*(pi/180))*Omega_max;
sigma_b3_max4(i) = -E4*H3*cos(alpha4)^4*cos(psi(i)*(pi/180))*Omega_max;
sigma_b_max4(i) = sigma_b2_max4(i) + sigma_b3_max4(i);

sigma_0_cr4(i) = sigma_f4(i)+ sigma_b_cr4(i);
sigma_0_max4(i) = sigma_f4(i)+ sigma_b_max4(i);
end

% ++++++++++++++++++++++++++++++++++++++++++++++++++++++++++++++++
%                       POST PROCESSING
%                       INNER ARMOUR
% ++++++++++++++++++++++++++++++++++++++++++++++++++++++++++++++++
```

```
figure
plot(psi,sigma_f,'r', psi,sigma_b_max,'b', psi,sigma_0_max,'g')
legend('Friction stress','Bending stress','Total stress')
axis([0,360,-500,500]);
xlabel('Circumferential location [deg]');
ylabel('Stress [MPa]');
print -depsc validationB2_bft3_psi.eps
% =========================================================
%                @ outrados  psi = 180 degrees
%                @ northeast psi = 225 degrees
%==========================================================
%response values
% @ outrados
sigma_f_180 = [0 sigma_f(181) sigma_f(181)]
sigma_b2_180 = [0 sigma_b2_cr(181) sigma_b2_max(181)];
sigma_b3_180 = [0 sigma_b3_cr(181) sigma_b3_max(181)];
sigma_b_180 = [0 sigma_b_cr(181) sigma_b_max(181)];
sigma_0_180 = [0 sigma_0_cr(181) sigma_0_max(181)];

%@ psi = 225 degrees
sigma_f_225 = [0 sigma_f(226) sigma_f(226)]
sigma_b2_225 = [0 sigma_b2_cr(226) sigma_b2_max(226)];
sigma_b3_225 = [0 sigma_b3_cr(226) sigma_b3_max(226)];
sigma_b_225= [0 sigma_b_cr(226) sigma_b_max(226)];
sigma_0_225 = [0 sigma_0_cr(226) sigma_0_max(226)];


% ++++++++++++++++++++++++++++++++++++++++++++++++++++++++++++++
%                       POST PROCESSING
%                       OUTER ARMOUR
% ++++++++++++++++++++++++++++++++++++++++++++++++++++++++++++++
figure
plot(psi,sigma_f4,'r', psi,sigma_b_max4,'b', psi,sigma_0_max4,'g')
legend('Friction stress','Bending stress','Total stress')
axis([0,360,-500,500]);
xlabel('Circumferential location [deg]');
ylabel('Stress [MPa]');
print -depsc validationB2_bft4_psi.eps

% =========================================================
%                @ outrados  psi = 180 degrees
%                @ northeast psi = 225 degrees
%==========================================================
%response values
% @ outrados
sigma4_f_180 = [0 sigma_f4(181) sigma_f4(181)]
sigma4_b2_180 = [0 sigma_b2_cr4(181) sigma_b2_max4(181)];
sigma4_b3_180 = [0 sigma_b3_cr4(181) sigma_b3_max4(181)];
sigma4_b_180 = [0 sigma_b_cr4(181) sigma_b_max4(181)];
sigma4_0_180 = [0 sigma_0_cr4(181) sigma_0_max4(181)];

%@ psi = 225 degrees
sigma4_f_225 = [0 sigma_f4(226) sigma_f4(226)]
sigma4_b2_225 = [0 sigma_b2_cr4(226) sigma_b2_max4(226)];
sigma4_b3_225 = [0 sigma_b3_cr4(226) sigma_b3_max4(226)];
```

```
sigma4_b_225= [0 sigma_b_cr4(226) sigma_b_max4(226)];
sigma4_0_225 = [0 sigma_0_cr4(226) sigma_0_max4(226)];


% +++++++++++++++++++++++++++++++++++++++++++++++++++++++++++++++
%                       POST PROCESSING
%                       VALIDATION FRICTION STRESSES
% +++++++++++++++++++++++++++++++++++++++++++++++++++++++++++++++
psi = [0 180 360;];

sigmaL3 = [430 740 430];
sigmaB3 = [428 746 428];
sigmaB3mean = [587 587 587];
sigmaL3mean = [585 585 585];

sigmaL4 = [530 420 530];
sigmaB4 = [635 531 635];
sigmaBc4 = [527 423 527];
sigmaL4mean = [475 475 475];
sigmaB4mean = [583 583 583];

figure
plot(psi,sigmaB3, 'r', psi,sigmaL3, 'r-.',psi,sigmaB3mean, 'r',psi,
    sigmaL3mean, 'r-.')
legend('ABC_{in}', 'Life6_{in}')
axis([0,360,350,800]);
xlabel('Circumferential location [deg]');
ylabel('Stress [MPa]');
print -depsc validationB2_in.eps

figure
plot(psi,sigmaBc4, 'r', psi,sigmaL4, 'r-.',psi,sigmaB4mean, 'r',psi,
    sigmaL4mean, 'r-.')
legend('ABC_{out}*', 'Life6_{out}')
axis([0,360,350,600]);
xlabel('Circumferential location [deg]');
ylabel('Stress [MPa]');
print -depsc validationB2_out.eps

% figure
% plot(psi,sigmaB3, 'k', psi,sigmaL3, 'k-.',psi,sigmaB4, 'm', psi,sigmaL4,
    'm-.',psi,sigmaL4mean, 'm-.',psi,sigmaL3mean, 'k-.')
% legend('ABC_{in}', 'Life6_{in}','ABC_{out}', 'Life6_{out}')
% axis([0,360,350,800]);
% xlabel('Circumferential location [deg]');
% ylabel('Stress [MPa]');
% print -depsc validationB2_psif.eps

figure
plot(psi,sigmaB3, 'k', psi,sigmaL3, 'k-.',psi,sigmaBc4, 'm', psi,sigmaL4, '
    m-.',psi,sigmaB3mean, 'k',psi,sigmaL4mean, 'm-.',psi,sigmaL3mean, 'k-.')
legend('ABC_{in}', 'Life6_{in}','ABC_{out}*', 'Life6_{out}')
axis([0,360,350,800]);
xlabel('Circumferential location [deg]');
ylabel('Stress [MPa]');
```

```
print -depsc validationB2corr_psif.eps
```

B-2 Response graphs

B-2-1 B1: Helica

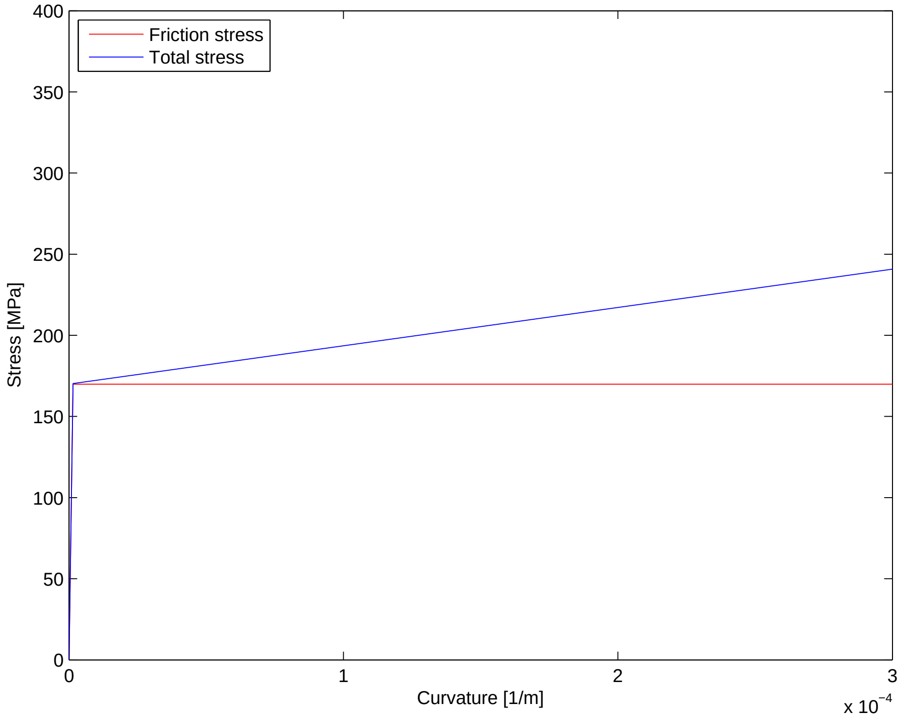

Figure B-1: Stress accumulation $\psi = 180$ deg, outrados

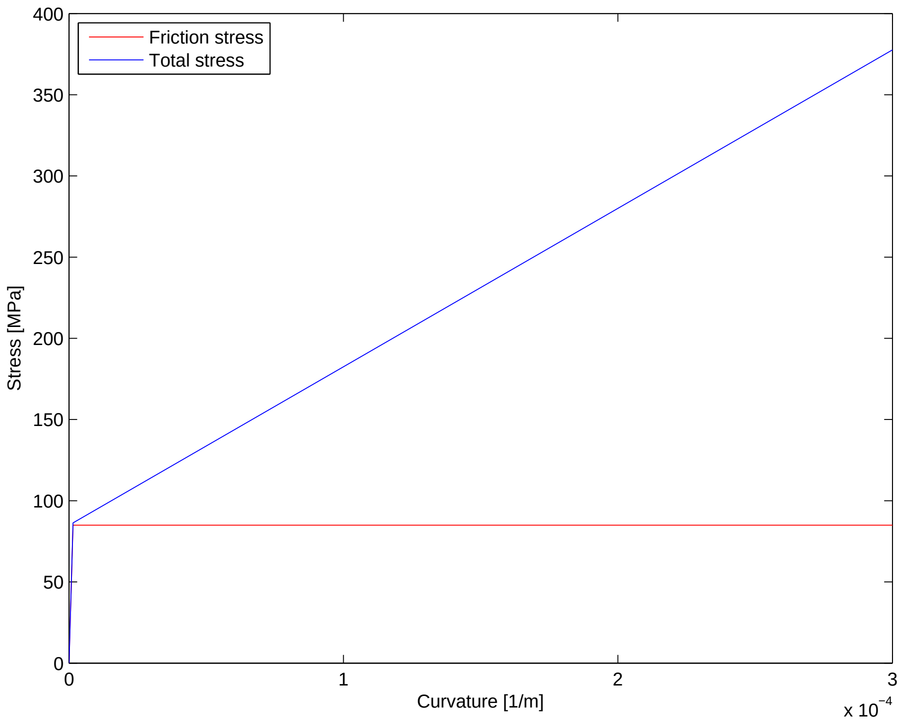

Figure B-2: Stress accumulation $\psi = 225$ deg, north-east

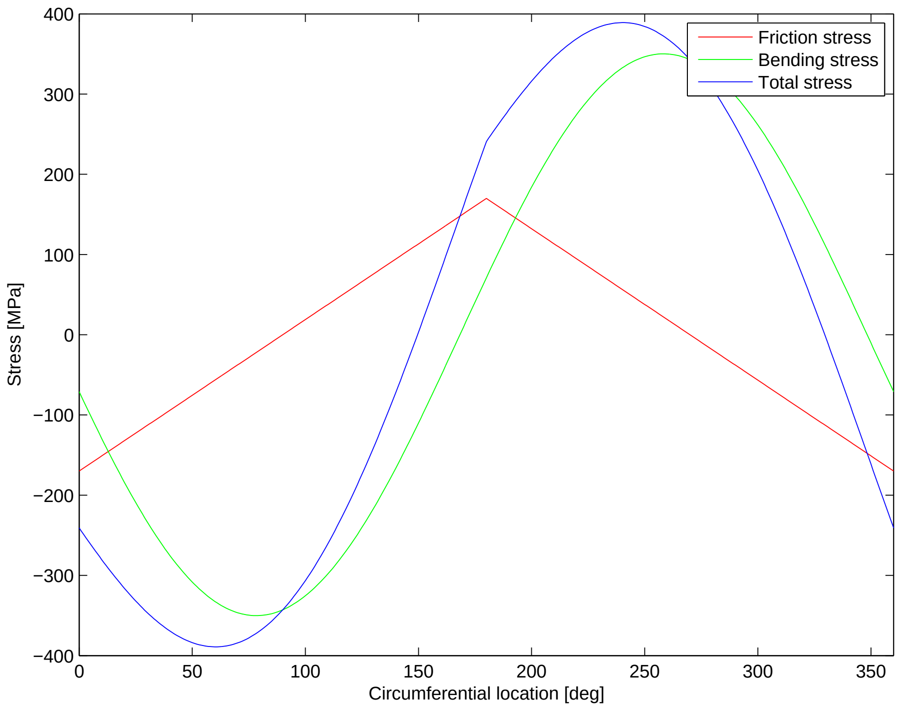

Figure B-3: Circumferential stress distribution, top right $\Omega = 0.3$ 1/m

B-2-2 B2: Life6

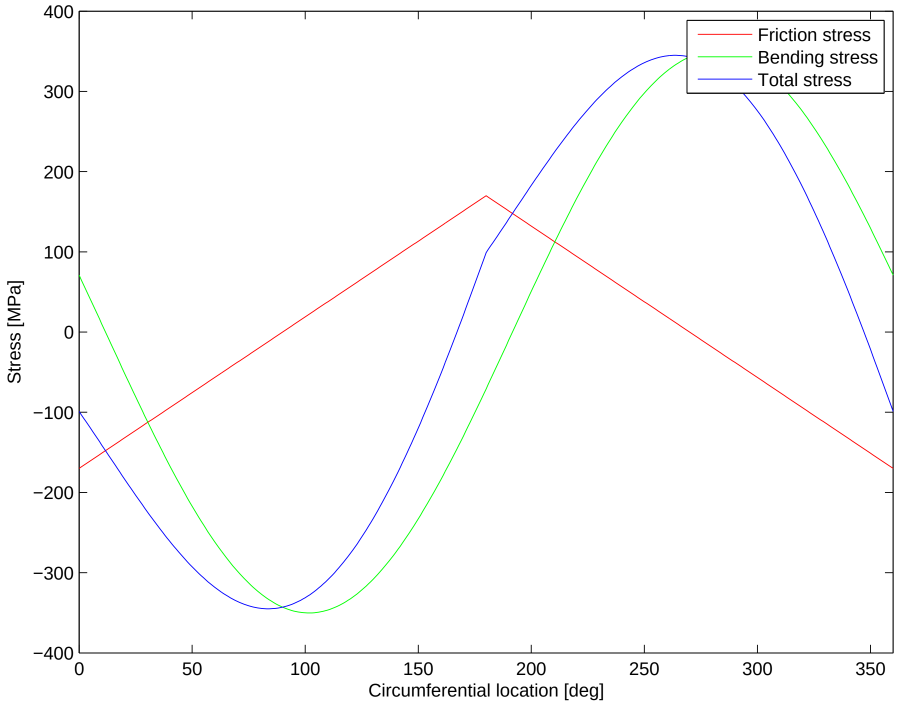

Figure B-4: Circumferential stress distribution, bottom right $\Omega = 0.3$ 1/m

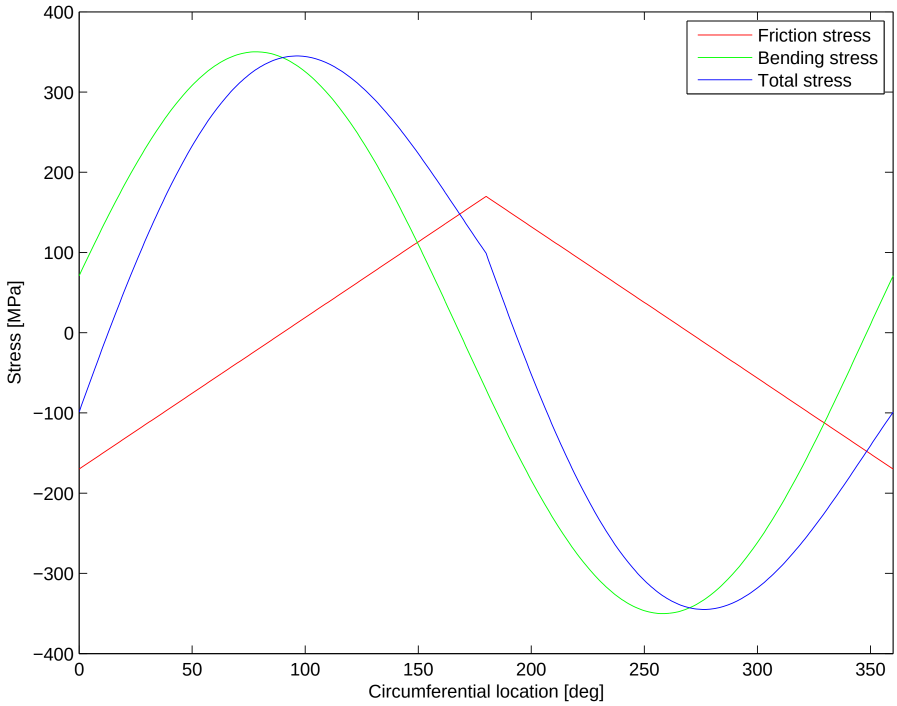

Figure B-5: Circumferential stress distribution, bottom left $\Omega = 0.3$ 1/m

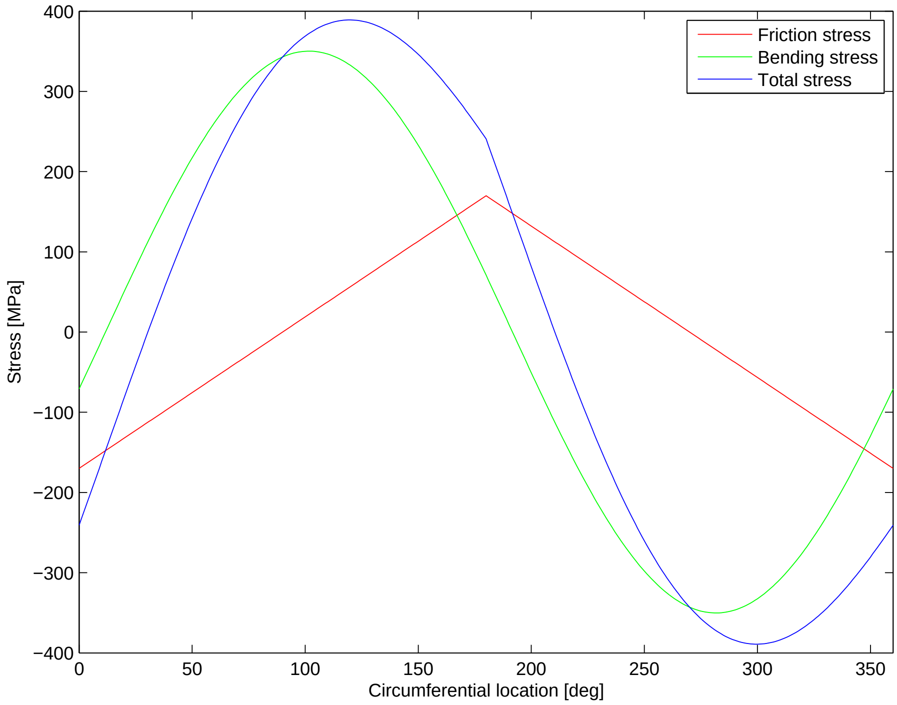

Figure B-6: Circumferential stress distribution, top left $\Omega = 0.3$ 1/m

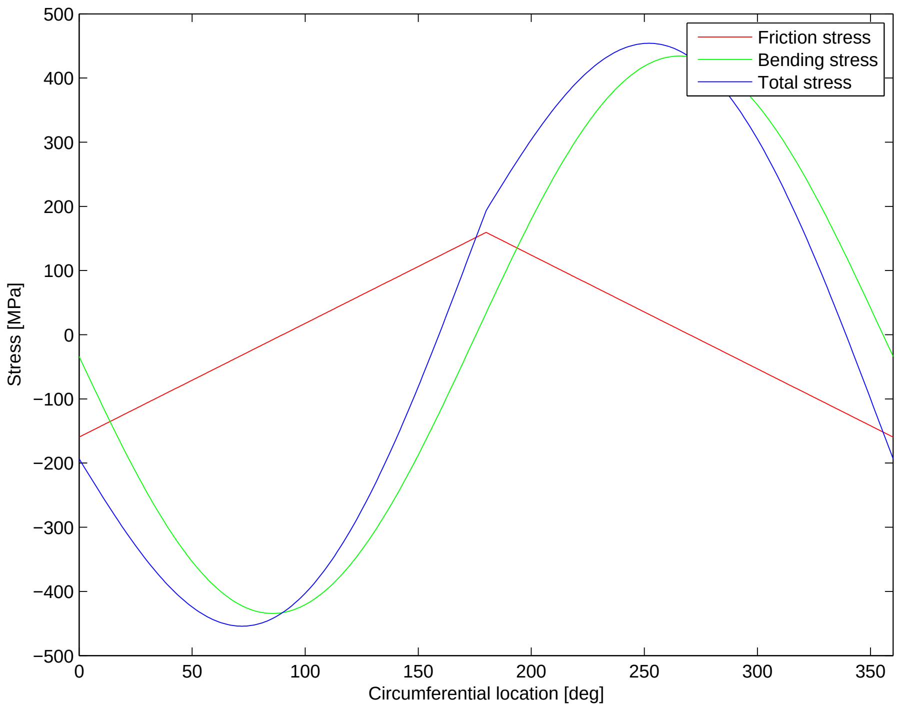

Figure B-7: Circumferential stress distribution inner tensile armour $\Omega = 0.2$ 1/m

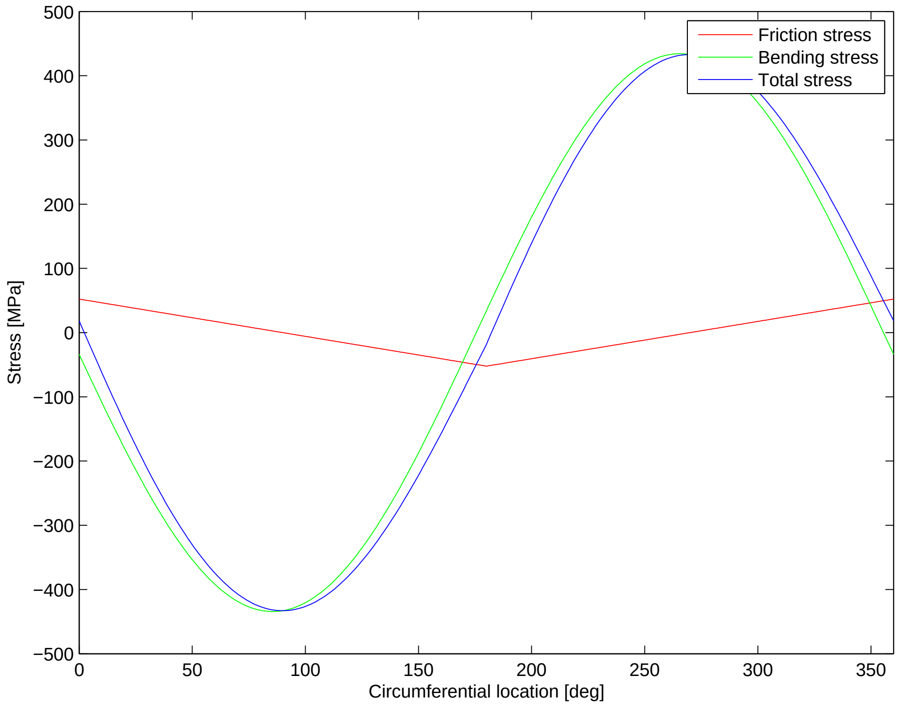

Figure B-8: Circumferential stress distribution, outer tensile armour $\Omega = 0.2$ 1/m

Appendix C

Benchmark Case-Study: Response Graphs

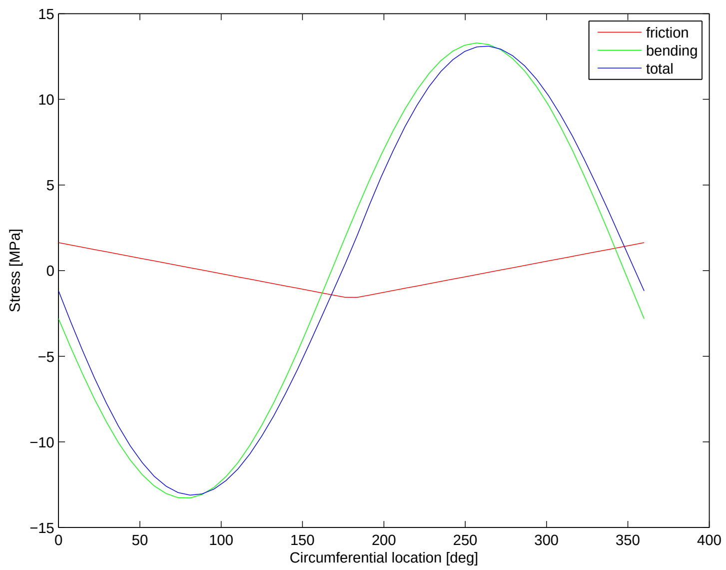

(a) Minimum 5 MPa

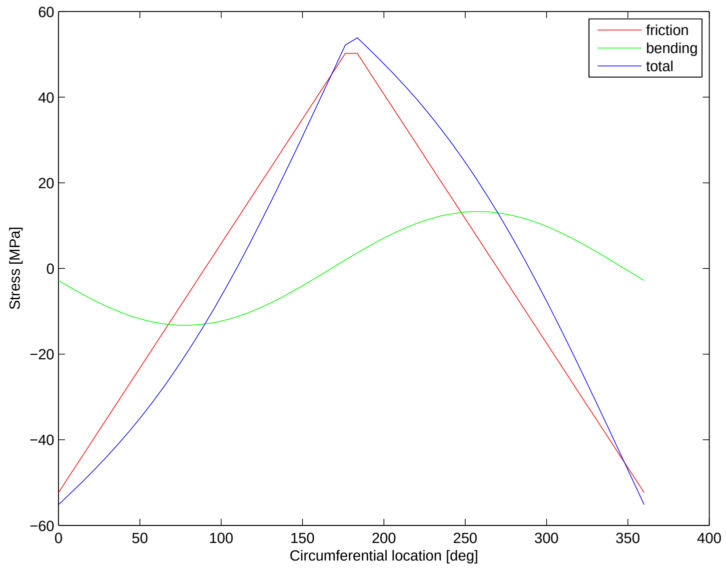

(b) Benchmark 25 Mpa

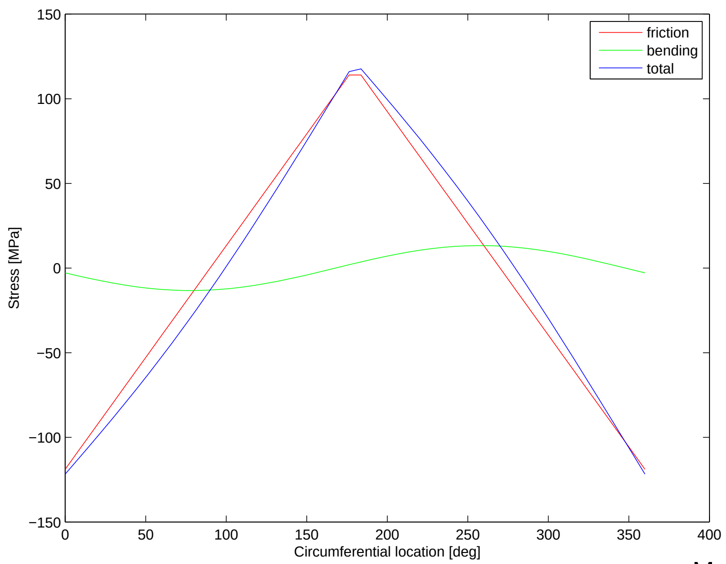

(c) Maximum 50 MPa

Figure C-1: Experiment 1: circumferential stress distributions pressure range

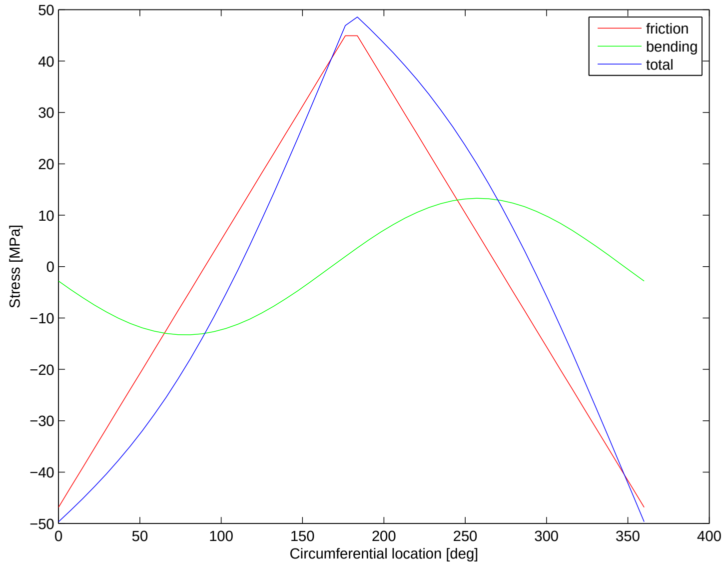

(a) Minimum 20 kN

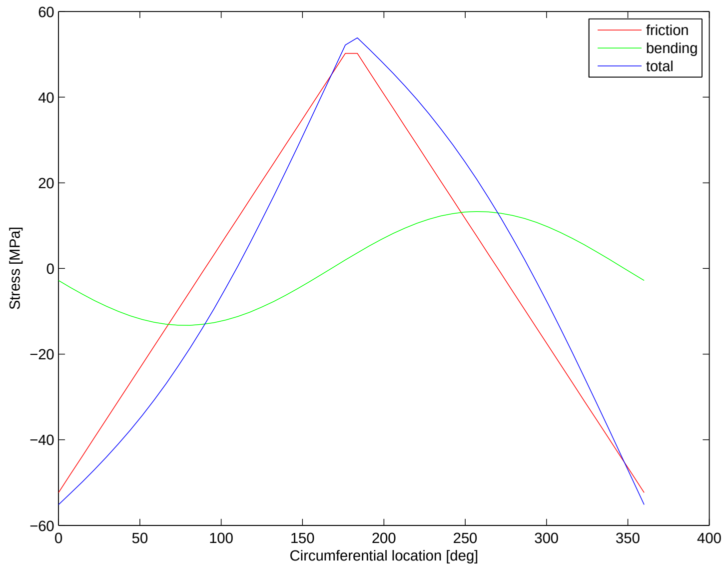

(b) Benchmark 100 kN

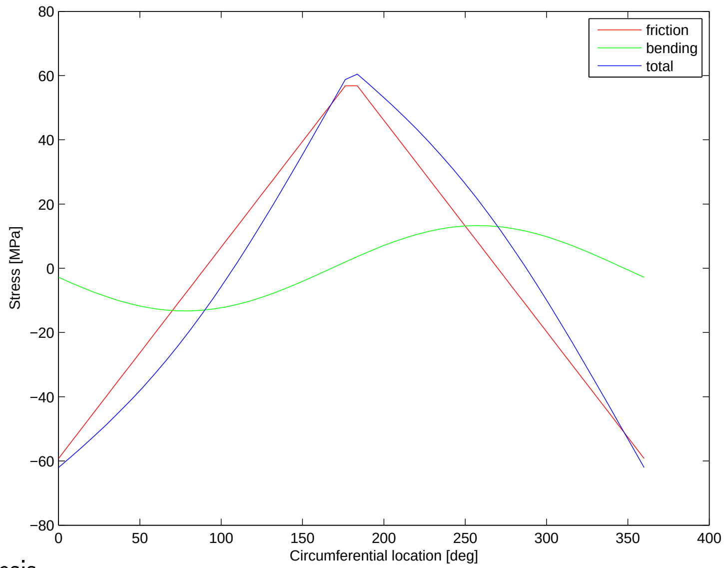

(c) Maximum 200 kN

Figure C-2: Experiment 2: Circumferential stress distributions tension range

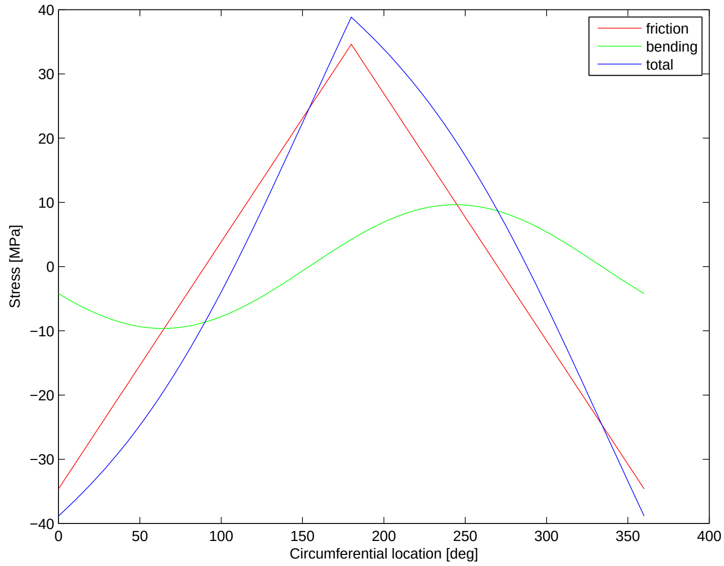

(a) Minimum 8 mm

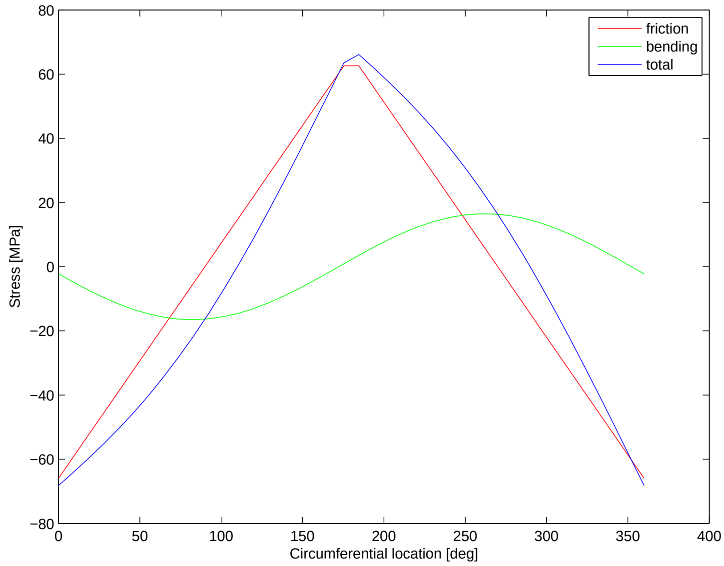

(b) Benchmark 12 mm

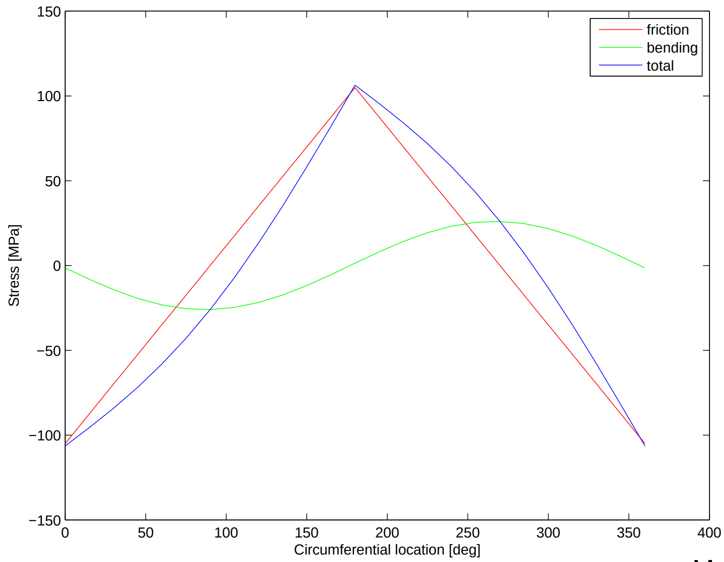

(c) Maximum 24 mm

Figure C-3: Experiment 3: Circumferential stress distributions wire width range

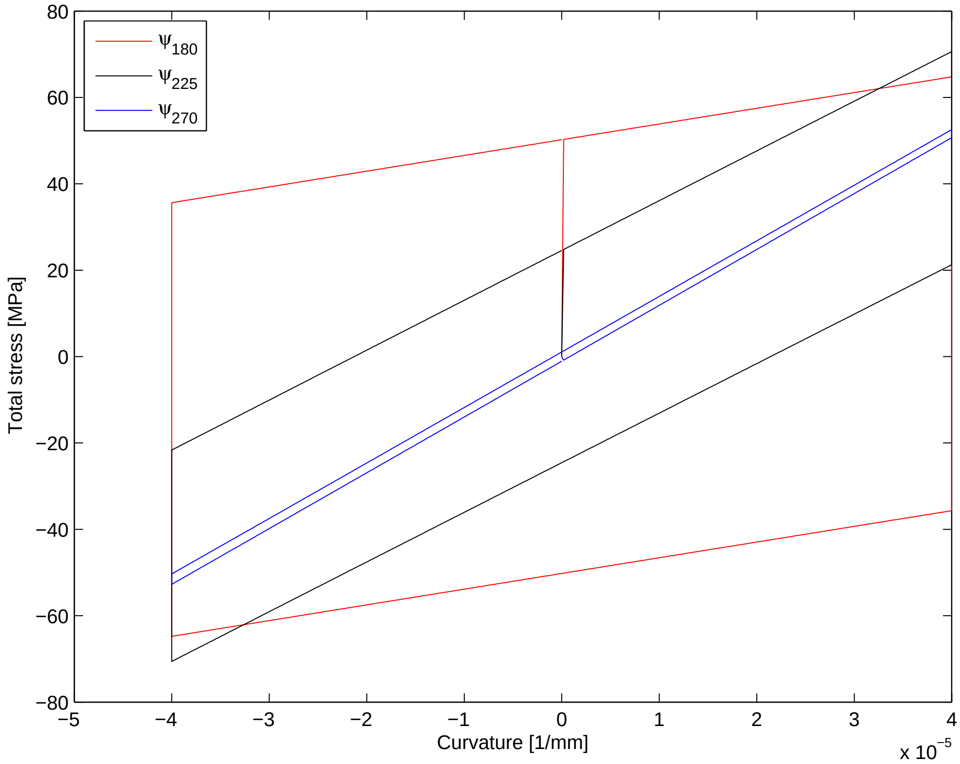

(a) Three different circumferential locations

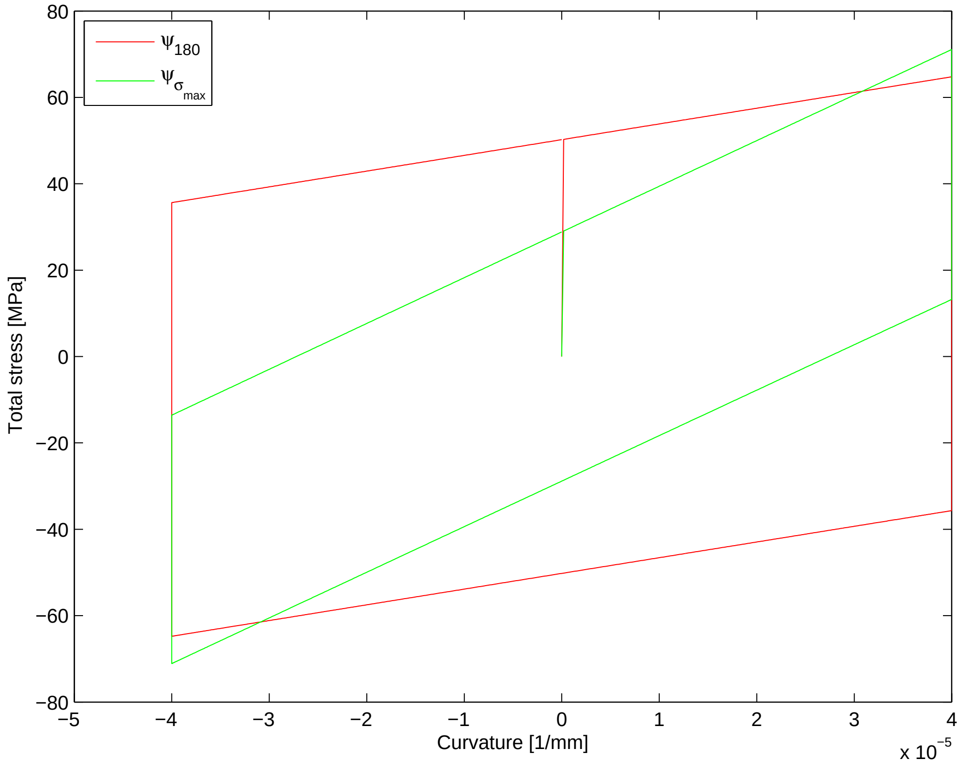

(b) Comparison maximum and outrados

Figure C-4: Experiment 4: Curvature-stress responses

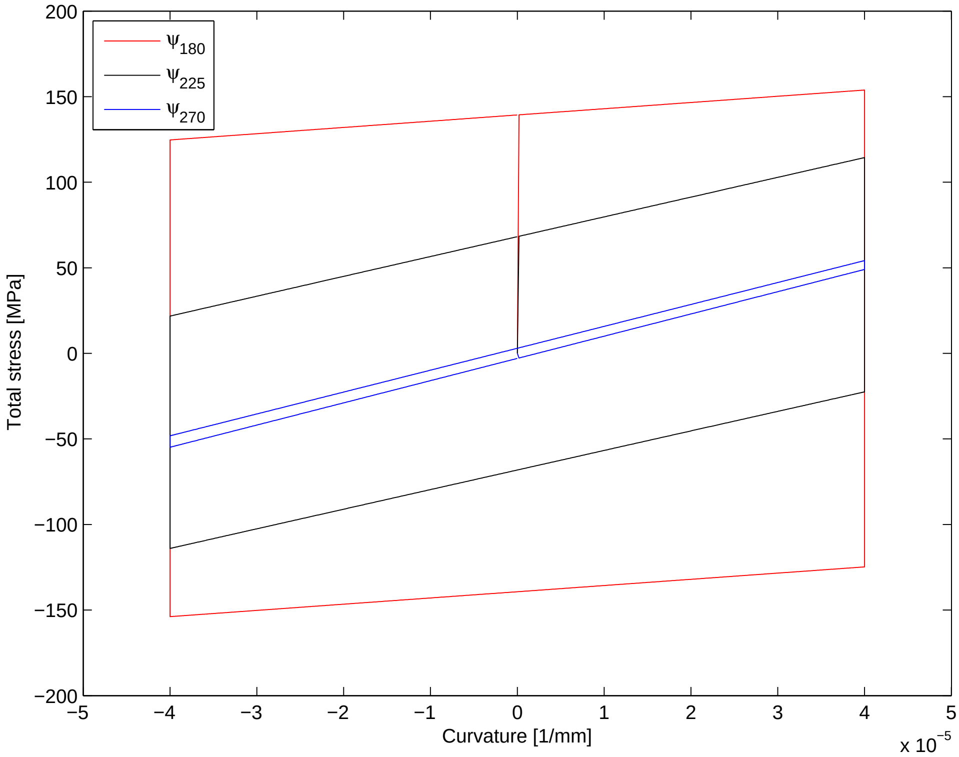

(a) Three different circumferential locations

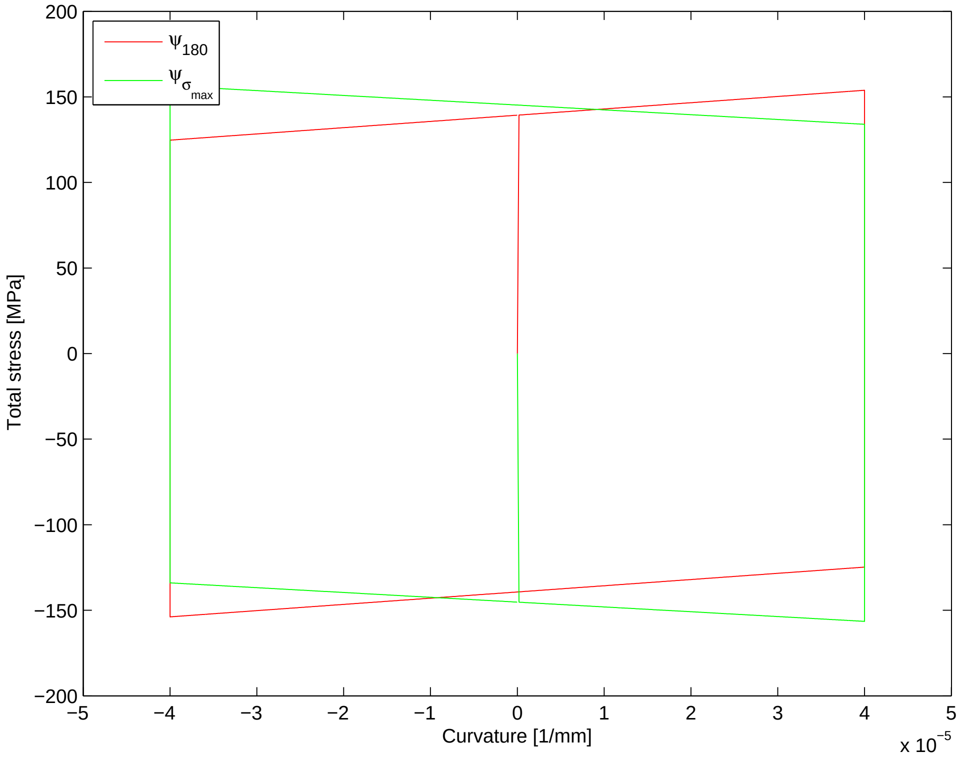

(b) Comparison maximum and outrados

Figure C-5: Experiment 5: Curvature-stress responses high pressure

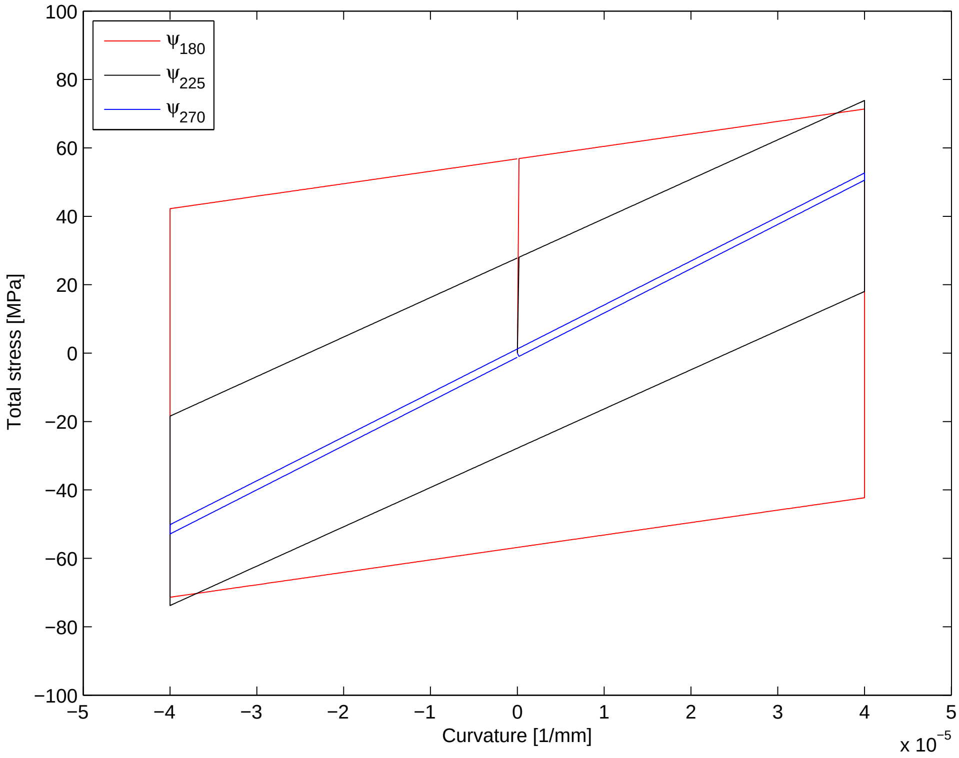

(a) Three different circumferential locations

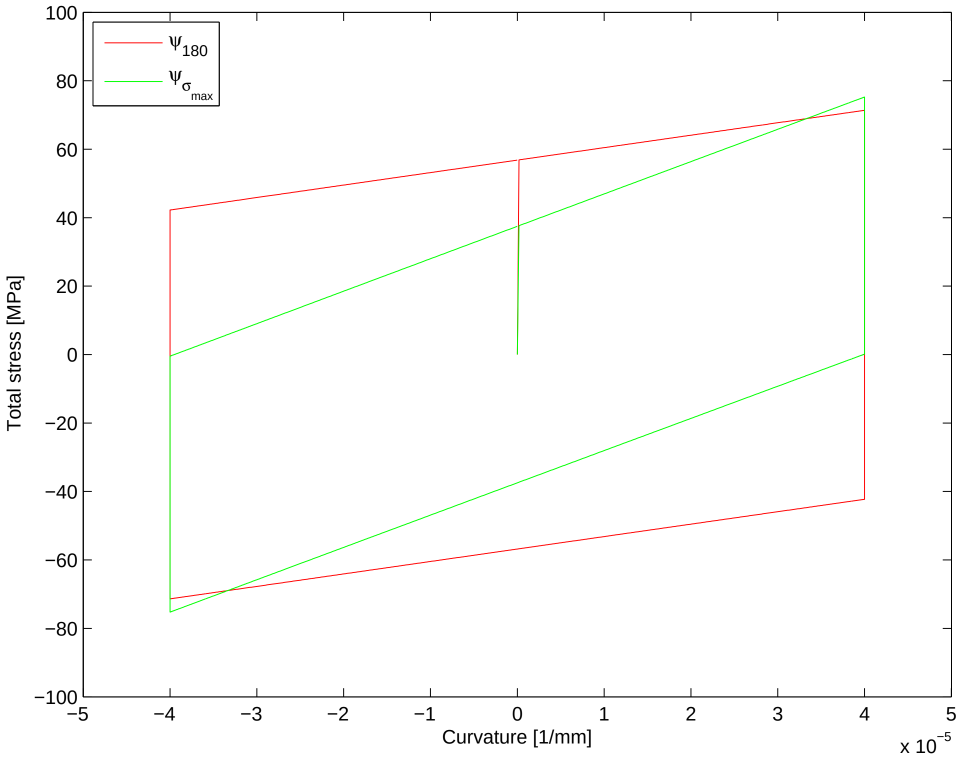

(b) Comparison maximum and outrados

Figure C-6: Experiment 5: Curvature-stress responses high tension

Appendix D

Model C

```
clear all
clc
close all
format loose
format shortg

ABC = fopen('ABC.txt','w');
experiment = 2;

%++++++++++++++++++++++++++++++++++++++++++++++++++++++++++++++++++++++++
%
    T_ex    = 100000;      %[N] External tension
    p_in   = 25;   %[MPa] Inner bore pressure
    p_out   = -1;      %[MPa] Outer (hydrostatic) pressure
%
%++++++++++++++++++++++++++++++++++++++++++++++++++++++++++++++++++++++++

%%%%%%%%%%%%%%%%% GEOMETRY RISER %%%%%%%%%%%%%%%%
%input riser geometry
a_in    = 108.1;    %[mm] Inner bore radius
a_out   = 124.6;   %[mm] Outer pipe radius
L       = 15000;  %[mm] Length local pipe section
N       = 4;      %[-] Number of metallic layers

%%%%%%%%%%%%%%%%% MATERIAL LAYERS %%%%%%%%%%%%%%%%
%Elastic modulus
E1 = 200E3;
E2 = 200E3;
E3 = 200E3;
E4 = 200E3;

%%%%%%%%%%%% GEOMETRY LAYERS %%%%%%%%%%%%%%%%%%
%Wire laying angle
alpha1 = -86.1*(pi/180); %[rad]
```

```
alpha2 = 87.6*(pi/180);
alpha3 = 30*(pi/180);
alpha4 = -30*(pi/180);

%Layer radius
a1 = 108.1;
a2 = 113;
a3 = 118.2;
a4 = 124.6;

%Layer number of wires
n1 = 2;
n2 = 2;
n3 = 50;
n4 = 53;

%Layer Area of wire
A1 = 218.7;
A2 = 45.3;
A3 = 60;
A4 = 60;


%
    ============================================================================
% Part A
%============================================================================
sigma1_L = (E1*cos(alpha1)^2)/L;
sigma1_a = (E1*sin(alpha1)^2)/a1;

sigma2_L = (E2*cos(alpha2)^2)/L;
sigma2_a = (E2*sin(alpha2)^2)/a2;

sigma3_L = (E3*cos(alpha3)^2)/L;
sigma3_a = (E3*sin(alpha3)^2)/a3;

sigma4_L = (E4*cos(alpha4)^2)/L;
sigma4_a = (E4*sin(alpha4)^2)/a4;

F_1 = n1*A1*cos(alpha1);
F_2 = n2*A2*cos(alpha2);
F_3 = n3*A3*cos(alpha3);
F_4 = n4*A4*cos(alpha4);

%Summation for F_i and i=1:N
F_L = F_1*sigma1_L+F_2*sigma2_L+F_3*sigma3_L+F_4*sigma4_L;

F_a = F_1*sigma1_a+F_2*sigma2_a+F_3*sigma3_a+F_4*sigma4_a;

F_0c = T_ex + pi*p_in*a_in^2-pi*p_out*a_out^2;
F_0lin = (pi*p_in-pi*p_out)*2;
F_0nl = (pi*p_in-pi*p_out);

p_1 = (n1*A1*sin(alpha1)*tan(alpha1))/(2*pi*a1);
```

```
p_2 = (n2*A2*sin(alpha2)*tan(alpha2))/(2*pi*a2);
p_3 = (n3*A3*sin(alpha3)*tan(alpha3))/(2*pi*a3);
p_4 = (n4*A4*sin(alpha4)*tan(alpha4))/(2*pi*a4);

%Summation for p_i and i=1:N
p_L = p_1*sigma1_L+p_2*sigma2_L+p_3*sigma3_L+p_4*sigma4_L;
p_a = p_1*sigma1_a+p_2*sigma2_a+p_3*sigma3_a+p_4*sigma4_a;

p_0c = p_in*a_in - p_out*a_out;
p_0lin = p_in-p_out;

% Newton Raphson solution of two nonlinear algebraic equations
% set up the iteration
error1 = 1.e8;
xx(1) = 1; % Da (radial expansion)
xx(2) =10; %DL (elongation)
iter=0;
itermax=30;

% begin iteration
while error1>1.e-12
iter=iter+1;
x = xx(1); % Da expansion
y = xx(2); % DL elongation
% calculate the functions
f(1)= F_L*y +F_a*x - F_0c -F_0lin*x -F_0nl*x^2;
f(2)= p_L*y +p_a*x - p_0c -p_0lin*x;
% calculate the Jacobian
J(1,1) = F_a - F_0lin -2*F_0nl*x;
J(1,2) = F_L;
J(2,1) = p_a - p_0lin;
J(2,2) = p_L;
% solve the linear equations
yy = -J\f ;
% move the solution, xx(k+1) - xx(k), to xx(k+1)
xx = xx + yy ;
% calculate norms
error1=sqrt(yy(1)*yy(1)+yy(2)*yy(2));
error(iter)=sqrt(f(1)*f(1)+f(2)*f(2));
ii(iter)=iter;
if (iter > itermax)
error1 = 0.;
s=sprintf('****Did not converge within %3.0f iterations.****',itermax);
disp(s)
end
% check if error1 < 1.e-12
end
x = xx(1);
y = xx(2);
f(1)= F_L*y +F_a*x - F_0c -F_0lin*x -F_0nl*x^2;
f(2)= p_L*y +p_a*x - p_0c -p_0lin*x;
% print results
f;
xx;
iter;
```

```
% % plot results
% semilogy(ii,error)
% xlabel('iteration number')
% ylabel('norm of functions')
% clear ii
% clear error

% Wall tension
F_0deformed = F_L*y + F_a*x;
F_0load = F_0c +F_0lin*x + F_0nl*x^2;

%%%%%%%%%%%% OUTPUT PART A %%%%%%%%%%%%%%%%%%
%%%%%%%%%%% AXISYMMETRIC WIRE STRESS %%%%%%%%%%%%%%%%%%
sigma1 = sigma1_L*y + sigma1_a*x;
sigma2 = sigma2_L*y + sigma2_a*x;
sigma3 = sigma3_L*y + sigma3_a*x;
sigma4 = sigma4_L*y + sigma4_a*x;

%Calculate pressure differential
Dp1= (n1*A1*sigma1*sin(alpha1)*tan(alpha1))/(2*pi*a1^2);
Dp2= (n2*A2*sigma2*sin(alpha2)*tan(alpha2))/(2*pi*a2^2);
Dp3= (n3*A3*sigma3*sin(alpha3)*tan(alpha3))/(2*pi*a3^2);
Dp4= (n4*A4*sigma4*sin(alpha4)*tan(alpha4))/(2*pi*a4^2);
Dp = [Dp1 Dp2 Dp3 Dp4];

%%%%%%%%%%% CONTACT PRESSURE %%%%%%%%%%%%%%%%%%
pC1 = p_in;
pC2 = pC1 - Dp1;
pC3 = pC2 - Dp2;
pC4 = pC3 - Dp3;
pC5 = pC4 - Dp4;
pC = [pC3; pC4; pC5];
%display(pC);

%%
%=====================================================================
%CURVATURE STEPS
%quarterpitch =  round((L_p-5)/4) %points between zero and max curvature.
cycles = 10;
%=====================================================================

%Constants
L_p = round((2*pi*a3)/(tan(alpha3)))+2   ;    %mm pitch length
f3 = 1/(L_p)  ; % 1/s frequency cyclic curvature

% Total number of points in time
% c78 = 7/8 + (9/8-7/8)*rand(cycles-2,1);
% cycle78 = round((L_p)*(c78));
% cycle78 = cycle78';
% cyclepoints = [ round(L_p) cycle78 round(L_p)];

%Experiment 2.4
c34 = 3/4 + (5/4-3/4)*rand(cycles-2,1);
cycle34 = round((L_p)*(c34));
cycle34 = cycle34 ;
```

```
cyclepoints = [ round(L_p) cycle34 round(L_p)];

%N random numbers in the interval [a,b] with the formula r = a + (b-a).*rand(N,1).

% Circumferential positions = n wires
wires = n3 ; %number of wires
PSI = wires;

%initial wire locations
psi_0 = linspace(0,360,PSI) ;   %initial positions around circumference(deg)
H_0 = zeros(1,PSI);

%First definition of initial curvature and circumferential location
psi_end = psi_0;
Omega_end = 0;
t_top = 1;

%=========================================================
% VARIABLE: CURVATURE (E2.3 E2.4)
%==========================================================
%define omega max
Omega_max = 0.04;
r = 0.0001 + (Omega_max-0.0001)*rand(cycles-1,1);
Omega_max = [Omega_max r ];

%N random numbers in the interval [a,b] with the formula r = a + (b-a).*rand(N,1).

Omega_max(cycles)= Omega_max(1);

% Omega_max'
% Omega_min'
%=========================================================
Omega_min = -0.04;
r = -0.0001 + (Omega_min+0.0001)*rand(cycles-1,1);
Omega_min = [Omega_min r ];

Omega_min(cycles) = Omega_min(1);


for e=1:cycles
%=======================================================

%=======================================================

var = Omega_max;
var2 = Omega_min;


%input values
Omega_pos = Omega_max(e); %1/m
Omega_neg = Omega_min(e);  %1/m
Omega_ampl = (Omega_pos + abs(Omega_neg))/2;    %1/m
```

```
Omega_mean = (Omega_neg + Omega_ampl);            %1/m

%Friction factor (equal for all layers)
mu = 0.15;

%Wire dimensions
b = 12;     %mm
t_w = 5;    %mm

%Curvature range and amplitude
Omega_neg = Omega_neg/1000;     %1/mm
Omega_pos = Omega_pos/1000;     %1/mm
Omega_ampl = Omega_ampl/1000;    %1/mm
Omega_mean = Omega_mean/1000;   %1/mm

%Critical curvatures
Omega_cr3 = (mu*(pC3 +pC4))/(E3*A3*cos(alpha3)^2*sin(alpha3))*(4/pi);    %1/mm

%Hotspot positions
H2=0.5*b;    %mm
H3=0.5*t_w; %mm

%time
t_max = cyclepoints(e);
t_top1 = round(L_p/4);
t_0 = linspace(0,t_max,cyclepoints(e));             % time discretization (one cycle)

c_H =1000* a3^2*(cos(alpha3)^2/sin(alpha3));               %displacement constant
c_f = (mu*a3*(pC3+pC4))/(t_w*sin(alpha3));          %friction stress constant

%pre-allocation friction stress
theta_left = zeros(cyclepoints(e),PSI);
theta_right = zeros(cyclepoints(e),PSI);

for s=2:cyclepoints(e)
 t(s) = t_0(s);
for w = 1:PSI
psi(1,w) = psi_0(1,w) + (psi_end(1,w) - psi_0(1,w));    %initial positions around circumference(deg)
H(1,w) = psi(1,w)*(L_p/360);                             %initial positions along the helix wire(mm)
dH(1,w) = 0.000000001;

% NEW Wire position and displacement
Omega(s) = Omega_ampl*sin(2*pi*f3*t(s))+ Omega_end;
dOmega(s) = Omega_ampl*2*pi*f3*cos(2*pi*f3*t(s));

if  abs(dOmega(s-1)) < 10^-20 && sum(dOmega(s)) < Omega_cr3
    %display('stick');
    dH(s,w) = 0;
elseif abs(dOmega(s-2)) < 10^-20 && sum(dOmega(s)) < Omega_cr3
```

```
    dH(s,w) = 0;
elseif abs(dOmega(s-3)) < 10^-20 && sum(dOmega(s)) < Omega_cr3
    dH(s,w) = 0;
elseif abs(dOmega(s-4)) < 10^-20 && sum(dOmega(s)) < Omega_cr3
    dH(s,w) = 0;
elseif abs(dOmega(s-5)) < 10^-20 && sum(dOmega(s)) < Omega_cr3
    dH(s,w) = 0;
else
    dH(s,w)= c_H*sin(psi(s-1,w)*(pi/180))*(Omega(s)-Omega(s-1));
end;

%Define new position along the helix and around circumference
H(s,w)= H(s-1,w) + dH(s,w);
%dH(s,w)= H(1,w) + H(s,w);
psi(s,w) = (360/L_p)*H(s,w);

%Friction stress
    if psi(s,w) <= 180 %LEFT SIDE OF CROSS SECTION
    % Friction stress
        theta_left(1,w) =(psi(1,w)*pi)/(180)-pi/2;
        %sigma_f(1,i) = c_f*theta_left(1,i);

        theta_left(s,w) =(psi(s,w)*pi)/(180)-pi/2  ;

        if dOmega(s)> 0
        sigma_f(s,w) = c_f*theta_left(s,w);
        else
        sigma_f(s,w) = -c_f*theta_left(s,w);
        end;

    else  %RIGHT SIDE OF CROSS SECTION
        theta_right(1,w) = pi/2-((pi/180)*(psi(1,w)-180));
        %sigma_f(1,i) = c_f*theta_right(1,i);

        theta_right(s,w) = pi/2-((pi/180)*(psi(s,w)-180));

        % Friction stress
        if dOmega(s) > 0
        sigma_f(s,w) = c_f*theta_right(s,w);
        else
        sigma_f(s,w) = -c_f*theta_right(s,w);
        end;
    end;

% Local bending Stress @ max curvature
sigma_b2(1,w) = -E3*H2*cos(alpha3)*(1+sin(alpha3)^2)*sin(psi(1,w)*(pi/180))
    *Omega(1);
sigma_b3(1,w) = -E3*H3*cos(alpha3)^4*cos(psi(1,w)*(pi/180))*Omega(1);
sigma_b(1,w) = sigma_b2(1,w) + sigma_b3(1,w);

sigma_b2(s,w) = -E3*H2*cos(alpha3)*(1+sin(alpha3)^2)*sin(psi(s,w)*(pi/180))
    *Omega(s);
sigma_b3(s,w) = -E3*H3*cos(alpha3)^4*cos(psi(s,w)*(pi/180))*Omega(s);
sigma_b(s,w) = sigma_b2(s,w) + sigma_b3(s,w);

```

```
sigma_0(1,w) = sigma_f(1,w)+ sigma_b(1,w);
sigma_0(s,w) = sigma_f(s,w)+ sigma_b(s,w);

end;

end

Omega_end = Omega(cyclepoints(e));
psi_end = psi(cyclepoints(e),:);

%Given that wire 26 32 and 38 have initial positions closest to 180 225 270
w_180 = 26;
w_225 = 32;
w_270 = 38;

psi_w0 = psi(32);
H_w0 = H_0(32);

%=====================================================================
%                           RESPONSE DATA
%=====================================================================

% MODEL A
sigma_s = sigma3;
p_C3 = pC3;
p_C4 = pC4;

% MODEL B
Omega_cr = Omega_cr3;
sigmaf_top = [sigma_f(t_top1,w_180) sigma_f(t_top1,w_225) sigma_f(t_top1,
    w_270)];
sigmab_top= [sigma_b(t_top1,w_180) sigma_b(t_top1,w_225) sigma_b(t_top1,
    w_270)];
sigma_top = [sigma_0(t_top1,w_180) sigma_0(t_top1,w_225) sigma_0(t_top1,
    w_270)];

%MODEL C
psi_w = psi(t_max,w_225)
H_w = H(t_max,w_225)
dH_w = sum(dH(:,w_225))

sigma_topmax = sigma_0(t_max-3*t_top1,w_225);
sigma_crestmax = sigma_0(t_max-t_top1,w_225);
sigma_tmax = sigma_0(t_max,w_225);

Dsigma = abs(sigma_topmax) + abs(sigma_crestmax);

R = [cyclepoints(e) Dsigma psi_w H_w Omega_max(e) Omega_min(e)]
display(e);
fprintf(ABC, '%g %g %g %g %g %g \r\n',R);
%=====================================================================
%                           OUTPUT PLOTS
%=====================================================================

figure
```

```
plot( psi(t_top1,:),sigma_f(t_top1,:),'r',psi(t_top1,:),sigma_b(t_top1,:),'
    g',psi(t_top1,:),sigma_0(t_top1,:),'b')
legend('friction','bending','total')
xlabel('Circumferential location [deg]');
ylabel('Stress [MPa]');
title('\psi,\sigma_{total} max positive curvature');
end

figure
plot( psi(t_top1,:),sigma_f(t_top1,:),'r',psi(t_top1,:),sigma_b(t_top1,:),'
    g',psi(t_top1,:),sigma_0(t_top1,:),'b')
legend('friction','bending','total')
xlabel('Circumferential location [deg]');
ylabel('Stress [MPa]');
title('\psi,\sigma_{total} max positive curvature');

figure
plot( psi(3*t_top1-1,:),sigma_f(3*t_top1-1,:),'r',psi(3*t_top1,:),sigma_b
    (3*t_top1-1,:),'g',psi(3*t_top1-1,:),sigma_0(3*t_top1-1,:),'b')
legend('friction','bending','total')
xlabel('Circumferential location [deg]');
ylabel('Stress [MPa]');
title('\psi,\sigma_{total} max negative curvature');

Omega = Omega ;
figure
plot(Omega,sigma_0(:,wire_max),'g', Omega,sigma_0(:,w_180),'r', Omega,
    sigma_0(:,w_225),'k',Omega,sigma_0(:,w_270),'m')
legend('wiremax', 'wiremin','225','270')
% axis([-0.00002,0.00002,-50,50]);
xlabel('Curvature [1/mm]');
ylabel('Total stress [MPa]');
print -depsc validationfin.eps
```

Bibliography

4Subsea. Un-bonded flexible risers - recent field experience and actions for increased robustness. Technical report, 4Subsea.

S. Berge and A. Olufsen. *Handbook on Design and Operaiton of Flexible Pipes*. SINTEF, 1992.

David Charlesworth, Bill D'All, Cecile Zimmerlin, Elias Remita, Nina Langhelle, and Ting Wang. Operational experience of the fatigue performance of a flexible riser with a flooded annulus. *Offshore Technology Conference*, 2011.

Carsten S. Dahl, Bo Andersen, and Mikael Groenne. Developments in managing flexible risers and pipelines, a suppliers perspective. *Offshore Technology Conference*, 2011.

Ali Fatemi. Chapter 4; fatigue tests and s-n approach. Technical report, The University of Toledo.

Jany Feret and Jean-Marc Leroy. Calculation of stresses and slips in flexible armour layers with layers interaction. *OMAE, Pipeline Technology volume V*, 1995.

J.J. Feret and C.L. Bournazel. Calculation of stresses and slip in structural layers of unbonded flexible pipes. *Journal of Offshore Mechanics and Arctic Engineering*, 1987.

F. Grealish, R. Smith, and J. Zimmerman. New industry guidelines for fatigue analysis of unbonded flexible risers. *Offshore Technology Conference*, 2006.

Russel C. Hibbeler. *Mechanics of Materials*. Pearson, 2013.

MCS Kenny. Cook risers fatigue assessment. Technical report, MCS Kenny.

R.H. Knapp. Helical wire stresses in bent cables. *OMAE International Mechanics and Arctic Engineering Symposium*, 1987.

Bogi Laksafoss and Christian Bergenstof Nielsen (NOV). Deepwater jip - data request present work. Email conversation, June 2015.

Carl Martin Larsen, Svein Saevik, and Jacob Qvist. *Handbook on Design and Operation of Flexible Pipes; B1 Design Analysis*. MARINTEK / NTNU / 4Subsea, 2014. Development of this Handbook is made possible through the Joint Industry Project: Safe and Cost Effective Operation of Flexible Pipes, 2011-2013.

Jean-Marc Leroy, Timothee Perdrizet, Vincent Le Corre, and Pascal Estrier. Stress assessment in armour layers of flexible risers. *Proceedings of the ASME*, 2010.

J.M. Leroy and P. Estrier. Calculation of stresses and slips in helical layers of dynamically bent flexible pipes. *Oil and Gas Science and Technology*, 2001.

Ramon Loback, B.B. Matos, Celso Velasco Raposo, and Kumar Rajesh. Flexible pipe integrity analysis using event trees. *Offshore Technology Conference*, 2010.

S.A. Lotveit and O. Often. Increased reliability througgh a unified analysis tool for bonded and non-bonded pipes. *Advances in Subsea Pipeline Engineering and Technology*, 1990.

Patrich Obrien, Chris Overton, Ian Macleod, John Picksley, Keith Anderson, and Euan Meldrum. Outcomes from the sureflex joint industry project - an international initiative on flexible pipe integrity assurance. *Offshore Technology Conference*, 2011.

J.M.M. Out. On the prediction of the endurance strength of flexible pipe. *Offshore Technology Conference*, 1989.

J.M.M Out. Integrity management of flexible pipe: Chasing failure mechanisms. *Offshore Technology Conference*, 2012.

J.M.M. Out and B.J. von Morgen. Slippage of helical reinforcing on a bent cylinder. *Engineering Structures*, 1997.

Svein Saevik. *On Stresses and Fatigue in Flexible Pipes*. PhD thesis, University of Trondheim, Norway.

Geir Skeie, Nils Sodahl, and Oddrun Steinkjer. Efficient fatigue analysis of helix elements in umbilicals and flexible risers: Theory and applications. *Journal of Applied Mathematics*, 2012.

Russel Smith and F. Grealish. Real life jip: Fatigue analysis methodology guidelines. Technical report, MCS Kenny.

James Stewart. *Calculus*. Cengage Learning, 2007.

Technip. Cook risers design report. Technical report, Technip.

Tatiana Vargas-Londono, Jose Renato M. De Sousa, Carlos Magluta, and Ney Roitman. A theoretical and experimental analysis of the bending behaviour of unbonded flexible pipes. *Proceedings of the ASME*, 2014.

J.A. Witz. A case study in the cross-seciton analysis of flexible risers. *Marine Structures*, 1995.

J.A. Witz and Z. Tan. On the axial-torsional structural behaviour of flexible pipes, umbilicals and marine cables. *Marine Structures*, 1992.